

XEROGEL COATINGS FOR BIOMEDICAL SENSING APPLICATIONS

by
Kevin Perry Dobmeier

A dissertation submitted to the faculty of the University of North Carolina at Chapel Hill in partial fulfillment of the requirements for the degree of Doctor of Philosophy in the Department of Chemistry (Analytical Chemistry).

Chapel Hill
2007

Approved by

Professor Mark H. Schoenfish

Professor Gary L. Glish

Professor Royce W. Murray

Professor Valerie Sheares Ashby

Professor Sergei S. Sheiko

ABSTRACT

Kevin Perry Dobmeier: Xerogel Coatings for Biomedical Sensing Applications
(Under the direction of Professor Mark H. Schoenfisch)

New strategies for utilizing sol-gel chemistry to improve sensor compatibility with physiological environments and produce xerogel membranes for novel optical sensor applications are described. Incorporation of nitric oxide (NO)-donor functionalities into a material is an established means of creating more biocompatible blood and tissue-contacting surfaces. A NO-releasing optical pH sensor designed for intravascular use was developed through covalent attachment of *N*-diazeniumdiolate (NONOate) NO donors to aminoalkoxysilane-derived xerogels. A two-layer sensor configuration was employed wherein a NONOate-modified xerogel and porous tetramethyl orthosilicate xerogel containing a fluorescent pH indicator were sequentially dip-coated onto a tapered fiber-optic probe. The resulting sensors were capable of rapid and linear optical pH detection throughout the physiological pH range (7.0 - 7.8 pH) and generated NO fluxes $>0.4 \text{ pmol cm}^{-2} \text{ s}^{-1}$ for ~ 16 h. Significant reductions of platelet adhesion to the NO-releasing materials versus controls were observed after exposure to platelet-enriched porcine plasma.

An alternate class of NO-releasing xerogels was formed by co-condensation of mercaptoalkoxysilane and alkylalkoxysilane sol-gel precursors. Subsequent thiol nitrosation resulted in *S*-nitrosothiol (RSNO)-modified xerogels capable of generating NO-fluxes $>0.5 \text{ pmol cm}^{-2} \text{ s}^{-1}$ for up to 14 d in 37 °C phosphate-buffered saline (PBS). The

films displayed excellent solution stability with larger percentages of NO-donor inclusion than NONOate-modified films. Reductions observed in platelet and *Pseudomonas aeruginosa* adhesion to nitrosated films versus non-nitrosated controls confirmed the antithrombotic and antibacterial properties of the materials.

Aminoalkoxysilane-derived xerogels were further employed to create optical sensor coatings for quantitative detection of nitroxyl (HNO), the one-electron reduced congener of NO. A kinetic strategy was used to quantify HNO via the spectroscopically observed rates of HNO-induced reductive manganese(III) *meso*-tetrakis(4-sulfonatophenyl) porphyrinate (Mn^{III}TPPS) nitrosylation. The stability of the Mn^{II}(NO)TPPS reaction product was significantly increased when encapsulated in the anaerobic interior of an (aminoethylaminomethyl)phenethyltrimethoxysilane (AEMP3)-derived xerogel film. Nitroxyl diffusion through the xerogel materials was selectively enhanced via the covalent incorporation of trimethoxysilyl-terminated poly(amidoamine-organosilicon) (PAMAMOS) dendrimers, resulting in substantially increased sensitivity to HNO. The HNO-sensing films were subsequently employed in a 96-well microtitre plate format to characterize HNO release from a recently described HNO/NO donor compound, sodium-1-(isopropylamino)diazene-1-ium-1,2-diolate (IPA/NO).

TABLE OF CONTENTS

LIST OF TABLES	ix
LIST OF FIGURES	x
LIST OF ABBREVIATIONS AND SYMBOLS	xiii
Chapter 1. Xerogel Technology in Sensor Applications	1
1.1. Xerogels.....	1
1.1.1. Sol-Gel Chemistry.....	2
1.1.2. Xerogel Properties.....	5
1.2. Xerogel-Based Sensors.....	7
1.2.1. Optical Xerogel Sensors.....	7
1.2.2. Electrochemical Xerogel Sensors.....	11
1.3. Sensor Biocompatibility	13
1.3.1. Sensor Biofouling.....	14
1.3.2. Nitric Oxide-Releasing Xerogels	16
1.3.3. NO-releasing Xerogel Sensors	20
1.4. S-Nitrosothiol-Modified Xerogels.....	22
1.5. Nitroxyl Sensing via Aminoalkoxysilane Xerogels	24
1.6. Summary of Dissertation Research	26

1.7. References.....	28
Chapter 2. Nitric Oxide-Releasing Xerogel-Based Fiber-Optic pH Sensors.....	39
2.1. Introduction.....	39
2.2. Materials and Methods	43
2.2.1. NO-Releasing Xerogel Preparation	43
2.2.2. pH-Sensing Xerogel Preparation	43
2.2.3. Sensor Fabrication	44
2.2.4. Apparatus.....	44
2.2.5. Characterization of NO Release	45
2.2.6. Platelet Adhesion Studies	46
2.3. Results and Discussion	47
2.3.1. Two-Layer Sensors.....	48
2.3.2. Sensitivity and Reproducibility	48
2.3.3. Pretreatment and Response Time	51
2.3.4. Nitric Oxide Release.....	55
2.3.5. In vitro Platelet Adhesion Studies	57
2.4. Conclusions.....	57
2.5. References.....	60
Chapter 3. Preparation and Characterization of <i>S</i> -Nitrosothiol (RSNO)-Modified Xerogels.....	65
3.1. Introduction.....	65
3.2. Materials and Methods	68

3.2.1. Xerogel Film Synthesis	69
3.2.2. Nitrosothiol Formation	69
3.2.3. Characterization of NO Release	70
3.2.4. Xerogel Film Stability	70
3.2.5. Bacterial Adhesion to RSNO Xerogels	71
3.2.6. Platelet Adhesion to RSNO Xerogels	72
3.3. Results and Discussion	72
3.3.1. Xerogel Characterization	72
3.3.2. Antibacterial Properties of RSNO-Xerogels	80
3.3.3. Antithrombotic Properties of RSNO-Xerogels	83
3.4. Conclusions	86
3.5. References	88
Chapter 4. Xerogel Optical Sensor Films for Quantitative Detection of Nitroxyl	94
4.1. Introduction	94
4.2. Materials and Methods	99
4.2.1. Response of Mn ^{III} TPPS to NO and HNO	100
4.2.2. Xerogel Film Preparation	100
4.2.3. Film Characterization	100
4.2.4. Kinetic HNO Quantification	101
4.2.5. Xerogel-Coating of 96-well Microtitre Plates	103
4.2.6. Microtitre Plate Sensor Optimization	103
4.2.7. Oxygen Permeability Testing	103

4.2.8. HNO-Generation from IPA/NO	105
4.3. Results and Discussion	106
4.3.1. Mn ^{III} TPPS HNO Selectivity	106
4.3.2. Mn ^{II} (NO)TPPS Formation in Xerogel Films	108
4.3.3. Microtitre Plate Sensor Optimization via PAMAMOS	110
4.3.4. Oxygen Permeability in PAMAMOS-Modified Films	113
4.3.5. Nitroxyl Sensing	115
4.4. Conclusions	122
4.5. References	123
 Chapter 5. Summary and Future Directions	 127
5.1. Summary	127
5.2. Future Research Directions	130
5.3. References	134
 Appendix 1. Antibacterial Properties of NO-Releasing Xerogel Microarrays	 135
A1.1. Introduction	135
A1.2. Materials and Methods	136
A1.2.1. Xerogel Micropatterning	137
A1.2.2. NO-Release	138
A1.2.3. Array Stability	138
A1.2.4. Evaluation of Bacterial Retention	138
A1.3. Results and Discussion	139
A1.4. Conclusions	143

A1.5. References.....	145
-----------------------	-----

LIST OF TABLES

Table 2.1.	Reference emission ratios, sensitivity, linearity, and signal reproducibility of 40:60% (v:v) AHAP3/ETMOS-TMOS NO-releasing sensors	52
Table 4.1.	Oxygen permeability of 0-2% (v:v) PAMAMOS-modified AEMP3/MTMOS xerogels and controls	114
Table A1.1.	Average bacterial surface coverage on 20% AEMP3 / 80% MTMOS xerogel arrays.....	142

LIST OF FIGURES

Figure 1.1.	Mechanism of sol-gel precursor hydrolysis under (A) acid-catalyzed and (B) base catalyzed conditions	4
Figure 1.2.	General (A) extrinsic and (B) intrinsic xerogel optical sensor configurations	9
Figure 1.3.	Biofouling of sensor surfaces upon (A) intravascular or (B) subcutaneous implantation	15
Figure 1.4.	Mechanism of <i>N</i> -diazoniumdiolate formation and subsequent NO release	17
Figure 1.5.	Alkylalkoxysilanes and aminoalkoxysilanes used in production of <i>N</i> -diazoniumdiolated NO-releasing xerogels	19
Figure 1.6.	Common <i>S</i> -nitrosothiol decomposition pathways	23
Figure 2.1.	Fluorescence emission spectra from a 40:60% (v:v) AHAP3/ETMOS-TMOS optical pH sensor immersed in phosphate buffered saline at pH (A) 7.0; (B) 7.4; and (C) 7.8.....	49
Figure 2.2.	Time-resolved response from 40:60% (v:v) AHAP3/ETMOS-TMOS optical pH sensor immersed in pH 7.0-7.8 PBS solutions.....	50
Figure 2.3.	Timed response of 40:60% (v:v) AHAP3/ETMOS-TMOS optical pH sensor as a function of pH (7.0-7.8).....	54
Figure 2.4.	Nitric oxide release from (A) 40:60% and (B) 20:80% (v:v) AHAP3/ETMOS xerogels; and, (C) 20:80% (v:v) AHAP3/ETMOS xerogel with a TMOS overlayer film, immersed in 37 °C PBS (pH 7.4).....	56
Figure 2.5.	Representative scanning electron micrographs illustrating platelet adhesion to (A) NO-releasing and (C) control 40:60% (v:v) AHAP3/ETMOS films, and equivalent (B) NO-releasing and (D) control films with TMOS overcoats.....	58

Figure 3.1.	Chemical structures of (A) mercaptopropyltrimethoxysilane (MPTMS); (B) methyltrimethoxysilane (MTMOS); (C) ethyltrimethoxysilane (ETMOS); and (D) isobutyltrimethoxysilane (BTMOS)	74
Figure 3.2.	Absorbance spectrum of MTMOS films containing (—) 20% MPTMS; (---) 40% MPTMS; (···) 60% MPTMS; and (---) 80% MPTMS (v:v total silane).....	76
Figure 3.3.	Average NO flux from RSNO-modified MPTMS/MTMOS films in 37 °C PBS/DTPA. Data points correspond to the average of 3 films incorporating (■) 80%; (●) 60%; (▲) 40% and (▼) 20% MPTMS (v:v total silane). [Inset: Magnified view of 2 – 14 d NO release.].....	77
Figure 3.4.	Nitric oxide flux from RSNO-modified 40% (v:v total silane) MPTMS/MTMOS films in pH 7.4 PBS / 100 μM DTPA solutions held at (A) 37 °C; (B) 25 °C; or (C) 0 °C	79
Figure 3.5.	Average <i>P. aeruginosa</i> adhesion to 60% (v:v total silane) MPTMS/MTMOS films during 1 h immersion in ~10 ⁸ cfu/mL bacterial suspensions. Average values were calculated from the mean of 5 images on control or RSNO-modified films (N = 3) soaked 0 or 24 h in 37 °C PBS/GSH	81
Figure 3.6.	Representative phase-contrast images of platelet adhesion to (A) control and (B) RSNO-modified 40% (v:v total silane) MPTMS/MTMOS films after 1 h exposure to porcine PRP	85
Figure 4.1.	Chemical structures of (A) Mn ^{III} TPPS and (B) generation-zero trimethoxysilyl-terminated PAMAMOS dendrimers.....	97
Figure 4.2.	The UV/Vis spectral response of (—) Mn ^{III} TPPS in pH 7.4 PBS upon exposure to 100 μM (---) Angeli's salt and (···) NO. Spectra were recorded 8 min after the addition of Angeli's salt or NO.....	107
Figure 4.3.	Mn ^{II} (NO)TPPS formation in (■) AEMP3/MTMOS or (x) free in aerobic PBS as measured by absorbance at 432 or 423 nm, respectively, after the addition of 100 μM Angeli's salt	109

Figure 4.4.	Initial rates of Mn ^{II} (NO)TPPS formation detected as 430 nm absorbance in AEMP3/MTMOS films modified with 0-2% (v:v total silane) trimethoxysilyl-terminated PAMAMOS dendrimers upon the addition of 320 μM Angeli's salt/PBS.....	112
Figure 4.5.	Initial rates of Mn ^{II} (NO)TPPS formation in 40/60% (v:v total silane) AEMP3/MTMOS films modified with 0.25% (v:v total silane) trimethoxysilyl-terminated PAMAMOS dendrimers. Data corresponds to the average of 7 individual films. [Inset: Magnified view of linear region.].....	116
Figure 4.6.	Time-resolved HNO concentrations obtained from (■) 700 μM and (x) 50 μM Angeli's salt in pH 7.4 PBS. Rates were acquired over 60 s intervals.....	118
Figure 4.7.	Effect of pH on HNO production from 6.1 mM IPA/NO in PBS. Data corresponds to the average of 7 individual films.....	120
Figure 4.8.	Concentrations of HNO versus required donor concentrations of (■) IPA/NO or (x) Angeli's salt in pH 7.4 PBS. Data corresponds to the average of 7 individual films. Note the scale break along the x-axis.....	121
Figure A1.1.	<i>P. aeruginosa</i> adhesion on A) control and B) NO-releasing 10 μm xerogel lines separated by 50 μm spacings. Cells are white.....	141

LIST OF ABBREVIATIONS AND SYMBOLS

°C	degree(s) Celsius
%	percentage(s)
±	statistical margin of error or tolerance
[...]	concentration
·	radical
$\partial / \partial t$	partial derivative with respect to time
ε	extinction coefficient
μL	microliter(s)
μm	micrometer(s)
μmol	micromole(s)
τ_{90}	time to reach 90% of the steady-state response
ACD	acid citrate dextrose
AEAP3	<i>N</i> -(2-aminoethyl)-3-aminopropyltrimethoxysilane
AEMP3	(aminoethylaminomethyl)phenethyltrimethoxysilane
AFM	atomic force microscopy/microscope
Ag	silver
AgCl	silver chloride
AHAP3	<i>N</i> -(6-aminohexyl)aminopropyltrimethoxysilane
Al	aluminum
ANOVA	analysis of variance
APTES	aminopropyltriethoxysilane
aq	aqueous
Ar	argon gas
AS	Angeli's Salt; disodium diazen-1-ium-1,2,2,-triolate
atm	atmosphere(s)
B	boron
BTMOS	isobutyltrimethoxysilane
C18	octadecyl-
C8-TMOS	octyltrimethoxysilane
Ca^{2+}	calcium ion
cfu	colony forming unit(s)
Cl^-	chloride ion
cm	centimeter(s)

cm ²	square centimeter(s)
CO ₂	carbon dioxide gas
Cu	copper
Cu ²⁺	copper ion
CuZnSOD	copper-zinc superoxide dismutase
d	day(s)
DCP-OES	direct current plasma optical emission spectroscopy/spectrometer
DET3	<i>N</i> -[3-(trimethoxysilyl)propyl]diethylenetriamine
DTPA	diethylenetriamine-pentaacetic acid
e.g.	for example
<i>et al.</i>	and others
etc.	and so forth
ETMOS	ethyltrimethoxysilane
EtOH	ethanol
Fe	iron
fmol	femtomole(s)
g	gram(s)
GSH	glutathione
GOx	glucose oxidase
GSNO	<i>S</i> -nitrosoglutathione
h	hour(s)
H ⁺	hydrogen ion
H ₂ O	water
H ₂ O ₂	hydrogen peroxide
HCl	hydrochloric acid
HMDS	hexamethyldisilazane
HNO	nitroxyl
HPU	hydrophilic polyurethane
i.d.	inside diameter
i.e.	that is
IPA/NO	sodium-1-(isopropylamino)diazene-1-ium-1,2-diolate
<i>k</i>	kinetic coefficient
K	kelvin
K ⁺	potassium ion
KCl	potassium chloride
L	liter(s)

M	molar concentration
MeOH	methanol
mg	milligram(s)
MIMIC	micromolding in capillaries
min	minute(s)
mL	milliliter(s)
mM	millimolar concentration
mm	millimeter(s)
mmol	millimole(s)
Mn	manganese
Mn ^{III} TPPS	manganese(III) <i>meso</i> -tetrakis(4-sulfonatophenyl) porphyrinate
mol	mole(s)
MPTMS	mercaptopropyltrimethoxysilane
MTMOS	methyltrimethoxysilane
N	number of samples
<i>N</i> -	nitrogen bound
<i>N</i> -diazoniumdiolate	1-amino-substituted diazen-1-ium-1,2-diolate
NA	numerical aperture
N ₂	nitrogen gas
N ₂ O ₃	dinitrogen trioxide
Na ⁺	sodium ion
Na ₂ N ₂ O ₃	Angeli's Salt; disodium diazen-1-ium-1,2,2,-triolate
NaCl	sodium chloride
NHE	normal hydrogen electrode
NH ₄ ⁺	ammonium cation
nm	nanometer(s)
nM	nanomolar concentration
N ₂ O	nitrous oxide
NO	nitric oxide
NO ⁻	nitroxyl anion
NONOate	<i>N</i> -diazoniumdiolate moiety
NO ₂	nitrogen dioxide
NO ₂ ⁻	nitrite
NO ₃ ⁻	nitrate
o.d.	outside diameter
O ₂	oxygen gas

O ₃	ozone
OD _{λ=600}	optical density at 600 nm of wavelength
OEt	ethoxy group
OH ⁻	hydroxide ion
OMe	methoxy group
ONOO ⁻	peroxynitrite
<i>P. aeruginosa</i>	<i>Pseudomonas aeruginosa</i>
PAMAMOS	poly(amidoamine-organosilicon)
PBS	phosphate-buffered saline
PCO ₂	partial pressure of carbon dioxide
PDMS	poly(dimethylsiloxane)
PEG	poly(ethylene glycol)
pH	-log of proton concentration
pmol	picomole(s)
PO ₂	partial pressure of oxygen
ppb	part(s) per billion
ppm	part(s) per million
PRP	platelet enriched plasma
PVC	poly(vinyl chloride)
PVP	polyvinylpyrrolidone
R, R', R ₁ , R ₂	organic functional group
rpm	rotation(s) per minute
RSNO	<i>S</i> -nitrosothiol
Ru(dpp) ₃ ²⁺	ruthenium tris(4,7-diphenyl-1,10-phenanthroline)
<i>S</i> -	sulfur bound
s, sec	second(s)
SEM	scanning electron microscope
Si	silicon
SiN ₃	silicon nitride
SNAC	<i>S</i> -nitroso- <i>N</i> -acetyl-L-cysteine
SNARF-1	seminaphthorhodamine-1 carboxylate
t	time
TEOS	tetraethyl orthosilicate
Ti	titanium
TMOS	tetramethyl orthosilicate
TSB	tryptic soy broth

UV	ultraviolet
V	vanadium
V	volts
v:v	volume/volume
Vis	visible
vs.	versus
W	watt(s)
Zr	zirconium

Chapter 1:

Xerogel Technology in Sensor Applications

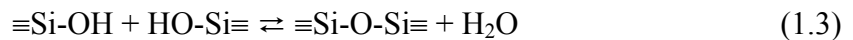
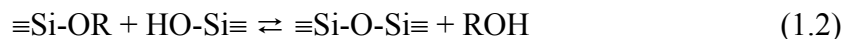
1.1. Xerogels

Sol-gel chemistry is a useful and versatile means of producing ceramic materials from simple metal or metalloid precursors. During the sol-gel process, three-dimensional networking transforms a stabilized colloidal suspension of particles, termed a sol, into a unified macroscopic molecule extending throughout the liquid bulk, termed a gel.¹ Subsequent removal of the solvent results in the formation of a solid ceramic material called a xerogel, the character and morphology of which can be widely controlled through changes over various aspects of the sol-gel process, including the starting reagents,^{2, 3} catalyst,^{4, 5} reaction environment,^{6, 7} and drying conditions utilized.^{8, 9} Because of the relatively mild reaction conditions and fine control allowed over the physical and chemical properties of the resultant material, sol-gel processing has been widely employed in analytical chemistry as a means of producing scaffolds and host matrices for chemical indicators and transducing molecules in the fabrication of chemical sensors.^{10, 11} My doctoral work has focused on strategies to best employ the unique capabilities of sol-gel processing for the design and development of coatings for biomedical sensors and devices.

1.1.1. Sol-Gel Chemistry

The history of sol-gel chemistry can be traced as far back as 1845 and the first reported synthesis of an alkoxysilane reagent, tetraethylorthosilicate ($\text{Si}(\text{OEt})_4$; TEOS) by Ebelmen.¹² Ebelmen observed that TEOS solutions exposed to the atmosphere would gel over time, and this has been the basis for all sol-gel chemistry that has followed. Sol-gel derived materials may be formed from a large number of metal alkoxide compounds, including the early transition metals (e.g., Ti, V, Zr) and Group IIIB metals such as B and Al. The most widely studied and developed sol-gel materials by far are silicate ceramics formed by reaction of alkoxysilane precursors.¹ Such materials are favored due to the inert nature of the final silicate network and relative simplicity of the chemistry of tetravalent Si compared to other transition metals. As nearly all sol-gel-derived sensors rely on silica-based materials,^{10, 11} the following discussion will focus exclusively on alkoxysilane-based xerogels.

Sol-gel chemistry is based on three reactions: the hydrolysis, and the alcohol and water condensation of alkoxysilane precursors into siloxane-bonded networks (Reactions 1.1-1.3, respectively).



All three reactions proceed simultaneously. Water and alkoxysilanes are immiscible and thus an alcohol co-solvent (e.g., ethanol or methanol) is typically employed to speed hydrolysis, though it is not always required. Alcohol produced as a byproduct of Reactions 1.1 and 1.2

has been found sufficient to homogenize the solution in some cases.¹³ Hydrolysis and condensation reactions are responsible for both initial colloid nucleation and subsequent networking and gel formation. The relative rates of the three reactions determine in large part the final properties of the xerogel material. Under conditions where hydrolysis rates exceed condensation, high concentrations of readily accessible reactive monomer in solution lead to the production of large silane aggregates and large particulate sols. The result upon drying is a bulky, porous, highly branched xerogel network. Conversely, if condensation rates far outstrip the reservoir of hydrolyzed monomers, weakly branched polymeric sols comprised of long interwoven siloxane chains are formed. Xerogels formed under these conditions tend to be denser and less porous materials.

The kinetics of hydrolysis and condensation, and thus the final properties of a homogenous xerogel material, are affected mainly by 3 reaction parameters: the water to silane molar ratio,⁶ the pH of the sol,⁴ and the steric accessibility of the alkoxy leaving group.¹⁴ A high water to silane ratio will speed hydrolysis reactions and retard rates of condensation. Conversely, bulky alkoxy functionalities or branched alkyl-side chains on silane precursors can sterically hinder hydrolysis, shifting the relative rates of reaction in favor of condensation. Sol pH provides a third avenue of control. Sol-gel reactions are typically catalyzed by the addition of acid or base, most often mineral acids (e.g., HCl) or ammonia, respectively.¹ As shown in Figure 1.1, the catalyst employed affects the mechanism of gel hydrolysis. In general, more acidic conditions favor condensation over hydrolysis resulting in the production of denser films. At $\text{pH} < 2$ where the polymerization rate is proportional to $[\text{H}]^+$, silica solubility is low and gel networks are formed of small particles with diameters $< 2 \text{ nm}$.¹⁵ From pH 2-6, gelation rates increase with increasing

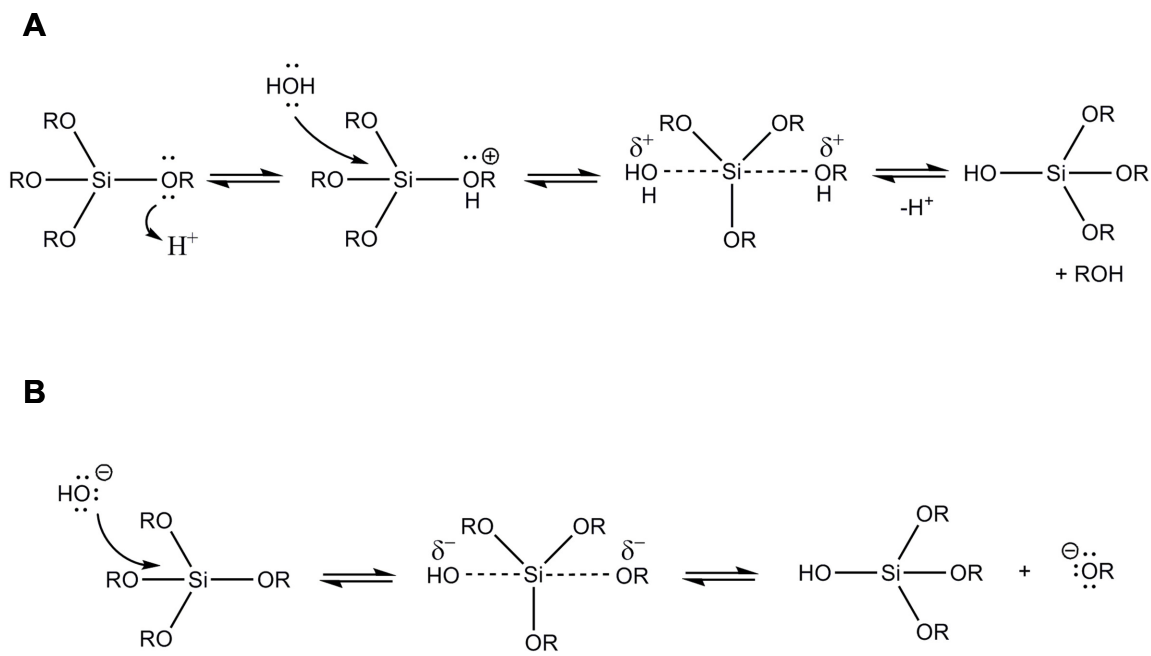


Figure 1.1. Mechanism of sol-gel precursor hydrolysis under (A) acid-catalyzed and (B) base-catalyzed conditions.

[OH]⁻ and particles grow by the preferential condensation of highly condensed oligomers with smaller neutral species to diameters of ~2-4 nm. At pH > 7, condensed species are largely ionized, leading to greatly increased silica solubility and charge-charge repulsion between particles. Particles grow via Ostwald ripening and the dissolution of smaller particles and deposition of silica onto larger particles.¹ Silica solubility (and hence maximum particle diameter) is controlled largely by temperature. Particles can reach sizes >100 nm.¹⁵ In this manner, stable sols containing large diameter silica nanoparticles may be created in high pH conditions.

1.1.2. Xerogel Properties

Xerogels have a number of physical and chemical properties that prove useful for the production of chemical sensors and biosensors. Xerogels formed via the reaction of tetraalkoxysilane precursors such as TEOS or tetramethyl orthosilicate (TMOS) are chemically inert, glass-like materials with a high degree of mechanical and chemical stability. Such films are generally porous, and the pore-size distribution is easily controlled via the reaction conditions employed (*vide supra*). Xerogels often exhibit useful optical properties such as high refractive indices and transparency to visible light.¹⁶ They adhere well to glass and silica substrates and may form covalent linkages to terminal silanol groups on the glass surface.^{17, 18} Xerogels may also be produced at low temperatures, allowing for the incorporation of organic molecules and polymers and sustaining the activity of doped enzymes and biomolecules.¹⁹

Perhaps the greatest overall advantage of sol-gel chemistry is the extreme versatility and ease of xerogel network modification. The structure of a sol-gel derived material can vary greatly depending on the processing and drying conditions employed. Thin films, fibers,

monoliths, and powders may all be formed.^{3, 20} Extremely porous aerogels having solid volume fractions as low as 1% may be created under supercritical-drying conditions whereby gel shrinkage due to capillary pressure from the liquid/vapor interface is avoided.²¹ Each material form has advantages. Thin films may be applied to a variety of sensing platforms and offer short analyte diffusion path lengths through the material.¹⁰ Bulk monoliths may be molded to a desired form and offer longer optical path lengths for spectroscopic measurements.²² Powders and aerogels are not typically employed in analytical sensing applications, but their high surface areas are of practical use in catalysis.^{21, 23} By exerting proper control over sol-gel processing conditions, the final material is readily tailored to a desired application.

Another common avenue of xerogel modification is through the use of organically modified silane precursors, wherein one or more alkoxy groups of a silane is replaced with a desired organic side chain. Incorporating organic character into the silicate network can produce fundamental changes in the properties of the xerogel. For example, Rao et al. reported increased hydrophobicity of aerogels formed from alkylalkoxysilane precursors with an increasing number of alkyl units in the organic side chain.² Organoalkoxysilanes allow numerous functionalities (e.g., amines, thiols, epoxides) to be covalently incorporated as pendant additions to the siloxane backbone.^{3, 20} The result can affect not only bulk physical properties of the xerogel material,^{16, 24} but also provides a means of including specific localized reaction sites in the xerogel microenvironment. Thus appropriate organoalkoxysilanes may be employed for sensor applications to create more open or lipophilic sensor membranes or provide sites for direct covalent attachment of chemical indicators.

1.2. Xerogel-Based Sensors

1.2.1. Optical Xerogel Sensors

The chemical stability, porosity, and optically transparency of xerogels make them nearly ideal as a host matrix for optical dyes and indicators, and it is in this sensing format that xerogels have been most often used in sensing applications. Since Avnir and co-workers first reported the incorporation of Rhodamine 6G, a fluorescent indicator molecule, in a xerogel matrix in 1984,²⁵ xerogel-based optical sensing has advanced rapidly. Three general methods may be employed to immobilize fluorophores or colorimetric indicators in a host xerogel: impregnation, covalent binding, or doping.^{26, 27} Impregnation involves simple physical or chemical adsorption (e.g., electrostatic interaction) of optical indicator species onto the glass surface of a preformed xerogel. Dye/matrix association is generally short-lived in these cases, making impregnation typically unsuitable for most sensing applications.²⁸ Covalent binding of an indicator to the xerogel matrix via specific organic functionalities allows permanent immobilization of dyes in a sensor and ends leaching concerns.^{29, 30} Unfortunately, covalent binding also has a tendency to lengthen sensor response times and decrease overall sensitivity due to reductions in the bound fluorophore's degrees of freedom and corresponding fluorescence intensity.³¹ Doping strategies, wherein optical indicators and dyes are incorporated into the sol prior to gel formation, are the most widely employed means of creating xerogel optical sensors.²⁸ After gel formation and curing procedures, the dyes become physically entrapped in the cross-linked xerogel matrix. As such, indicator retention in the xerogel is enhanced while fluorophore rotational freedom is maintained. While dye leaching can still pose a problem during long term exposure of

indicator-doped xerogels to solution,^{32, 33} numerous xerogel-based optical sensors with rapid response times and high signal stability have been reported.^{11, 26}

Optical sensors may be formed from indicator-doped xerogel materials in a number of ways. The most common strategy is deposition of a thin xerogel film onto the surface of an optical fiber or waveguide material.²⁶ Numerous studies have utilized xerogel thin films in this manner to create optical sensors using both extrinsic and intrinsic sensing configurations (Figure 1.2).¹¹ For extrinsic optical sensor configurations (Fig 1.2A), light is guided to and from the indicator via optical fibers or waveguides. The xerogel matrix is used strictly as a scaffold or support for the indicator species. For example, Li et al. recently described a wide-range optical pH sensor formed by doping a novel pH indicator, 10-(4-aminophenyl)-5,15-dimesitylcorrole, in a TEOS xerogel membrane.³⁴ The indicator-doped-xerogel material was coated onto glass slides immersed in a flow-cell chamber. A bifurcated optical fiber was used to shuttle excitation light and the resultant fluorescent emission to and from the sample. Conversely, intrinsic sensing configurations (Fig 1.2B) utilize the xerogel coating itself as an integral part of the sensor design. The refractive properties of the xerogel are utilized to guide exciting and emitted light. Interrogation of an encapsulated fluorescent indicator is often accomplished via the penetration of an evanescent wave from the light-guide core to the doped-xerogel cladding material. For example, O’Keeffe and co-workers described the fabrication of a LED-driven O₂ sensor based on the quenching of Ru^{II}-tris(4,7-diphenyl-1,10-phenanthroline) (Ru(dpp)₃²⁺) encapsulated in xerogel surrounding a de-clad multi-mode optical fiber.³⁵ A subsequent study illustrated that the observed fluorescence-quenching behavior could be tailored for specific O₂ concentrations and environments through manipulation of the xerogel cladding properties.³⁶ Intrinsic configurations have a number

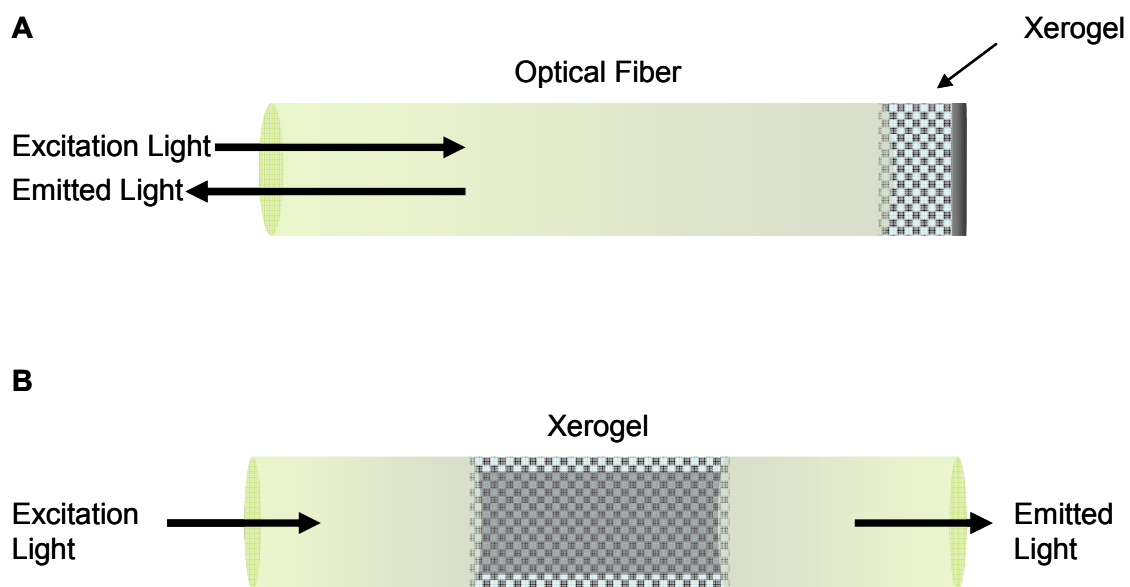


Figure 1.2. General (A) extrinsic and (B) intrinsic xerogel optical sensor configurations.

of benefits over extrinsic sensing schemes. As the interrogating light remains guided in the material, optical transparency of the surrounding sample is not required.³⁷ Additionally, the integrated nature of the light propagation and sensing elements lends itself to easy miniaturization. Both of these properties are important for sensors that are to be used in biological environments.¹¹

As mentioned above, the high level of control allowed over xerogel properties makes them useful for imparting selective analyte permeability to sensor membranes. This versatility makes xerogels particularly useful as sensor membranes for dissolved gas analytes.¹¹ By tuning the hydrophobicity and wettability of the xerogel network through the inclusion of lipophilic alkyl side chains on the sol-gel precursors employed, selectivity for dissolved gas species can be enhanced over other interfering species in solution. Bright and co-workers have examined the effect of xerogel network modification on luminophore-doped xerogel O₂ sensors extensively.³⁸⁻⁴⁰ Tao et al. characterized the effect of alkyl side-chain length on sensitivity using pin-printed microarrays of Ru(dpp)₃²⁺-doped xerogels formed from TMOS and TEOS precursors and organoalkoxysilanes with alkyl side-chains ranging from 1 to 12 carbon units.⁴⁰ Sensitivity was found to follow O₂ diffusion coefficients and solubility in the xerogel matrix. Maximum sensitivity was achieved with an 8-carbon chain (C8-TMOS). A subsequent study by Tang et al. demonstrated that the extent of hydrolysis and condensation of C8-TMOS/TMOS sols, as determined by sol aging time prior to casting, also played a major role in determining film porosity and final O₂ sensitivity.³⁸ Bukowski et al. found that even greater O₂ sensitivities could be achieved using hydrophobic fluorinated alkylalkoxysilane precursors in Ru(dpp)₃²⁺-doped xerogels.³⁹ Clearly, modification of

optical membrane properties through sol-gel chemistry provides a powerful means of enhancing sensor performance.

1.2.2. Electrochemical Xerogel Sensors

Xerogels have also been employed as electrochemical sensing platforms.⁴¹ Similar to optical sensing formats, xerogels in electrochemical sensors are used in two basic configurations. In the most basic format, xerogels are simply coated as thin films onto the surface of conventional macro or microelectrodes. These films act as scaffolds and membranes in a similar manner to extrinsic optical sensors. An alternate strategy is to disperse a conductive material (e.g., carbon powder,⁴² or gold⁴³) throughout the sol prior to curing of the gel. When the gel is subsequently dried in monolith form, a composite electrode is formed. Though their fabrication is more complicated, sol-gel derived composite electrodes have a number of benefits over the more simply prepared coated-metallic electrodes. The monoliths provide a homogenous structure that may be molded to a desired form. Additionally, the conductive surface area of the porous composite material tends to be large and fresh surface can be regenerated through simple polishing.⁴⁴

Xerogels provide many of the same benefits discussed for optical sensors when used in electrochemical sensors. For example, proper choice of sol-gel processing conditions and alkoxy silane precursors can be utilized to control the wettability and gas permeability of composite ceramic carbon electrodes.⁴⁵ Xerogels can also provide a number of benefits more tailored to the specific needs of electrochemical sensors. By incorporating the correct functionalities into the xerogel host network, preconcentration of a target analyte may be accomplished, resulting in enhanced sensitivity. Preadsorption of ephedrine onto C18-modified gels⁴⁶ or metal ion complexation with covalently bound thiols⁴⁷ or amines⁴⁸ are

each examples of xerogel-based preconcentration strategies. In a similar manner, permselective membranes for selective screening of charged analytes from solution may also be formed by the incorporation of suitable $-\text{NH}_3^+$ or $-\text{COO}^-$ groups in the xerogel.^{49, 50} Xerogel coatings and composite electrodes also lend themselves well to electrocatalysis. Organic or organometallic catalytic sites may be covalently bound or doped into the material to alter electron transfer kinetics and reduce necessary overpotentials for certain analytes. For example, Wang et al. described a methyltrimethoxysilane (MTMOS)-based composite electrode system containing silicomolybdic acid for the catalytic reduction and detection of nitrite.⁵¹ Tsionsky et al. used a similar cobalt porphyrin-doped xerogel composite electrode for the detection of sulfur dioxide, carbon dioxide, and O_2 .⁵² Xerogel-doping strategies are not limited to amperometric sensing platforms. Numerous potentiometric xerogel sensors containing covalently bound or physically doped ionophores for the detection of ionic species (e.g., chloride^{53, 54} and perchlorate⁵⁵ anions) have been described.

One of the most beneficial attributes of xerogel-based electrochemical membranes and electrodes is the controllable porosity of the xerogel material. Small redox-active analytes retain large diffusion rates in the open porous silicate network of TEOS and TMOS-based films. High sensitivity and rapid response at xerogel-modified electrodes is thus maintained. At the same time, pore size distribution may be tuned to better retain larger signal transduction molecules or electrochemical mediators. This property makes xerogel-modified electrodes particularly well-suited for fabricating enzyme-based biosensors, wherein the reaction between an immobilized enzyme and target substrate results in the production of a redox-active species that can be monitored amperometrically.⁴⁴ Bulky enzymes are easily retained within the confines of a doped-xerogel network, while smaller substrates and

reaction products are free to diffuse throughout the xerogel scaffold. Ellerby and co-workers first pioneered the fabrication of xerogel-based biosensors by reporting a technique to retain the activity of enzymes copper-zinc superoxide dismutase (CuZnSOD), cytochrome c, and myoglobin in a sol by returning the sol to neutral pH via the addition of buffer solution after acid-catalysis procedures of TMOS xerogels.⁵⁶ A report of glucose oxidase (GOx) immobilization using the same technique soon followed,⁵⁷ thus creating the basis for the design of future amperometric glucose biosensors for continuous subcutaneous glucose monitoring – a goal steadily pursued for the last 15 years.⁵⁸ Sanchez and co-workers were the first to monitor GOx activity amperometrically in TMOS-coated electrodes via the electro-oxidation of a ferrocene mediator.⁵⁹ Narang et al. later reported a popular “sandwich” configuration where GOx was immobilized between two TEOS xerogel layers on the surface of indium tin oxide electrodes.⁶⁰ Glucose was monitored via amperometric response to hydrogen peroxide (H₂O₂), formed during the enzymatic transformation of glucose to gluconic acid. This general scheme has since been utilized multiple times in subsequent reports of xerogel-based glucose sensors and other enzyme-doped biosensors.⁴⁴

1.3. Sensor Biocompatibility

Regardless of the performance of xerogel-based sensors in the laboratory, the environment in which a sensor is employed can have equally as large an effect on the sensor’s performance as the strategies used in its fabrication. When a sensor is to be used in the body, for example, the physiological environment often complicates sensor operation in many important ways.⁶¹ The term “biocompatibility” is often used to describe how well an indwelling sensor is integrated into and functions within biological environments.^{62, 63} With

proper choice of silane precursor molecules and selective incorporation of nitric oxide (NO)-donor moieties into xerogel materials, strategies have been developed to increase xerogel biocompatibility.

1.3.1. Sensor Biofouling

When a sensor is inserted into blood or tissue, a cascade of events begin that ultimately affect sensor performance.⁶¹ Blood-contacting devices are quickly coated with plasma proteins, and platelets that begin to activate and adhere to the surface of the sensor.⁶⁴ Further aggregation of platelets and the formation of a polymeric fibrin mesh throughout the mass of cells results in a blood clot, or thrombus. Thrombus formation is a serious impediment to the function of intravascular sensors as the sensor is blocked from the bulk blood environment and analytes of interest (Figure 1.3A).⁶⁵ In worst case scenarios, the mass of platelets and cells can lead to severe health problems such as vessel occlusion. Even if complete thrombus formation is avoided, the metabolic processes of adhered cells and platelets skew localized analyte concentrations and negatively impact the accuracy of sensor measurements.^{64, 66}

While the threat of thrombus formation is less of a factor for subcutaneous sensors, tissue-contacting devices fall victim to other problems. The body's natural response to foreign materials results in the sequestration of tissue-implanted biomaterials within a dense avascular collagen capsule, thereby limiting interaction of the device with the surrounding environment (Figure 1.3B).^{67, 68} Additionally, the presence of inflammatory cells and macrophages recruited to the wound site skew localized analyte concentrations in a similar manner as platelet metabolism affects intravascular sensors.⁶⁹ With all implanted materials, the risk that bacteria adherent to the sensor upon implantation may later result in infection is

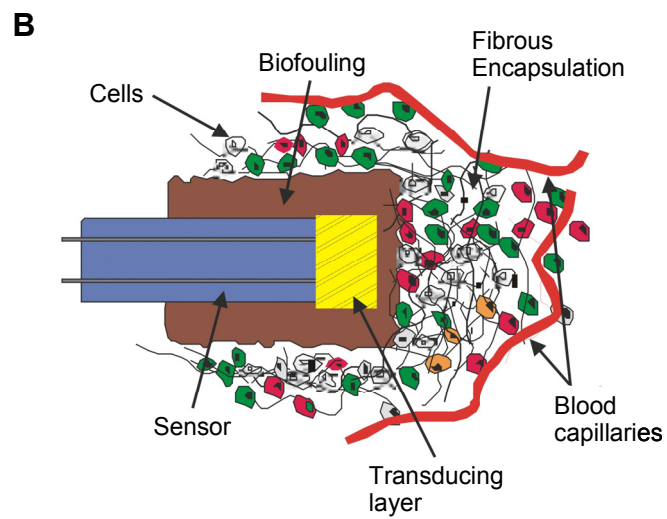
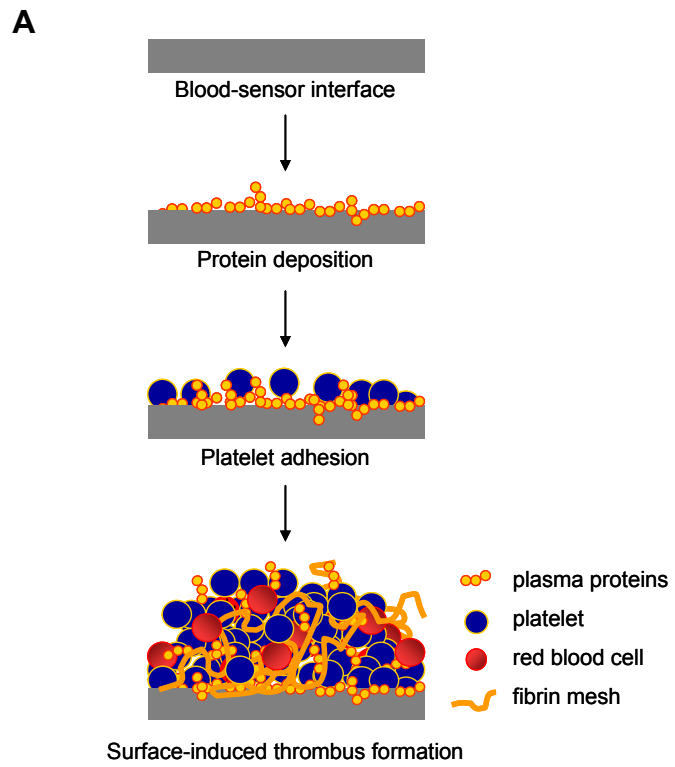


Figure 1.3. Biofouling of sensor surfaces upon (A) intravascular or (B) subcutaneous implantation.

great.⁷⁰ Though stringent sterilization procedures are employed, implant-associated infection remains a serious problem. Indwelling medical devices are responsible for >1,000,000 hospital-acquired infections per year in the U.S. alone.⁷¹ The problem is further exacerbated by the tendency of many surface adherent bacteria to form protective exopolysaccharide layers called biofilms.⁷⁰ Biofilms surrounding bacteria act to keep nutrients in and antibiotics out, significantly limiting treatment options if an infection does occur. In many cases, ultimate removal of the sensor or biomedical implant is required.⁷¹

1.3.2. Nitric Oxide-Releasing Xerogels

Nitric oxide (NO), a diatomic free radical produced endogenously by heme proteins known as NO synthases,⁷² may provide a potentially universal solution to several of the previously mentioned biofouling issues. Nitric oxide plays myriad roles in the body and functions in processes ranging from vasodilation to neurotransmission.^{72, 73} Most importantly with regards to enhancing sensor biocompatibility, NO is instrumental in the processes governing platelet activation,⁷⁴ wound-healing,⁷⁵ angiogenesis,^{76, 77} and body's immune response to foreign pathogens.⁷⁸ By modifying polymeric sensor coatings to release NO, significant antithrombotic,^{63, 79} antibacterial,⁸⁰ and tissue-integration⁸¹ benefits may be achieved.

Sol-gel chemistry is easily tailored to allow the creation of NO-releasing xerogel coatings. These materials have traditionally been formed by covalently incorporating NO-donor functionalities termed *N*-diazeniumdiolates (NONOates) into the siloxane polymer backbone. Zwitterionic NONOates are formed by exposure of secondary amines to high pressures (e.g., 5 atm) of NO under basic conditions.⁸² The amine reversibly binds two molecules of NO into a stable NONOate structure (Figure 1.4) that essentially stores or

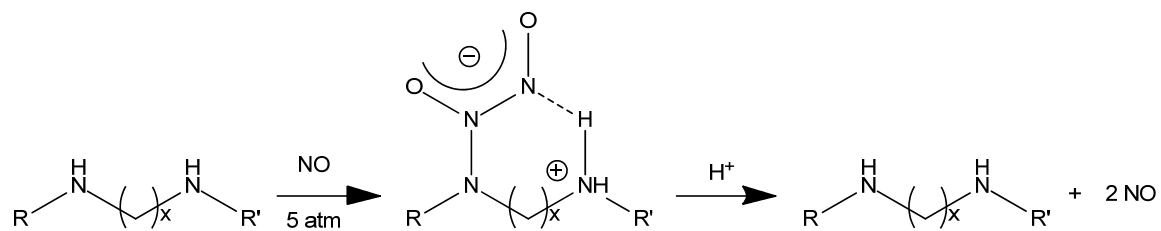
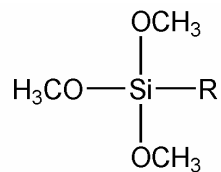


Figure 1.4. Mechanism of *N*-diazeniumdiolate formation and subsequent NO release.

transports NO until exposed to a proton source (e.g., water). Reprotonation of the parent amine results in NONOate decomposition and the release of two equivalents of NO. Nablo et al. first reported the synthesis of a NO-releasing xerogel coating by co-condensing (3-trimethoxysilylpropyl)diethylenetriamine (DET3) with isobutyltrimethoxysilane (BTMOS) to form a stable xerogel film.⁸³ After curing and drying of the gel, exposure of the pendant triamine side-chain of DET3 to 5 atm NO resulted in NONOate formation. The resulting films released NO continuously for up to 24 h. A number of NONOate-modified xerogels have since been reported by our lab utilizing a variety of aminoalkoxysilanes and alkylalkoxysilane precursors (Figure 1.5).⁸⁴⁻⁸⁸ Of note, amine-terminated xerogel films formed from 100% aminoalkoxysilanes are not feasible due to poor stability during immersion in solution, likely due to charge-charge repulsion of the diamine and triamine side chains.⁸⁸ Incorporation of inert alkylalkoxysilanes in the xerogel network was found to drastically increase stability. As such, NONOate-modified films were generally formed from sols limited to $\leq 40\%$ aminoalkoxysilane (v:v total silane). Under these constraints, xerogel films capable of generating NO fluxes $>0.5 \text{ pmol cm}^{-2} \text{ s}^{-1}$ for up to 72 h at physiological temperatures have been reported.⁸¹

The biocompatibility benefits of NO-releasing xerogel coatings have been thoroughly examined. Robbins et al. reported on the efficacy of *N*-diazoniumdiolated (aminoethylaminomethylphenethyl)trimethoxysilane (AEMP3)/MTMOS xerogel films and microarrays for inhibiting platelet activation and adhesion onto glass substrates.⁸⁶ Nitric oxide fluxes as low as $0.4 \text{ pmol cm}^{-2} \text{ s}^{-1}$ from micropatterned arrays of raised xerogel lines were capable of reducing the thrombogenicity of glass surfaces versus controls during exposure to platelet rich porcine plasma. Nablo et al. examined the antibacterial effects of

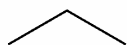


ALKYLALKOXYSILANES (R group)

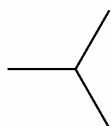
methyltrimethoxysilane
(MTMOS)



ethyltrimethoxysilane
(ETMOS)

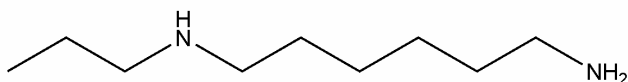


isobutyltrimethoxysilane
(BTMOS)

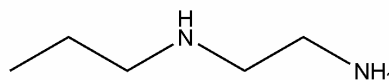


AMINOALKOXYSILANES (R group)

N-(6-aminoethyl)aminopropyltrimethoxysilane
(AHAP3)



N-(2-aminoethyl)-3-aminopropyltrimethoxysilane
(AEAP3)



(Aminoethylaminomethyl)phenethyltrimethoxysilane
(AEMP3)

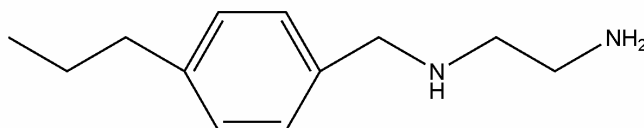


Figure 1.5. Alkylalkoxysilanes and aminoalkoxysilanes used in production of *N*-diazoniumdiolated NO-releasing xerogels.

NO-releasing aminohexylaminopropyltrimethoxysilane (AHAP3)/BTMOS xerogel films on stainless steel substrates.⁸⁷ Significant reductions of adhesion by three medically relevant bacterial species (i.e., *Pseudomonas aeruginosa*, *Staphylococcus aureus*, and *Staphylococcus epidermidis*) on NO-releasing films versus controls were observed during immersion in concentrated bacterial cell suspensions. Subsequent studies have confirmed that the antibacterial benefits are maintained with the presence of a protective polyvinylchloride (PVC) overlayer,⁸⁹ under flow-cell conditions,⁹⁰ and in vivo (rat model.)⁹¹ Benefits to overall tissue integration imparted by NO-releasing xerogels have also been examined by Hetrick and co-workers.⁸¹ During 6 week implantation in a rat model, NO-releasing AHAP3/BTMOS xerogel-coated silicone rubber demonstrated decreased fibrous capsule formation and enhanced vascularization relative to controls, indicating that NO is useful for minimizing the detrimental sequestration of implant materials by the natural foreign body response.

1.3.3. NO-Releasing Xerogel Sensors

While significant biocompatibility benefits for implanted materials may be achieved via NONOate-modified xerogel coatings, specific drawbacks associated with their use in sensor applications exist. Exposure to high pressures of NO (necessary for NONOate modification) has been found to dramatically increase xerogel cross-linking and decrease porosity.⁹² As such, diffusion of analytes into NO-releasing xerogel membranes is reduced, leading to lengthened sensor response times and decreased overall sensitivity. When attempting to utilize NONOate modified xerogel coatings as electrochemical sensor membranes, sensor design strategies beyond simple xerogel coating of the electrode must be employed. Using a multilayer glucose biosensor format, Shin et al. doped NO-releasing

AHAP3/MTMOS xerogel particles into a polyurethane overlayer surrounding GOx/MTMOS at the surface of an electrode. In this manner, the benefits of NO-release could be achieved while maintaining glucose diffusion through the polyurethane to the underlying enzyme layer. Oh et al. used a similar multilayer format using micropatterned arrays of AEMP3/MTMOS xerogel lines to create a NO-releasing glucose microsensor.⁹³ In this respect, bare regions of GOx/MTMOS-modified electrode between NO-releasing microstructures were retained. Polymer-doping strategies have also been employed to improve analyte diffusion through NO-releasing xerogel materials. Marxer et al. utilized hydrophilic polyurethane (HPU) in conjunction with AHAP3 and ethyltrimethoxysilane (ETMOS) to create oxygen-permeable hybrid films for the creation of a NO-releasing amperometric oxygen sensor.⁸⁵ Schoenfisch et al. reported a similar strategy using water-soluble poly(vinylpyrrolidone) (PVP) in AHAP3/BTMOS films to create hydrophilic pockets in a NO-releasing glucose sensor membrane.⁹⁴

While the previous strategies may be used to create functional NO-releasing electrochemical sensors, the common drawback of these membrane modification procedures is a reduced overall volume of NO-generating material. Attainable NO flux intensities and durations are thus greatly reduced. Optical-sensing formats have not been previously utilized in the fabrication of NO-releasing xerogel sensors. The dense cross-linking of NONOate modified xerogels may be less problematic for optical sensing configurations, as analyte or enzyme-product transport to an underlying electrode surface is not required. While solution permeability is reduced in NONOate modified xerogels, visible light propagation through the transparent material should remain unhindered. Optical sensing strategies should allow the use of NONOate modified xerogels without requiring extensive microfabrication or doping

procedures, thereby increasing the amount of NO attainable from the sensor. Evaluating NONOate-modified xerogels films as optical sensor membranes was one goal of my doctoral work.

1.4. S-Nitrosothiol-Modified Xerogels

Alternative NO-donor functionalities may also prove useful for improving the biocompatibility and function of NO-releasing sensors. *S*-nitrosothiols (RSNOs) are one class of NO donors that have significant potential in this area. *S*-nitrosothiols are readily formed by reaction of thiols with reactive nitrogen oxide species (e.g., N_2O_3 , HNO_2).⁹⁵ The solution phase antimicrobial^{96, 97} and antithrombotic^{98, 99} effects of small-molecule RSNOs have been well characterized. For example, Langford et al. reported on the efficacy of *S*-nitrosoglutathione (GSNO) treatment of patients undergoing percutaneous transluminal coronary angioplasty.⁹⁸ A significant reduction of platelet activation in the GSNO-treated patients was observed with no measurable increase in blood pressure. While NO production from RSNOs is not as straightforward as the proton-initiated decomposition of NONOates, a number of mechanisms have been described triggering NO release from RSNOs. These reactions include thermal and light-initiated homolytic cleavage of the S-N bond,¹⁰⁰ catalytic reaction with Cu^+ ,¹⁰¹ or a two-step mechanism with other thiols through a nitroxyl (HNO) intermediate (Figure 1.6).¹⁰² Direct transnitrosation reactions between RSNOs and other thiols have also been described,¹⁰³ indicating that the production of an NO intermediate may not be required to achieve some of the observed beneficial physiological effects of RSNOs.

At present, reports on RSNO-modified materials as coatings for sensors and biomedical devices¹⁰⁴⁻¹⁰⁶ have been limited. Frost and co-workers described the production

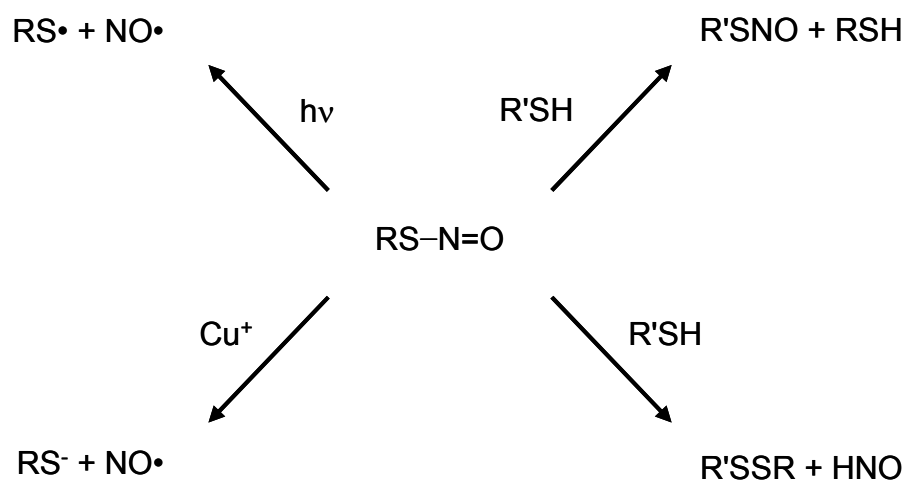


Figure 1.6. Common *S*-nitrosothiol decomposition pathways.

of photo-triggered NO-releasing films by encapsulating RSNO-modified silica particles in tri-layer polymer films.¹⁰⁶ These films were capable of generating significant NO fluxes ($\geq 1.7 \text{ pmol cm}^{-2} \text{ s}^{-1}$) for up to 12 h under bright illumination. Although not yet demonstrated, the incorporation of RSNOs into xerogel films should be readily achieved in an analogous manner to NONOate-modified xerogels via the use of mercaptoalkoxysilane precursors. Hydrolysis and condensation of the thiol-terminated alkoxysilane precursors should allow the covalent binding of pendant thiol moieties into the siloxane backbone of the xerogel, which may be subsequently nitrosated via reaction with acidified nitrite.¹⁰⁷ It is anticipated that these materials may provide a means of overcoming some of the short-comings of NONOate-modified xerogels. Charge-charge repulsion effects of RSNO-modified films should be minimal compared to *N*-diazoniumdiolated films, leading to increased stability of the material in solution at greater NO donor loading conditions. Thus enhanced NO flux and duration may be achievable. The synthesis and characterization of RSNO-modified xerogel films as an alternative strategy for creating NO-releasing xerogels was a second goal of my doctoral research.

1.5. Nitroxyl Sensing via Aminoalkoxysilane Xerogels

The dense, cross-linked nature of aminoalkoxysilane-derived xerogels need not always be viewed as problematic. Despite the hinderance low permeability may present for the creation of certain sensors (e.g., NO-releasing glucose sensors), the same property may be beneficial for the fabrication of other sensors. For example, Shin and co-workers used the low porosity of *N*-diazoniumdiolated AEMP3/MTMOS xerogels to fabricate an amperometric NO sensor with enhanced NO sensitivity compared to previously reported

sensors.¹⁰⁸ Sensors fabricated with aminoalkoxysilane derived membranes showed $\sim 10^6$ -fold increased selectivity for NO over nitrite, ascorbic acid, uric acid, and acetaminophen, common interfering species in biological environments. Likewise, whereas the low oxygen permeability of aminoalkoxysilane-derived xerogels presented a problem for Marxer's development of a NO-releasing amperometric oxygen sensor,⁸⁵ the same property may be beneficial for applications where an anaerobic interior environment of the xerogel is desired.

One application where decreased oxygen permeability may be a benefit is in the production of optical sensor membranes for the detection of nitroxyl (HNO), a one-electron-reduced congener of NO.¹⁰⁹ Despite their similarities, HNO's chemistry and reactivity is distinct from NO,¹¹⁰⁻¹¹³ and the potential benefits of its pharmaceutical application are just beginning to be elucidated.¹¹⁴ For example, Pagliaro and co-workers demonstrated that exposure of cardiac muscle to HNO prior to ischemic injury, wherein the heart is deprived of oxygen for extended periods, decreased both tissue damage and infarct size and increased post-ischemic contractility.¹¹⁵ Similarly, Paolocci et al. examined the effects of HNO in dogs with failing hearts.¹¹⁶ Treatment with HNO resulted in both enhanced left ventricular contractility and selective venodilation, in effect making the heart beat more strongly without increasing its overall rate, a benefit that makes HNO a strong candidate for the treatment of congestive heart failure. Nitroxyl has also been shown to be a key reactive product in the targeted inhibition of aldehyde dehydrogenase by the antialcoholism drug cyanamide,^{117, 118} leading Nagasawa and co-workers to develop a series of HNO donors and prodrugs for the treatment of alcohol abuse.¹¹⁹⁻¹²¹ Such applications may be indicative of a general role for HNO in targeted enzyme inhibition through reaction with active-site thiol-terminated residues.

Despite the potential pharmaceutical benefits of HNO, research related to HNO chemistry and the development of HNO-donor compounds lags significantly behind that of NO.^{122, 123} Much of the difficulty of working with HNO lies in its high reactivity and problems associated with its detection.¹²⁴ While highly specialized spectroscopic techniques may be used to detect HNO directly,¹²⁵ generally, indirect means of screening for HNO (e.g., absorbance shifts associated with reductive nitrosylation of heme proteins)¹²⁶ have been employed. These absorbance techniques are generally non-quantitative as the resulting metal-NO complexes are unstable in the presence of oxygen. By encapsulating HNO sensitive heme proteins (or their simplified porphyrin analogs^{127, 128}) in the anaerobic interior of aminoalkoxysilane xerogel membranes, it may become possible to stabilize the nitrosylated complex and enable quantitative detection of HNO. A third focus of my doctoral research involved the synthesis of HNO-sensing aminoalkoxysilane-derived xerogel films suitable for quantitative detection of HNO in an optical sensor format.

1.6. Summary of Dissertation Research

My doctoral research has focused on maximizing the potential of sol-gel-derived materials for use in the creation of biomedical sensors and more biocompatible interfaces. This work has involved both modifying the core structure of the gel with new NO-donor functionalities to enhance the integration of sensors into surrounding blood and tissue, and also developing novel techniques and sensing platforms to best utilize the unique properties of previously developed aminoalkoxysilane-derived xerogel films. The specific aims of my research included:

- 1) the design, fabrication, and characterization of a optical fiber-based NO-releasing pH sensor using NONOate-modified xerogel films;
- 2) the evaluation of NO-release and antithrombogenic benefits achievable using NONOate-modified xerogels in an optical sensor format;
- 3) the synthesis of RSNO-modified films via nitrosation of mercaptoalkoxysilane-derived xerogels;
- 4) the evaluation of the NO-release capability, solution stability, and antibacterial and antithrombogenic properties of RSNO-modified xerogels;
- 5) the fabrication and characterization of aminoalkoxysilane-based HNO-sensing films for optical quantification of HNO;
- 6) the optimization of HNO-sensing xerogel film properties for application in a 96-well microtitre plate optical sensor format.

The goal of Chapter 1 was to provide a brief overview of sol-gel chemistry and the versatility and benefits xerogels provide in sensor development. Chapter 2 will focus on the fabrication of a NO-releasing optical pH sensor and the improvements in sensor response and NO release that can be achieved by using NONOate-modified xerogels in optical sensing formats versus previously described electrochemical designs.¹²⁹ Chapter 3 focuses on the synthesis of novel RSNO-modified xerogel coatings with improved stability and extended durations of NO generation compared to NONOate modified films. Finally, Chapter 4 discusses a novel application of aminoalkoxysilane-derived xerogels in the development of HNO-sensing optical films.¹³⁰

1.7. References

- (1) Brinker, C. J.; Scherer, G. W. *Sol-Gel Science*. Academic Press, Inc.: New York, 1990.
- (2) Rao, A. V.; Kulkarni, M. M.; Amalnerkar, D. P.; Seth, T. "Surface chemical modification of silica aerogels using various alkyl-alkoxy/chloro silanes." *Applied Surface Science* **2003**, *206*, 262-270.
- (3) Collinson, M. M. "Recent trends in analytical applications of organically modified silicate materials." *Trends in Analytical Chemistry* **2002**, *21*, 30-38.
- (4) Elferink, W. J.; Nair, B. N.; DeVos, R. M.; Keizer, K.; Verweij, H. "Sol-gel synthesis and characterization of microporous silica membranes .2. Tailor-making porosity." *Journal of Colloid and Interface Science* **1996**, *180*, 127-134.
- (5) Liu, Y.; Zhang, L. Y.; Yao, X.; Xu, C. N. "Development of porous silica thick films by a new base-catalyzed sol-gel route." *Materials Letters* **2001**, *49*, 102-107.
- (6) Wang, J.; Park, D. S.; Pamidi, P. V. A. "Tailoring the macroporosity and performance of sol-gel derived carbon composite glucose sensors." *Journal of Electroanalytical Chemistry* **1997**, *434*, 185-189.
- (7) Zarzycki, J. "Sonogels." *Heterogeneous Chemistry Reviews* **1994**, *1*, 243-253.
- (8) Matsuda, A.; Matsuno, Y.; Tatsumisago, M.; Minami, T. "Changes in porosity and amounts of adsorbed water in sol-gel derived porous silica films with heat treatment." *Journal of Sol-Gel Science and Technology* **2001**, *20*, 129-134.
- (9) Takemori, M. "Low temperature synthesis of a silica-based glass-like adherent film by a sol-gel method." *Journal of Materials Science Letters* **2001**, *20*, 151-154.
- (10) Collinson, M. M.; Howells, A. R. "Sol-gels and electrochemistry: Research at the intersection." *Analytical Chemistry* **2000**, *72*, 702A-709A.
- (11) Jeronimo, P. C. A.; Araujo, A. N.; Montenegro, M. "Optical sensors and biosensors based on sol-gel films." *Talanta* **2007**, *72*, 13-27.
- (12) Ebelmen, M. *Annales de Chimie et de Physique* **1845**, *15*, 319.
- (13) Avnir, D.; Kaufman, V. R. "Alcohol is an unnecessary additive in the silicon alkoxide sol-gel process." *Journal of Non-Crystalline Solids* **1987**, *92*, 180-182.

- (14) Chambers, R. C.; Jones, W. E.; Haruvy, Y.; Webber, S. E.; Fox, M. A. "Influence of steric effects on the kinetics of ethyltrimethoxysilane hydrolysis in a fast sol-gel system." *Chemistry of Materials* **1993**, *5*, 1481-1486.
- (15) Iler, R. K. *The Chemistry of Silica*. Wiley: New York, 1979.
- (16) Sanchez, C.; Lebeau, B.; Chaput, F.; Boilot, J. P. "Optical properties of functional hybrid organic-inorganic nanocomposites." *Advanced Materials* **2003**, *15*, 1969-1994.
- (17) Lebeau, B.; Fowler, C. E.; Mann, S.; Farcet, C.; Charleux, B.; Sanchez, C. "Synthesis of hierarchically ordered dye-functionalised mesoporous silica with macroporous architecture by dual templating." *Journal of Materials Chemistry* **2000**, *10*, 2105-2108.
- (18) Klimant, I.; Ruckruh, F.; Liebsch, G.; Stangelmayer, C.; Wolfbeis, O. S. "Fast response oxygen micro-optodes based on novel soluble ormosil glasses." *Mikrochimica Acta* **1999**, *131*, 35-46.
- (19) Loy, D. A.; Shea, K. J. "Bridged polysilsesquioxanes - Highly porous hybrid organic-inorganic materials." *Chemical Reviews* **1995**, *95*, 1431-1442.
- (20) Schottner, G. "Hybrid sol-gel-derived polymers: Applications of multifunctional materials." *Chemistry of Materials* **2001**, *13*, 3422-3435.
- (21) Pierre, A. C.; Pajonk, G. M. "Chemistry of aerogels and their applications." *Chemical Reviews* **2002**, *102*, 4243-4265.
- (22) Carrington, N. A.; Thomas, G. H.; Rodman, D. L.; Beach, D. B.; Xue, Z. L. "Optical determination of Cr(VI) using regenerable, functionalized sol-gel monoliths." *Analytica Chimica Acta* **2007**, *581*, 232-240.
- (23) Pajonk, G. M. "Aerogel catalysts." *Applied Catalysis* **1991**, *72*, 217-266.
- (24) Sanchez, C.; Soler-Illia, G.; Ribot, F.; Lalot, T.; Mayer, C. R.; Cabuil, V. "Designed hybrid organic-inorganic nanocomposites from functional nanobuilding blocks." *Chemistry of Materials* **2001**, *13*, 3061-3083.
- (25) Avnir, D.; Levy, D.; Reisfeld, R. "The nature of the silica cage as reflected by spectral changes and enhanced photostability of trapped Rhodamine-6g." *Journal of Physical Chemistry* **1984**, *88*, 5956-5959.
- (26) Basabe-Desmonts, L.; Reinhoudt, D. N.; Crego-Calama, M. "Design of fluorescent materials for chemical sensing." *Chemical Society Reviews* **2007**, *36*, 993-1017.

- (27) Schulz-Ekloff, G.; Wohrle, D.; van Duffel, B.; Schoonheydt, R. A. "Chromophores in porous silicas and minerals: preparation and optical properties." *Microporous and Mesoporous Materials* **2002**, *51*, 91-138.
- (28) Lin, J.; Brown, C. W. "Sol-gel glass as a matrix for chemical and biochemical sensing." *Trends in Analytical Chemistry* **1997**, *16*, 200-211.
- (29) Malins, C.; Fanni, S.; Glever, H. G.; Vos, J. G.; MacCraith, B. D. "The preparation of a sol-gel glass oxygen sensor incorporating a covalently bound fluorescent dye." *Analytical Communications* **1999**, *36*, 3-4.
- (30) Ayadim, M.; Jiwan, J. L. H.; DeSilva, A. P.; Soumillion, J. P. "Photosensing by a fluorescing probe covalently attached to the silica." *Tetrahedron Letters* **1996**, *37*, 7039-7042.
- (31) Lobnik, A.; Oehme, I.; Murkovic, I.; Wolfbeis, O. S. "pH optical sensors based on sol-gels: Chemical doping versus covalent immobilization." *Analytica Chimica Acta* **1998**, *367*, 159-165.
- (32) MacCraith, B. D.; McDonagh, C. M.; Okeeffe, G.; McEvoy, A. K.; Butler, T.; Sheridan, F. R. "Sol-gel coatings for optical chemical sensors and biosensors." *Sensors and Actuators B-Chemical* **1995**, *29*, 51-57.
- (33) Plaschke, M.; Czolk, R.; Ache, H. J. "Fluorometric-determination of mercury with a water-soluble porphyrin and porphyrin-doped sol-gel films." *Analytica Chimica Acta* **1995**, *304*, 107-113.
- (34) Li, C. Y.; Zhang, X. B.; Han, Z. X.; Akermark, B.; Sun, L. C.; Shen, G. L.; Yu, R. Q. "A wide pH range optical sensing system based on a sol-gel encapsulated amino-functionalised corrole." *Analyst* **2006**, *131*, 388-393.
- (35) Okeeffe, G.; MacCraith, B. D.; McEvoy, A. K.; McDonagh, C. M.; McGilp, J. F. "Development of a LED-based phase fluorometric oxygen sensor using evanescent-wave excitation of a sol-gel immobilized dye." *Sensors and Actuators B-Chemical* **1995**, *29*, 226-230.
- (36) McEvoy, A. K.; McDonagh, C.; MacCraith, B. D. "Optimisation of sol-gel-derived silica films for optical oxygen sensing." *Journal of Sol-Gel Science and Technology* **1997**, *8*, 1121-1125.
- (37) Maruszewski, K.; Streck, W.; Jasiorski, M.; Ucyk, A. "Technology and applications of sol-gel materials." *Radiation Effects and Defects in Solids* **2003**, *158*, 439-450.
- (38) Tang, Y.; Tao, Z. Y.; Bright, F. V. "Sol hydrolysis and condensation reaction time influence the sensitivity of class II xerogel-based sensing materials." *Journal of Sol-Gel Science and Technology* **2007**, *42*, 127-133.

- (39) Bukowski, R. M.; Davenport, M. D.; Titus, A. H.; Bright, F. V. "O₂-responsive chemical sensors based on hybrid xerogels that contain fluorinated precursors." *Applied Spectroscopy* **2006**, *60*, 951-957.
- (40) Tao, Z. Y.; Tehan, E. C.; Tang, Y.; Bright, F. V. "Stable sensors with tunable sensitivities based on class II xerogels." *Analytical Chemistry* **2006**, *78*, 1939-1945.
- (41) Walcarius, A.; Mandler, D.; Cox, J. A.; Collinson, M.; Lev, O. "Exciting new directions in the intersection of functionalized sol-gel materials with electrochemistry." *Journal of Materials Chemistry* **2005**, *15*, 3663-3689.
- (42) Tsionsky, M.; Gun, G.; Glezer, V.; Lev, O. "Sol-gel-derived ceramic-carbon composite electrodes - Introduction and scope of applications." *Analytical Chemistry* **1994**, *66*, 1747-1753.
- (43) Wang, J.; Pamidi, P. V. A. "Sol-gel-derived cold composite electrodes." *Analytical Chemistry* **1997**, *69*, 4490-4494.
- (44) Wang, J. "Sol-gel materials for electrochemical biosensors." *Analytica Chimica Acta* **1999**, *399*, 21-27.
- (45) Rabinovich, L.; Lev, O. "Sol-gel derived composite ceramic carbon electrodes." *Electroanalysis* **2001**, *13*, 265-275.
- (46) Chicharro, M.; Zapardiel, A.; Bermejo, E.; Perez, J. A.; Hernandez, L. "Ephedrine determination in human urine using a carbon-paste electrode modified with C-18 bonded silica-gel." *Analytical Letters* **1994**, *27*, 1809-1831.
- (47) Sayen, S.; Etienne, M.; Bessiere, J.; Walcarius, A. "Tuning the sensitivity of electrodes modified with an organic-inorganic hybrid by tailoring the structure of the nanocomposite material." *Electroanalysis* **2002**, *14*, 1521-1525.
- (48) Etienne, M.; Bessiere, J.; Walcarius, A. "Voltammetric detection of copper(II) at a carbon paste electrode containing an organically modified silica." *Sensors and Actuators B-Chemical* **2001**, *76*, 531-538.
- (49) Wei, H. J.; Collinson, M. M. "Functional-group effects on the ion-exchange properties of organically modified silicates." *Analytica Chimica Acta* **1999**, *397*, 113-121.
- (50) Hsueh, C. C.; Collinson, M. M. "Permeabilities and ion-exchange properties of organically modified sol-gel electrodes." *Journal of Electroanalytical Chemistry* **1997**, *420*, 243-249.

- (51) Wang, P.; Wang, X. P.; Bi, L. H.; Zhu, G. Y. "Renewable-surface amperometric nitrite sensor based on sol-gel-derived silicomolybdate-methylsilicate-graphite composite material." *Analyst* **2000**, *125*, 1291-1294.
- (52) Tsionsky, M.; Lev, O. "Electrochemical composite carbon-ceramic gas sensors - Introduction and oxygen sensing." *Analytical Chemistry* **1995**, *67*, 2409-2414.
- (53) Kim, W.; Chung, S.; Park, S. B.; Lee, S. C.; Kim, C. H.; Sung, D. D. "Sol-gel method for the matrix of chloride-selective membranes doped with tridodecylmethylammonium chloride." *Analytical Chemistry* **1997**, *69*, 95-98.
- (54) Kim, W.; Sung, D. D.; Cha, G. S.; Park, S. B. "Chloride-selective membranes prepared with different matrices including polymers obtained by the sol-gel method." *Analyst* **1998**, *123*, 379-382.
- (55) Lorencetti, L. L.; Gushikem, Y.; Kubota, L. T.; Neto, G. D.; Fernandes, J. R. "Potentiometric study using chemically-modified silica gel with pyridinium as membrane for ClO₄(-) ions." *Mikrochimica Acta* **1995**, *117*, 239-244.
- (56) Ellerby, L. M.; Nishida, C. R.; Nishida, F.; Yamanaka, S. A.; Dunn, B.; Valentine, J. S.; Zink, J. I. "Encapsulation of proteins in transparent porous silicate-glasses prepared by the sol-gel method." *Science* **1992**, *255*, 1113-1115.
- (57) Yamanaka, S. A.; Nishida, F.; Ellerby, L. M.; Nishida, C. R.; Dunn, B.; Valentine, J. S.; Zink, J. I. "Enzymatic activity of glucose-oxidase encapsulated in transparent glass by the sol-gel method." *Chemistry of Materials* **1992**, *4*, 495-497.
- (58) Pickup, J. C.; Hussain, F.; Evans, N. D.; Sachedina, N. "In vivo glucose monitoring: the clinical reality and the promise." *Biosensors & Bioelectronics* **2005**, *20*, 1897-1902.
- (59) Audebert, P.; Demaille, C.; Sanchez, C. "Electrochemical probing of the activity of glucose-oxidase embedded sol-gel matrices." *Chemistry of Materials* **1993**, *5*, 911-913.
- (60) Narang, U.; Prasad, P. N.; Bright, F. V.; Ramanathan, K.; Kumar, N. D.; Malhotra, B. D.; Kamalasanan, M. N.; Chandra, S. "Glucose biosensor based on a sol-gel-derived platform." *Analytical Chemistry* **1994**, *66*, 3139-3144.
- (61) Anderson, J. M. "Biological responses to materials." *Annual Review of Materials Research* **2001**, *31*, 81-110.
- (62) Frost, M. C.; Rudich, S. M.; Zhang, H. P.; Maraschio, M. A.; Meyerhoff, M. E. "In vivo biocompatibility and analytical performance of intravascular amperometric oxygen sensors prepared with improved nitric oxide-releasing silicone rubber coating." *Analytical Chemistry* **2002**, *74*, 5942-5947.

- (63) Shin, J. H.; Schoenfisch, M. H. "Improving the biocompatibility of in vivo sensors via nitric oxide release." *Analyst* **2006**, *131*, 609-615.
- (64) Meyerhoff, M. E. "In vivo blood-gas and electrolyte sensors - Progress and challenges." *Trends in Analytical Chemistry* **1993**, *12*, 257-266.
- (65) Frost, M. C.; Meyerhoff, M. E. "Implantable chemical sensors for real-time clinical monitoring: progress and challenges." *Current Opinion in Chemical Biology* **2002**, *6*, 633-641.
- (66) Wisniewski, N.; Moussy, F.; Reichert, W. M. "Characterization of implantable biosensor membrane biofouling." *Fresenius Journal of Analytical Chemistry* **2000**, *366*, 611-621.
- (67) Ratner, B. D. "Reducing capsular thickness and enhancing angiogenesis around implant drug release systems." *Journal of Controlled Release* **2002**, *78*, 211-218.
- (68) Ratner, B. D.; Bryant, S. J. "Biomaterials: Where we have been and where we are going." *Annual Review of Biomedical Engineering* **2004**, *6*, 41-75.
- (69) Wilson, G. S.; Hu, Y. B. "Enzyme based biosensors for in vivo measurements." *Chemical Reviews* **2000**, *100*, 2693-2704.
- (70) Vacheethasanee, K.; Marchant, R. E. In *Handbook of Bacterial Adhesion: Principles, Methods, and Applications*, An, Y. H.; Friedman, R. J., Eds. Humana Press: Totowa, NJ, 2000; pp 73-90.
- (71) Darouiche, R. O. "Current concepts - Treatment of infections associated with surgical implants." *New England Journal of Medicine* **2004**, *350*, 1422-1429.
- (72) Moncada, S.; Higgs, A. "The L-arginine nitric oxide pathway." *New England Journal of Medicine* **1993**, *329*, 2002-2012.
- (73) Marletta, M. A.; Tayeh, M. A.; Hevel, J. M. "Unraveling the biological significance of nitric oxide." *BioFactors* **1990**, 219-225.
- (74) Radomski, M. W.; Palmer, R. M. J.; Moncada, S. "An L-arginine nitric-oxide pathway present in human platelets regulates aggregation." *Proceedings of the National Academy of Sciences of the United States of America* **1990**, *87*, 5193-5197.
- (75) Efron, D. T.; Most, D.; Barbul, A. "Role of nitric oxide in wound healing." *Current Opinion in Clinical Nutrition and Metabolic Care* **2000**, *3*, 197-204.
- (76) Donnini, S.; Ziche, M. "Constitutive and inducible nitric oxide synthase: Role in angiogenesis." *Antioxidants & Redox Signaling* **2002**, *4*, 817-823.

- (77) Ziche, M.; Morbidelli, L.; Masini, E.; Amerini, S.; Granger, H. J.; Maggi, C. A.; Geppetti, P.; Ledda, F. "Nitric oxide mediates angiogenesis in-vivo and endothelial cell growth and migration in-vitro promoted by substance-P." *Journal of Clinical Investigation* **1994**, *94*, 2036-2044.
- (78) MacMicking, J.; Xie, Q. W.; Nathan, C. "Nitric oxide and macrophage function." *Annual Review of Immunology* **1997**, *15*, 323-350.
- (79) Frost, M. C.; Reynolds, M. M.; Meyerhoff, M. E. "Polymers incorporating nitric oxide releasing/generating substances for improved biocompatibility of blood-contacting medical devices." *Biomaterials* **2005**, *26*, 1685-1693.
- (80) Hetrick, E. M.; Schoenfisch, M. H. "Reducing implant-related infections: active release strategies." *Chemical Society Reviews* **2006**, *35*, 780-789.
- (81) Hetrick, E. M.; Prichard, H. L.; Klitzman, B.; Schoenfisch, M. H. "Reduced foreign body response at nitric oxide-releasing subcutaneous implants." *Biomaterials* **2007**, *28*, 4571-4580.
- (82) Hrabie, J. A.; Klose, J. R.; Wink, D. A.; Keefer, L. K. "New nitric oxide-releasing zwitterions derived from polyamines." *Journal of Organic Chemistry* **1993**, *58*, 1472-1476.
- (83) Nablo, B. J.; Chen, T. Y.; Schoenfisch, M. H. "Sol-gel derived nitric-oxide releasing materials that reduce bacterial adhesion." *Journal of the American Chemical Society* **2001**, *123*, 9712-9713.
- (84) Robbins, M. E.; Oh, B. K.; Hopper, E. D.; Schoenfisch, M. H. "Nitric oxide-releasing xerogel microarrays prepared with surface-tailored poly(dimethylsiloxane) templates." *Chemistry of Materials* **2005**, *17*, 3288-3296.
- (85) Marxer, S. M.; Robbins, M. E.; Schoenfisch, M. H. "Sol-gel derived nitric oxide-releasing oxygen sensors." *Analyst* **2005**, *130*, 206-212.
- (86) Robbins, M. E.; Hopper, E. D.; Schoenfisch, M. H. "Synthesis and characterization of nitric oxide-releasing sol-gel microarrays." *Langmuir* **2004**, *20*, 10296-10302.
- (87) Nablo, B. J.; Rothrock, A. R.; Schoenfisch, M. H. "Nitric oxide-releasing sol-gels as antibacterial coatings for orthopedic implants." *Biomaterials* **2005**, *26*, 917-924.
- (88) Marxer, S. M.; Rothrock, A. R.; Nablo, B. J.; Robbins, M. E.; Schoenfisch, M. H. "Preparation of nitric oxide (NO)-releasing sol-gels for biomaterial applications." *Chemistry of Materials* **2003**, *15*, 4193-4199.

- (89) Nablo, B. J.; Schoenfisch, M. H. "Poly(vinyl chloride)-coated sol-gels for studying the effects of nitric oxide release on bacterial adhesion." *Biomacromolecules* **2004**, *5*, 2034-2041.
- (90) Hetrick, E. M.; Schoenfisch, M. H. "Antibacterial nitric oxide-releasing xerogels: Cell viability and parallel plate flow cell adhesion studies." *Biomaterials* **2007**, *28*, 1948-1956.
- (91) Nablo, B. J.; Prichard, H. L.; Butler, R. D.; Klitzman, B.; Schoenfisch, M. H. "Inhibition of implant-associated infections via nitric oxide." *Biomaterials* **2005**, *26*, 6984-6990.
- (92) Shin, J. H.; Marxer, S. M.; Schoenfisch, M. H. "Nitric oxide-releasing sol-gel particle/polyurethane glucose biosensors." *Analytical Chemistry* **2004**, *76*, 4543-4549.
- (93) Oh, B. K.; Robbins, M. E.; Nablo, B. J.; Schoenfisch, M. H. "Miniaturized glucose biosensor modified with a nitric oxide-releasing xerogel microarray." *Biosensors & Bioelectronics* **2005**, *21*, 749-757.
- (94) Schoenfisch, M. H.; Rothrock, A. R.; Shin, J. H.; Polizzi, M. A.; Brinkley, M. F.; Dobmeier, K. P. "Poly(vinylpyrrolidone)-doped nitric oxide-releasing xerogels as glucose biosensor membranes." *Biosensors & Bioelectronics* **2006**, *22*, 306-312.
- (95) Williams, D. L. H. "The chemistry of S-nitrosothiols." *Accounts of Chemical Research* **1999**, *32*, 869-876.
- (96) de Souza, G. F. P.; Yokoyama-Yasunaka, J. K. U.; Seabra, A. B.; Miguel, D. C.; de Oliveira, M. G.; Uliana, S. R. B. "Leishmanicidal activity of primary S-nitrosothiols against *Leishmania major* and *Leishmania amazonensis*: Implications for the treatment of cutaneous leishmaniasis." *Nitric Oxide-Biology and Chemistry* **2006**, *15*, 209-216.
- (97) Fang, F. C. "Antimicrobial reactive oxygen and nitrogen species: Concepts and controversies." *Nature Reviews Microbiology* **2004**, *2*, 820-832.
- (98) Langford, E. J.; Brown, A. S.; Wainwright, R. J.; Debelder, A. J.; Thomas, M. R.; Smith, R. E. A.; Radomski, M. W.; Martin, J. F.; Moncada, S. "Inhibition of platelet activity by S-nitrosoglutathione during coronary angioplasty." *Lancet* **1994**, *344*, 1458-1460.
- (99) Salas, E.; Langford, E. J.; Marrinan, M. T.; Martin, J. F.; Moncada, S.; de Belder, A. J. "S-nitrosoglutathione inhibits platelet activation and deposition in coronary artery saphenous vein grafts in vitro and in vivo." *Heart* **1998**, *80*, 146-150.

- (100) Wood, P. D.; Mutus, B.; Redmond, R. W. "The mechanism of photochemical release of nitric oxide from S-nitrosoglutathione." *Photochemistry and Photobiology* **1996**, *64*, 518-524.
- (101) Singh, R. J.; Hogg, N.; Joseph, J.; Kalyanaraman, B. "Mechanism of nitric oxide release from S-nitrosothiols." *Journal of Biological Chemistry* **1996**, *271*, 18596-18603.
- (102) Wong, P. S. Y.; Hyun, J.; Fukuto, J. M.; Shiota, F. N.; DeMaster, E. G.; Shoeman, D. W.; Nagasawa, H. T. "Reaction between S-nitrosothiols and thiols: Generation of nitroxyl (HNO) and subsequent chemistry." *Biochemistry* **1998**, *37*, 5362-5371.
- (103) Hogg, N. "The kinetics of S-transnitrosation - A reversible second-order reaction." *Analytical Biochemistry* **1999**, *272*, 257-262.
- (104) Bohl, K. S.; West, J. L. "Nitric oxide-generating polymers reduce platelet adhesion and smooth muscle cell proliferation." *Biomaterials* **2000**, *21*, 2273-2278.
- (105) Masters, K. S. B.; Lipke, E. A.; Rice, E. E. H.; Liel, M. S.; Myler, H. A.; Zygourakis, C.; Tulis, D. A.; West, J. L. "Nitric oxide-generating hydrogels inhibit neointima formation." *Journal of Biomaterials Science-Polymer Edition* **2005**, *16*, 659-672.
- (106) Frost, M. C.; Meyerhoff, M. E. "Synthesis, characterization, and controlled nitric oxide release from S-nitrosothiol-derivatized fumed silica polymer filler particles." *Journal of Biomedical Materials Research Part A* **2005**, *72A*, 409-419.
- (107) Dasgupta, T. P.; Smith, J. N. Reactions of S-nitrosothiols with L-ascorbic acid in aqueous solution. In *Nitric Oxide, Pt D*, 2002; Vol. 359, pp 219-229.
- (108) Shin, J. H.; Weinman, S. W.; Schoenfisch, M. H. "Sol-gel derived amperometric nitric oxide microsensor." *Analytical Chemistry* **2005**, *77*, 3494-3501.
- (109) Fukuto, J. M.; Switzer, C. H.; Miranda, K. M.; Wink, D. A. "Nitroxyl (HNO): Chemistry, biochemistry, and pharmacology." *Annual Review of Pharmacology and Toxicology* **2005**, *45*, 335-355.
- (110) Miranda, K. M.; Nims, R. W.; Thomasa, D. D.; Espey, M. G.; Citrin, D.; Bartberger, M. D.; Paolocci, N.; Fukuto, J. M.; Feelisch, M.; Wink, D. A. "Comparison of the reactivity of nitric oxide and nitroxyl with heme proteins - A chemical discussion of the differential biological effects of these redox related products of NOS." *Journal of Inorganic Biochemistry* **2003**, *93*, 52-60.
- (111) Miranda, K. M.; Paolocci, N.; Katori, T.; Thomas, D. D.; Ford, E.; Bartberger, M. D.; Espey, M. G.; Kass, D. A.; Feelisch, M.; Fukuto, J. M.; Wink, D. A. "A biochemical rationale for the discrete behavior of nitroxyl and nitric oxide in the cardiovascular

- system." *Proceedings of the National Academy of Sciences of the United States of America* **2003**, *100*, 9196-9201.
- (112) Paolocci, N.; Jackson, M. I.; Lopez, B. E.; Miranda, K.; Tocchetti, C. G.; Wink, D. A.; Hobbs, A. J.; Fukuto, J. M. "The pharmacology of nitroxyl (HNO) and its therapeutic potential: Not just the janus face of NO." *Pharmacology & Therapeutics* **2007**, *113*, 442-458.
- (113) Wink, D. A.; Miranda, K. M.; Katori, T.; Mancardi, D.; Thomas, D. D.; Ridnour, L.; Espey, M. G.; Feelisch, M.; Colton, C. A.; Fukuto, J. M.; Pagliaro, P.; Kass, D. A.; Paolocci, N. "Orthogonal properties of the redox siblings nitroxyl and nitric oxide in the cardiovascular system: a novel redox paradigm." *American Journal of Physiology-Heart and Circulatory Physiology* **2003**, *285*, H2264-H2276.
- (114) Miranda, K. M.; Espey, M. G.; Paolocci, N.; Bartberger, M. D.; Colton, C. A.; Wink, D. A. "The chemistry of nitroxyl (HNO) and implications in various therapeutic applications." *Free Radical Biology and Medicine* **2001**, *31*, S72-S72.
- (115) Pagliaro, P.; Mancardi, D.; Rastaldo, R.; Penna, C.; Gattullo, D.; Miranda, K. M.; Feelisch, M.; Wink, D. A.; Kass, D. A.; Paolocci, N. "Nitroxyl affords thiol-sensitive myocardial protective effects akin to early preconditioning." *Free Radical Biology and Medicine* **2003**, *34*, 33-43.
- (116) Paolocci, N.; Saavedra, F. W.; Miranda, K. M.; Espey, M. G.; Isoda, T.; Wink, D. A.; Kass, D. A. "Novel and potent inotropic and selective venodilatory action of nitroxyl anion in intact dogs." *Circulation* **2000**, *102*, 161-161.
- (117) DeMaster, E. G.; Redfern, B.; Nagasawa, H. T. "Mechanisms of inhibition of aldehyde dehydrogenase by nitroxyl, the active metabolite of the alcohol deterrent agent cyanamide." *Biochemical Pharmacology* **1998**, *55*, 2007-2015.
- (118) Nagasawa, H. T.; Demaster, E. G.; Redfern, B.; Shirota, F. N.; Goon, J. W. "Evidence for nitroxyl in the catalase-mediated bioactivation of the alcohol deterrent agent cyanamide." *Journal of Medicinal Chemistry* **1990**, *33*, 3120-3122.
- (119) Conway, T. T.; DeMaster, E. G.; Lee, M. J. C.; Nagasawa, H. T. "Prodrugs of nitroxyl and nitrosobenzene as cascade latentiated inhibitors of aldehyde dehydrogenase." *Journal of Medicinal Chemistry* **1998**, *41*, 2903-2909.
- (120) Nagasawa, H. T.; Kawle, S. P.; Elberling, J. A.; Demaster, E. G.; Fukuto, J. M. "Prodrugs of nitroxyl as potential aldehyde dehydrogenase inhibitors vis-a-vis vascular smooth-muscle relaxants." *Journal of Medicinal Chemistry* **1995**, *38*, 1865-1871.

- (121) Nagasawa, H. T.; Yost, Y.; Elberling, J. A.; Shirota, F. N.; Demaster, E. G. "Nitroxyl analogs as inhibitors of aldehyde dehydrogenase - C-nitroso compounds." *Biochemical Pharmacology* **1993**, *45*, 2129-2134.
- (122) Miranda, K. M.; Katori, T.; de Holding, C. L. T.; Thomas, L.; Ridnour, L. A.; McLendon, W. J.; Cologna, S. M.; Dutton, A. S.; Champion, H. C.; Mancardi, D.; Tocchetti, C. G.; Saavedra, J. E.; Keefer, L. K.; Houk, K. N.; Fukuto, J. M.; Kass, D. A.; Paolucci, N.; Wink, D. A. "Comparison of the NO and HNO donating properties of diazeniumdiolates: Primary amine adducts release HNO in vivo." *Journal of Medicinal Chemistry* **2005**, *48*, 8220-8228.
- (123) Miranda, K. M.; Nagasawa, H. T.; Toscano, J. P. "Donors of HNO." *Current Topics in Medicinal Chemistry* **2005**, *5*, 647-664.
- (124) Donzelli, S.; Espey, M. G.; Thomas, D. D.; Mancardi, D.; Tocchetti, C. G.; Ridnour, L. A.; Paolucci, N.; King, S. B.; Miranda, K. M.; Lazzarino, G.; Fukuto, J. M.; Wink, D. A. "Discriminating formation of HNO from other reactive nitrogen oxide species." *Free Radical Biology and Medicine* **2006**, *40*, 1056-1066.
- (125) Butkovskaya, N. I.; Muravyov, A. A.; Setser, D. W. "Infrared chemiluminescence from the NO+HCO reaction: Observation of the 2 $\nu(1)$ - $\nu(1)$ hot band of HNO." *Chemical Physics Letters* **1997**, *266*, 223-226.
- (126) Bazylinski, D. A.; Hollocher, T. C. "Metmyoglobin and methemoglobin as efficient traps for nitrosyl hydride (nitroxyl) in neutral aqueous solution." *Journal of the American Chemical Society* **1985**, *107*, 7982-7986.
- (127) Bari, S. E.; Marti, M. A.; Amorebieta, V. T.; Estrin, D. A.; Doctorovich, F. "Fast nitroxyl trapping by ferric porphyrins." *Journal of the American Chemical Society* **2003**, *125*, 15272-15273.
- (128) Marti, M. A.; Bari, S. E.; Estrin, D. A.; Doctorovich, F. "Discrimination of nitroxyl and nitric oxide by water-soluble Mn(III) porphyrins." *Journal of the American Chemical Society* **2005**, *127*, 4680-4684.
- (129) Dobmeier, K. P.; Charville, G. W.; Schoenfish, M. H. "Nitric oxide-releasing xerogel-based fiber-optic pH sensors." *Analytical Chemistry* **2006**, *78*, 7461-7466.
- (130) Dobmeier, K. P.; Riccio, D. A.; Schoenfish, M. H. "Xerogel optical sensor films for quantitative detection of nitroxyl." *Analytical Chemistry* **2007**, *in press*.

Chapter 2:

Nitric Oxide-Releasing Xerogel-Based Fiber-Optic pH Sensors

2.1. Introduction

Blood pH, when measured in conjunction with PCO_2 , provides a useful window into respiratory, cardiovascular, and renal function.^{1,2} Strong shifts from arterial pH values of 7.4 due to alkalosis and acidosis conditions are often indicative of respiratory or metabolic distress. During thoracic surgeries and mechanical lung ventilation, blood gases (e.g., PO_2 , PCO_2) and pH may fluctuate rapidly.³ Throughout these critical periods, the common clinical practice of periodic arterial blood sampling followed by bench-top laboratory blood gas analysis does not provide an adequately fast means of tracking respiratory function. As such, real-time analysis strategies must be employed. Techniques such as capnometry and transcutaneous blood gas measurement provide real-time detection, but have important limitations. Capnometry requires normal pulmonary function to correctly estimate CO_2 concentration, which can lead to unreliable readings in critically-ill patients.³ Transcutaneous sensors are often hampered by skin and tissue variations in adult subjects.⁴ These issues may be circumvented by direct determination of blood gases through the implantation of miniaturized catheter sensors or sensor arrays into the arterial blood stream.

To date, most intravascular blood gas sensors have been based on amperometric (e.g., Clark-style dissolved oxygen electrodes) or fiber-optic-based photochemical platforms.⁵ Fiber-optic sensors may have greater appeal because of their high sensitivity, reduced

electrical interference, and ease of miniaturization for incorporation into bundled arrays.^{6, 7} Analyte concentrations are measured via their interaction with transducer dye molecules immobilized at the fiber surface, typically resulting in changes of absorbance or fluorescence intensity, lifetime, or phase.⁸ For example, the Paratrend 7+[®] (Diametrics Medical Inc.), a multiparameter continuous intravascular blood gas monitoring probe commercially available from 1999 to 2004, employed a bundle of three optical fiber probes modified to measure PO_2 via ruthenium dye fluorescence quenching, PCO_2 and pH via phenol red absorbance, and temperature via a thermocouple. Clinical trials confirmed that the real-time measurements made by these optical sensors compared well with intermittent laboratory blood gas analysis, the current clinical standard.^{3, 5, 9}

Despite favorable results in most cases, blood clot formation at the surface of fiber-optic intravascular sensors has been reported.^{10, 11} Platelet adhesion and aggregation at a sensor limits analyte diffusion to the transduction element, rendering the sensor largely inoperable.¹² At worst, subsequent dislodgement of the thrombus may lead to potentially serious health effects such as vessel occlusion. Recent research has focused on the synthesis and characterization of nitric oxide (NO)-releasing polymers as antithrombogenic sensor membranes to combat blood clot formation. Nitric oxide is released by human endothelial cells at femto- to picomolar fluxes where it helps regulate vasodilation and platelet activation.¹³ Indeed, polymers modified to release NO at physiological concentrations have demonstrated much lower proclivities for thrombus formation at a blood/material interface.¹⁴⁻
¹⁶ Unlike other systemically administered anticoagulants such as heparin, NO has a short half-life in blood (e.g., on the order of seconds), ensuring its antithrombogenic effects remain localized near the sensor/blood interface, precluding potentially detrimental side-effects.¹⁷

Nitric oxide release capability has been imparted to polymers through the inclusion of a number of NO donor functionalities, including nitrosothiols, nitrosamines, metal complexes, and diazeniumdiolates into the polymer via doping or covalent attachment.¹⁸ To date, nitrogen-bound diazeniumdiolates (*N*-diazeniumdiolates) represent the most widely employed NO donors for spontaneously generating NO from materials. Briefly, *N*-diazeniumdiolates are formed by exposing secondary amine precursors to high pressures of NO under basic conditions, resulting in the reversible binding of two NO molecules. Subsequent exposure to a proton source such as water initiates *N*-diazeniumdiolate decomposition and release of two equivalents of NO.¹⁹ Coatings utilizing this system have been employed to improve the biocompatibility of catheter and subcutaneous sensors for biologically relevant analytes. Previously described examples include amperometric PO_2 ²⁰,²¹ and glucose sensors,²² and potentiometric PCO_2 sensors.²³ Nitric oxide-releasing polymeric coatings suitable for fluorescence-based PO_2 detection have also been reported, although miniaturized sensors were neither fabricated nor evaluated.²⁴

In this chapter, a NO-releasing optical fiber-based pH sensor was fabricated via sol-gel chemistry. During the sol-gel process, hydrolysis and condensation of silicon alkoxide precursors form a robust, glassy silica network referred to as a xerogel.²⁵ Incorporation of aminoalkoxysilane precursors into the siloxane polymer backbone allows for the subsequent formation of covalently bound *N*-diazeniumdiolates, introducing NO-release capability to the xerogel.^{14, 26, 27} Nitric oxide-releasing xerogels with tunable NO-release kinetics have been reported previously, and their effectiveness in improving the biocompatibility of amperometric oxygen²⁸ and glucose^{29, 30} sensors has been demonstrated. Unfortunately, exposure of aminoalkoxysilane-based xerogels to high pressures of NO during *N*-diazeniumdiolate formation was shown to accelerate sol-gel polycondensation, resulting in

dense (i.e., non-permeable) xerogel coatings.²⁹ As such, sensors fabricated with such coatings often suffer from limited sensitivity and lengthened response times. Strategies for overcoming the reduced analyte diffusion have included doping xerogel particles into conventional sensor membranes²⁹ and utilizing soft-lithographic micropatterning techniques to selectively modify regions of the underlying electrode.³⁰ While effective, these techniques make sensor fabrication more complicated and limit the overall flux of NO attainable at such surfaces.

The dense nature of NO-releasing xerogel coatings may make them better suited to optical sensing platforms, where analyte diffusion to an electrode surface is not required. Optically transparent and chemically inert xerogels have long been recognized as a useful host matrix for fluorescent indicator molecules.³¹⁻³³ The siloxane network properties including membrane porosity and permeability are easily manipulated by varying the composition of the sol (e.g., water:silane ratio and/or acid concentration). Furthermore, physical entrapment of indicator dyes in the gel is straightforward. Herein, a miniaturized, NO-releasing xerogel-derived optical pH sensor suitable for intravascular use is described that combines the simplicity of sol-gel-based optical sensor fabrication with the added biocompatibility benefits of NO release. Using a two-layer immobilization strategy, xerogels containing both NO-producing *N*-diazeniumdiolates and the pH-sensitive fluorophore seminaphthorhodamine-1 carboxylate (SNARF-1) were immobilized onto optical fiber supports. The fabrication, analytical performance, and enhanced blood biocompatibility of the NO-releasing optical pH sensors are discussed.

2.2. Materials and Methods

Ethyltrimethoxysilane (ETMOS), isobutyltrimethoxysilane (BTMOS) methyltrimethoxysilane (MTMOS), (aminoethylaminomethyl)phenethyltrimethoxysilane (AEMP3), *N*-(6-aminohexyl)aminopropyltrimethoxysilane (AHAP3), and aminopropyltriethoxysilane (APTES), and were purchased from Gelest (Tullytown, PA). Tetramethyl orthosilicate (TMOS), glutaraldehyde (50% w:w in water), and hexamethyldisilazane (HMDS) were purchased from Aldrich (Milwaukee, WI). Seminaphthorhodamine-1 carboxylate (SNARF-1) pH indicator was purchased from Invitrogen (Carlsbad, CA). Nitric oxide (99.5%) was purchased from National Welders Supply (Durham, NC). Whole blood was obtained from healthy pigs at the Francis Owen Blood Research Laboratory (Chapel Hill, NC). Other solvents and chemicals were analytical-reagent grade and used as received. Distilled water was purified to 18.2 M Ω -cm with a Millipore Milli-Q Gradient A-10 water purification system (Bedford, MA). Optical fiber materials were purchased from Ocean Optics (Dunedin, FL).

2.2.1. *NO-releasing Xerogel Preparation*

Nitric oxide-releasing xerogels were prepared through the inclusion of 20 or 40% AHAP3 in ETMOS gels (v:v total silane). Ethanol (300 μ L) was mixed with ETMOS (160 or 120 μ L) and AHAP3 (40 or 80 μ L) in a vortex shaker for 5 min. Water (10 μ L) was added and shaken for an additional 5 min. The sol was then immobilized on optical fibers via dip-coating or drop-cast onto glass slides.

2.2.2. *pH-Sensing Xerogel Preparation*

Xerogels containing the SNARF-1 pH indicator were fabricated in a manner similar to that described by Grant and Glass.³⁴ Water (1000 μ L) was combined with TMOS (500

μL) and 0.04 M HCl (10 μL) and sonicated in an ice bath. After 30 min, a 75 μL aliquot of the sol was combined with 20 μL of a 5 mM SNARF-1/water stock solution and diluted with 300 μL pH 7.4 phosphate buffered saline (PBS). The sol was sonicated on ice for an additional minute prior to dip-coating procedures.

2.2.3. *Sensor Fabrication*

Two-layer NO-releasing pH sensors were created by sequential dip-coating of optical fibers in the AHAP3/ETMOS and TMOS sols. Unjacketed silica core/silica clad optical fiber (400 μm o.d., NA = 0.22) was cut into 8 cm segments and the polyimide sheathing around the fiber was removed by immersion in hot concentrated sulfuric acid. The fibers were tapered to enhance the coupling of fluorescent modes into the fiber core.³⁵ Approximately 1.0 cm of the bare silica fiber was immersed in a concentrated hydrofluoric acid bath with an overlying layer of toluene for 2.5 h,³⁶ resulting in the self-terminated tapering of approximately 0.5 cm of the distal end of the fiber down to 80 μm o.d. After rinsing, 2 cm of the tapered optical fibers were manually dip coated twice into the AHAP3/ETMOS sol, drying 1 min in a 75 °C oven between coats. Sensors were allowed to age for a minimum of 3 d under ambient conditions before 1 coat of the pH-sensing sol was applied in a similar manner. Again, sensors were aged for a minimum of 3 d under ambient conditions before *N*-diazoniumdiolate formation. Sensors were placed in an in-house reaction vessel and thoroughly flushed with Ar prior to exposure to 5 atm NO for 3 d. Unreacted NO was subsequently removed, and sensors were stored at -20 °C until use.

2.2.4. *Apparatus*

Sensors were evaluated with a simple optical fiber-based spectrophotometer system. The xerogel-coated probes were coupled directly to the common leg bundle of a solarization

resistant 200 μm o.d. bifurcated optical fiber assembly via an SMA905 connector and Ocean Optics SMA905 bare fiber adaptor. Excitation light was supplied through one leg of the bifurcated assembly by a Power Technology Inc. LDCU3/3663 10 mW, 532 nm laser (Alexander, AR) after passing through a 90% attenuation neutral density filter. Fluorescent emission from the xerogel coating was coupled back into the probe and partially transmitted through the second leg of the bifurcated assembly for detection at an Ocean Optics USB2000 Spectrometer. Sensor response characteristics were determined by sequential immersion of the probes in PBS solutions buffered across the common physiological pH range of blood (pH 7.0-7.8). Complete spectra in the 400-800 nm range were generated and saved with Ocean Optics OOIBase32 software. Fluorescence intensities at the 580 and 640 nm peak emission wavelengths of the SNARF-1 pH indicator, were later extracted and ratios generated using LabVIEWTM (National Instruments).

2.2.5. *Characterization of NO Release*

Real-time NO flux from AHAP/ETMOS xerogels prepared with and without TMOS overlayers was monitored using a Sievers NOATM 280 Chemiluminescence Nitric Oxide Analyzer (Boulder, CO). Xerogel films were cast onto glass slides via glutaraldehyde fixation procedures. The slides were cleaned in 10% nitric acid (v:v, water) at 70 °C for 30 min, rinsed with purified water, immersed in 10% APTES (v:v, PBS, pH 7.0) at 70 °C for 90 min, rinsed again, and then immersed in 10% glutaraldehyde (v:v, water) at 25 °C for 60 min. After rinsing the slides thoroughly with water, AHAP3/ETMOS gel solution (30 μL) was drop-cast onto the slides and allowed to dry under ambient conditions. After drying for 24 h, a TMOS overlayer was dip-coated over select gels by complete immersion of the xerogel-coated glass slides in the TMOS sol. Dip-coated gels were allowed to dry for an

additional 3 days under ambient conditions. The resulting xerogel films were then exposed to 5 atm NO for 3 d to form *N*-diazoniumdiolates as described above and stored at -20 °C until use. The Sievers NOA 280 instrument was calibrated before each experiment using air passed through a Sievers zero NO filter and 24.1 ppm NO gas (balance N₂). Individual slides were immersed in 20 mL PBS buffer (pH 7.4) at 37 °C and sparged with a 200 mL/min N₂ stream. Detected chemiluminescence due to NO was monitored continuously in 1 sec intervals for 16 h.

2.2.6. Platelet Adhesion Studies

Healthy porcine blood was drawn into acid citrate dextrose (ACD)-anticoagulated tubes (1 part ACD to 9 parts whole blood) and maintained at 37 °C for 1 h prior to use. Platelet enriched plasma (PRP) was obtained by centrifugation at 150g for 20 min at room temperature.³⁷ Normal platelet activity was reestablished by the addition of CaCl₂ to achieve a 0.5mM Ca²⁺ concentration. Individual NO-releasing xerogel films (prepared as described above) and controls were immersed in 2 mL PRP at 37 °C for 1 h. Loose platelets and cells were removed by rinsing with 37 °C Tyrodes buffer (137 mM NaCl, 2.7 mM KCl, 3.3 mM KH₂PO₄, 5.6 mM glucose, pH 7.35). The remaining adhered platelets were fixed by immersing the slides in a 1% glutaraldehyde solution (v:v, Tyrodes buffer) at 37 °C for 30 min. The slides were rinsed with Tyrodes buffer and water, and chemically dried as follows to preserve cell morphology. Slides were immersed in 50, 75, and 95% ethanol (v:v, water) for 5 min, 100% ethanol for 10 min, and HMDS overnight. Representative scanning electron microscope (SEM) images of all samples were obtained. Semiquantitative platelet surface coverages on NO-releasing samples were calculated via digital image processing and black/white thresholding from phase contrast images obtained with a Zeiss Axiovert 200

inverted microscope (Chester, VA). Average percent surface coverages were calculated from the overall average of five slides, with 5 images taken per slide.

2.3. Results and Discussion

The near-neutral dynamic range ($pK_a = 7.5$) and useful dual emission properties of the SNARF-1 fluorescent pH indicator make it an attractive choice for intravascular pH sensing.³⁸ Both acid and base isomers fluoresce strongly at 580 and 640 nm, respectively, and may be excited at a single wavelength. By monitoring the ratio of the fluorescent intensity at two emission maxima instead of intensity changes at only one wavelength, the dye provides a self-referencing means to compensate for common sources of signal drift such as photobleaching and light source inconsistencies. Fabrication of NO-releasing optical pH sensors was first attempted by direct encapsulation of SNARF-1 indicator within several aminoalkoxysilane/alkoxysilane systems, including AEMP3/MTMOS, AHAP3/ETMOS, and AHAP3/BTMOS xerogels. Unfortunately, sensors fabricated by direct SNARF-1 encapsulation in the aminoalkoxysilanes-modified xerogels proved unresponsive. No changes in fluorescent emission were observed when such sensors were immersed in PBS of pH 7.0 - 7.8 (data not shown). The lack of response can be explained by the nature of the aminoalkoxysilane xerogels used to host the SNARF-1 indicator. Stable, NO-releasing xerogels require aminosilane precursors in conjunction with more inert ethyl- or methyl-substituted alkoxysilanes.¹⁴ Such xerogel networks are inherently more hydrophobic than those formed strictly from inorganic silanes like tetramethyl and tetraethyl orthosilicates.³⁹ Additionally, when exposed to high pressures of NO to form *N*-diazoniumdiolates, aminoalkoxysilane xerogels suffer an extreme loss of permeability.²⁹ As such, it is unlikely that buffer was penetrating into the bulk of the xerogel and thus, the majority of the

fluorescent emission measured did not reflect the pH conditions of the surrounding buffer but rather the static interior pH of the bulk xerogel matrix.

2.3.1. *Two-Layer Sensors*

To improve the responsiveness of the NO-releasing optical pH sensors, a benefit of optical sensing platforms was utilized. Unlike amperometric sensors, fiber-optic sensors do not require that the analyte permeate through a polymeric membrane to an electrode. As long as fluorescent emission from the pH indicator is coupled back into the optical fiber, the indicator may be separated physically from the fiber surface. While xerogels modified with *N*-diazoniumdiolates suffer from low analyte permeability, they remain optically transparent. Thus, the application of a thin, NO-releasing xerogel directly to a fiber-optic surface will present minimal interference to the coupling of excitation and emission modes to and from an overlying xerogel layer encapsulating the pH indicator. Two-layer NO-releasing optodes comprised of a 40:60% (v:v) AHAP3/ETMOS NO-releasing xerogel as a base layer and a TMOS xerogel overlayer doped with the SNARF-1 indicator showed a significantly improved response (i.e., change in fluorescent emission at 580 and 640 nm) to buffer pH compared to single-layer sensors (Figure 2.1).

2.3.2. *Sensitivity and Reproducibility*

The response of the two-layer NO-releasing sensors was measured by sequential immersion of the optical fiber in PBS solutions buffered between pH 7.0 and 7.8 (Figure 2.2). The response of the sensors was linear ($R^2 \geq 0.986$) throughout the tested pH range. From the calibration curves generated, a minimum resolvable pH shift of approximately 0.04 pH units was estimated by doubling the average standard deviation of emission ratios at individual pH values. The sensitivity and signal reproducibility of five individual sensors, as

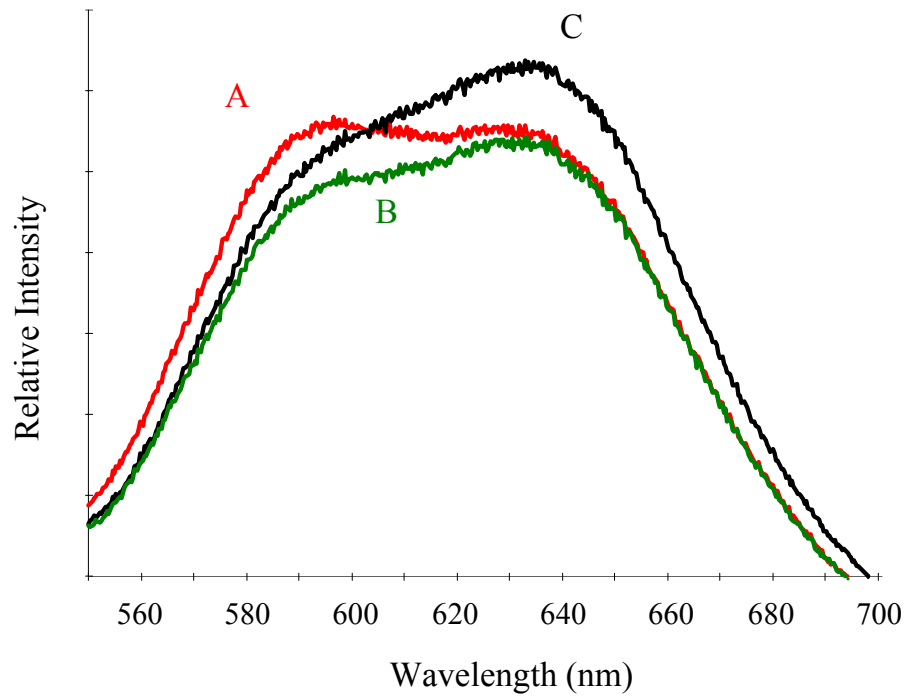


Figure 2.1. Fluorescence emission spectra from a 40:60% (v:v) AHAP3/ETMOS-TMOS optical pH sensor immersed in phosphate buffered saline at pH (A) 7.0; (B) 7.4; and (C) 7.8.

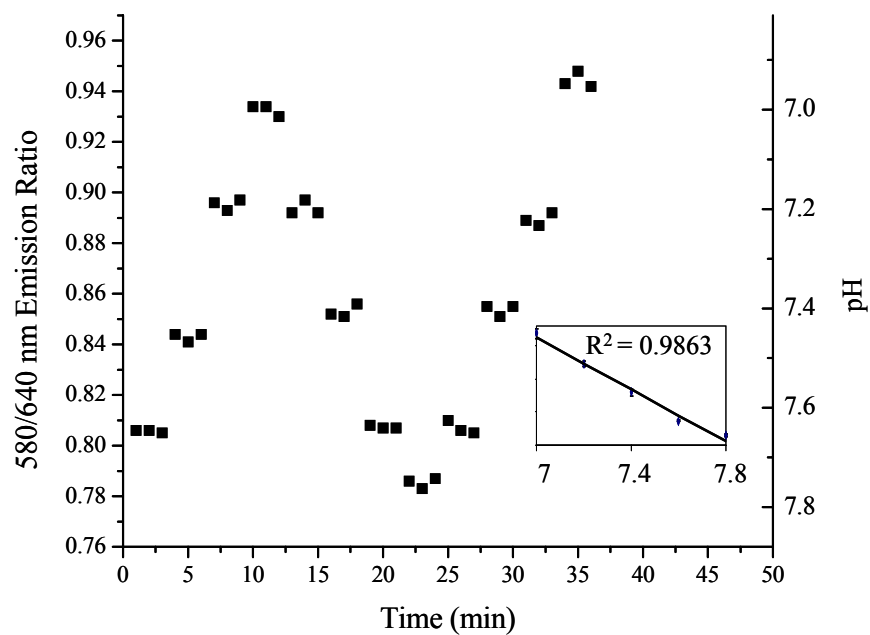


Figure 2.2. Time-resolved response from 40:60% (v:v) AHAP3/ETMOS-TMOS optical pH sensor immersed in pH 7.0-7.8 PBS solutions.

well as the average emission ratio of each sensor at pH 7.4, are provided in Table 2.1. As expected, variation between sensors was apparent. Such variability is attributed to inconsistencies in fiber tapering and coating. The TMOS gel employed for SNARF-1 encapsulation reacts and solidifies rapidly. Thus, a natural evolution of the gelation can be observed during the dip coating procedure. The sol coated onto fibers later in succession is generally more viscous, resulting in the deposition of a thicker xerogel layer.⁴⁰ While more stringent timing control and automated dip-coating procedures would likely reduce sensor-to-sensor variations, calibration of individual sensors prior to use is still necessary.

2.3.3. Pretreatment and Response Time

A common concern reported for xerogel-based sensors employed in aqueous solution is lengthy response times, which can range from seconds up to hours.⁴¹⁻⁴⁶ While porosity and gel hydrophobicity play an important role in determining diffusion rates through the material, Ismail et al. have demonstrated that hydrogen bonding at the gel/liquid interface has an equal, if not greater effect in many cases.⁴⁷ Xerogels may contain a large number of unreacted free silanol groups capable of forming hydrogen bonds with other nearby free silanols either directly or through the mediation of bridging water molecules. These hydrogen bond networks can serve as a barrier to rapid equilibrium of the exterior aqueous environment with the interior of the xerogel. Proton-exchange indicator molecules trapped in the xerogel can associate with residual protons and water molecules retained by hydrogen bonding until complete equilibrium of the material with its surrounding environment is achieved. The result is long response times and lengthy soaking requirements of xerogel-based sensors prior to use. Obviously, long response times are less than optimal for most sensing applications. Long presoak requirements are especially detrimental for sensors

Table 2.1. Reference emission ratios, sensitivity, linearity, and signal reproducibility of 40:60% (v:v) AHAP3/ETMOS-TMOS NO-releasing sensors.

Sensor	580 / 640 nm Emission Ratio ^a	Δ Emission Ratio / Δ pH	R ²	Average standard deviation	Resolvable pH Shift
1	0.850	0.196	0.986	0.00392	0.040
2	0.589	0.113	0.999	0.00203	0.036
3	0.707	0.116	0.999	0.00173	0.030
4	0.502	0.075	0.999	0.00138	0.037
5	0.581	0.079	0.998	0.00173	0.044

^a pH = 7.4

modified with NO-releasing coatings as NO release is initiated from diazeniumdiolate NO donors upon solution immersion. For NO-releasing xerogel based amperometric oxygen sensors, Marxer et al. was able to reduce the minimum presoaking time to 30 min (to obtain adequate sensitivity) by increasing the permeability of the xerogel via the inclusion of 1% (v:v) hydrophilic polyurethane in the gel.²⁸ Doping xerogel coatings to be used for optical sensors with such polymers, however, would lead to optically opaque films.

To ensure rapid response with minimal presoak requirements, the xerogel optical sensors were immersed in 0.5 M sodium hydroxide solution for 30 s prior to use, as described previously by Ismail et al.⁴⁷ Brief exposure to strongly basic solution allowed for rapid disruption of the silanol hydrogen bond networks present and substitution by sodium cations while having minimal effect on the proton-induced decomposition of *N*-diazeniumdiolates. The encapsulated SNARF-1 indicator was thus free to equilibrate with the surrounding buffer. The brief immersion in base may also serve to break siloxane bonds, further opening up the xerogel for more rapid analyte diffusion throughout the material. Such polymer breakdown was limited, however, as successive base immersions did not lead to changes in response or further reductions in fluorescent signal intensity. Following base immersion, the sensors were immediately used to monitor pH. Sensor response times were determined by tracking the shift of fluorescent emission ratios in 0.9 s increments as the two-layer sensor was moved from pH 7.8 to pH 7.0 buffer solutions. The time required to achieve 90% of the final response (τ_{90}) was determined by fitting the resulting data to a first order exponential decay model (Figure 2.3). The 40:60% (v:v) AHAP3/ETMOS-TMOS modified sensors exhibited extremely rapid response characteristics, with a calculated average τ_{90} of 14 ± 2 s ($n = 3$). Indicator leaching after base immersion was evaluated by monitoring the average intensity of 640 nm SNARF-1 fluorescence at hourly intervals from

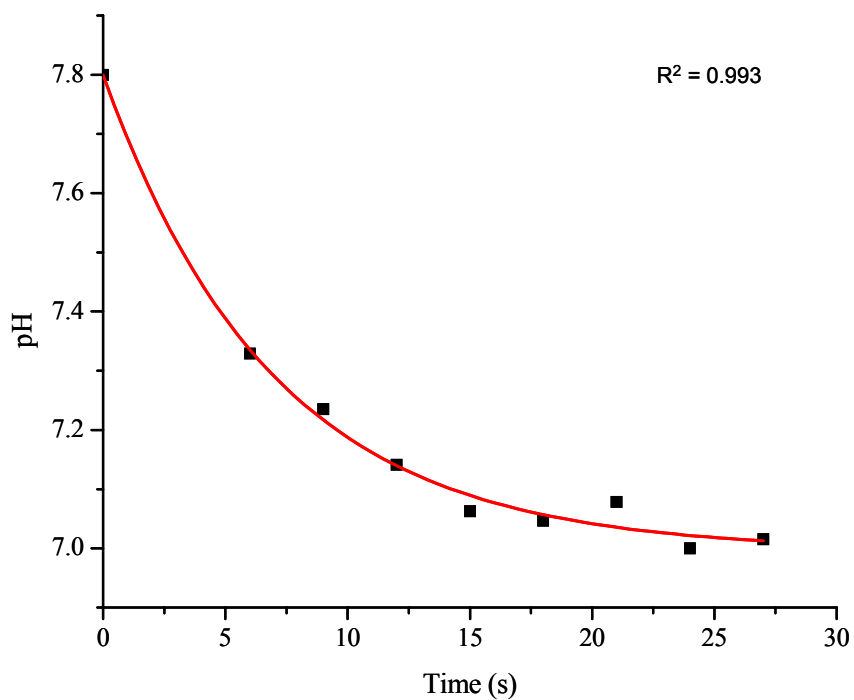


Figure 2.3. Timed response of 40:60% (v:v) AHAP3/ETMOS-TMOS optical pH sensor as a function of pH (7.0-7.8).

a sensor immersed in pH 7.4 PBS. Over the course of 20 h, the fluorescence intensity measured at 640 nm did not change (1070.1 ± 5.3 and 1068.0 ± 9.5 a.u. at 0 and 20 h, respectively). Thus, the AHAP3/ETMOS-TMOS coatings allowed immediate sensor use and rapid response with only a 30 s base pretreatment step.

2.3.4. Nitric Oxide Release

Manipulation of the identity and percentage of aminosilane employed in the original sol mixture allows control over the magnitude and duration of NO released by a *N*-diazoniumdiolate-modified xerogel film.²⁷ To evaluate the NO-release potential of the two-layer AHAP3/ETMOS-TMOS coatings employed in this study, real-time NO flux measurements were performed via chemiluminescence. Example NO release profiles demonstrating the NO flux generated by coatings comprised of 20 and 40% AHAP3 (v:v; balance ETMOS) are shown in Figure 2.4. The optimal NO flux for reducing thrombus formation at a blood/material interface is generally believed to fluctuate depending on the localized abundance of NO-scavengers (e.g., proteins, thiols, etc.) in the surrounding environment. Ramamurthi and Lewis have reported that surface NO fluxes as low as $0.6 \text{ fmol/cm}^2\text{s}$ were effective at reducing *in vitro* platelet adhesion.⁴⁸ Likewise, Robbins et al. demonstrated maintained thromboresistivity for up to 24 h at micropatterned xerogel arrays with NO surface fluxes of $0.4 \text{ pmol cm}^{-2} \text{ s}^{-1}$.⁴⁹ Considering $0.4 \text{ pmol cm}^{-2} \text{ s}^{-1}$ as a minimum threshold value for inhibiting platelet adhesion, sensors fabricated with 20% AHAP3 would be thromboresistant for approximately 6 h. Likewise, sensors prepared with 40% AHAP3 xerogels would maintain fluxes $> 0.4 \text{ pmol cm}^{-2} \text{ s}^{-1}$ for at least 16 h. Notably, the addition of a TMOS overlayer to the NO-releasing AHAP3/ETMOS films prior to *N*-diazoniumdiolate formation did not alter the NO-release profile significantly (Figure 2.4), suggesting that the

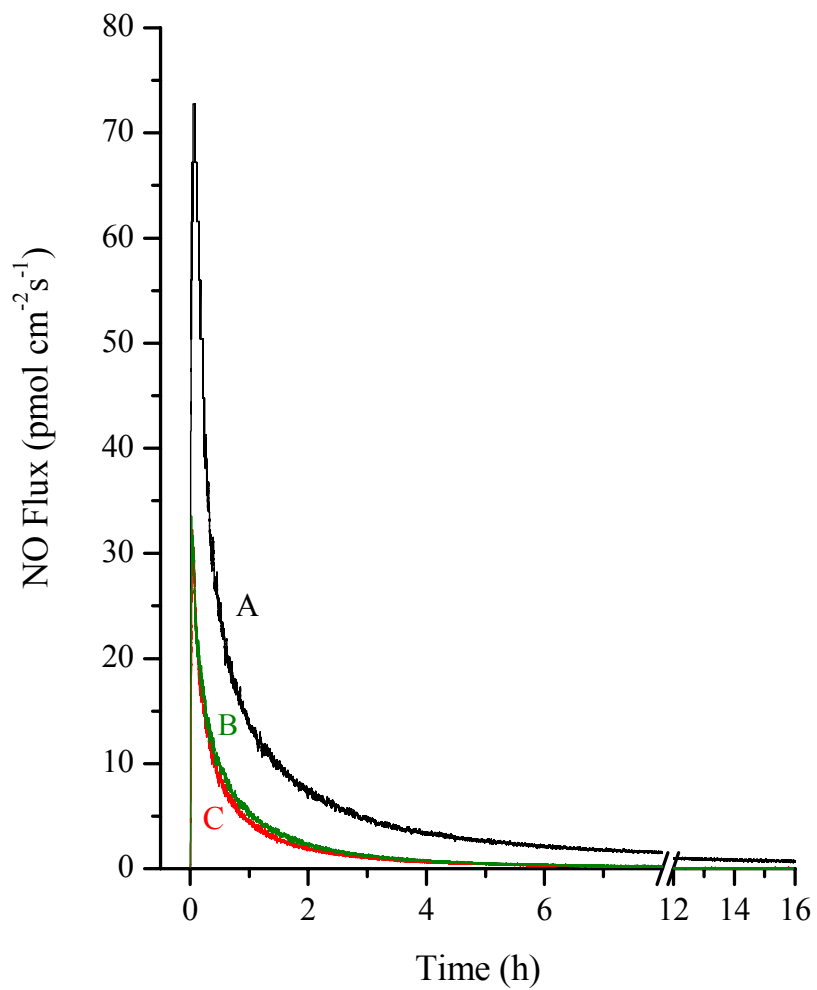


Figure 2.4. Nitric oxide release from (A) 40:60% and (B) 20:80% (v:v) AHAP3/ETMOS xerogels; and, (C) 20:80% (v:v) AHAP3/ETMOS xerogel with a TMOS overlayer film, immersed in 37 °C PBS (pH 7.4).

presence of the porous pH-sensing TMOS layer does not serve as an impediment to NO or proton transport through the gel.

2.3.5. *In vitro* Platelet Adhesion Studies

Platelet adhesion to slides coated with NO-releasing AHAP3/ETMOS (40:60%, v:v) xerogels with and without a TMOS overlayer was examined to evaluate the potential blood compatibility of the xerogel coatings. Representative scanning electron micrographs of platelet adhesion to the films are shown in Figure 2.5. After 1 h exposure to platelet enriched porcine plasma, platelet adhesion at both the single and two-layer NO-releasing films was significantly decreased compared to non-NO-releasing controls. As expected, NO contributes a strongly inhibitory effect on platelet adhesion, resulting in drastic reductions in overall coverage of platelets at xerogel coatings. As suggested by NO-flux measurements, the presence of the TMOS overcoat layer did not inhibit the effectiveness of the underlying NO-releasing film. In fact, TMOS-coated films showed slightly less platelet adhesion than AHAP3/ETMOS films (5.7 ± 1.5 versus 2.0 ± 0.9 percent coverage, respectively). Intravascular fiber optic pH sensors may be expected to exhibit similar biocompatibility benefits *in vivo* throughout the window of NO-release.

2.4. Conclusions

Introducing NO-release capability to a device implanted in the bloodstream may allow for significant reductions in platelet adhesion and thrombus formation at the material's surface and a concomitant improvement in the device's performance. For sensors, xerogel coatings modified with *N*-diazoniumdiolates provide a useful means of generating such NO release. To avoid the issue of low permeability observed for NO-releasing xerogel

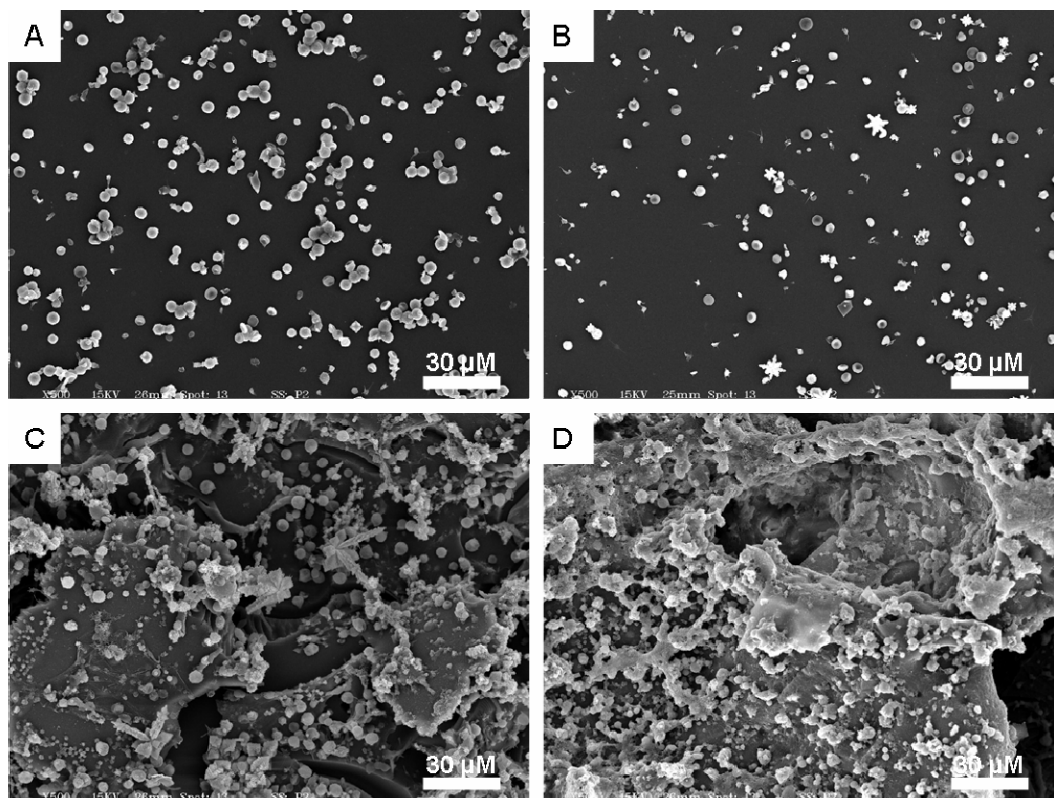


Figure 2.5. Representative scanning electron micrographs illustrating platelet adhesion to (A) NO-releasing and (C) control 40:60% (v:v) AHAP3/ETMOS films, and equivalent (B) NO-releasing and (D) control films with TMOS overcoats.

amperometric sensors, an optical sensing strategy was employed. Through straightforward dip-coating procedures, two-layer NO-releasing pH optical sensors were fabricated by depositing a porous pH-sensing xerogel layer over AHAP3/ETMOS NO-releasing xerogel-coated optical fibers. Sufficient resolution and response times were obtained from the resulting pH sensors after only a 30 s pretreatment step in sodium hydroxide solution. In vitro platelet adhesion studies indicated that the flux of NO ($>0.4 \text{ pmol cm}^{-2} \text{ s}^{-1}$ for 16 h) from the xerogel coatings was effective at reducing platelet adhesion. It is anticipated that the pH sensors and techniques described herein may be utilized in the fabrication of more biocompatible elements for intravascular blood gas sensor arrays and as the basic transduction mechanism for physiologically relevant chemical (e.g., CO_2 , NH_4^+) and enzyme-based (e.g., glucose, urea) biosensors.⁵⁰

2.5. References

- (1) Zhang, H. B.; Vincent, J. L. "Arteriovenous differences in PCO₂ and pH are good indicators of critical hypoperfusion." *American Review of Respiratory Disease* **1993**, *148*, 867-871.
- (2) Grundler, W.; Weil, M. H.; Rackow, E. C. "Arteriovenous carbon dioxide and pH gradients during cardiac arrest." *Circulation* **1986**, *74*, 1071-1074.
- (3) Ganter, M. T.; Hofer, C. K.; Zollinger, A.; Spahr, T.; Pasch, T.; Zalunardo, M. P. "Accuracy and performance of a modified continuous intravascular blood gas monitoring device during thoracoscopic surgery." *Journal of Cardiothoracic and Vascular Anesthesia* **2004**, *18*, 587-591.
- (4) Rithalia, S. V. S. "Developments in transcutaneous blood gas monitoring - A review." *Journal of Medical Engineering & Technology* **1991**, *15*, 143-153.
- (5) Ganter, M.; Zollinger, A. "Continuous intravascular blood gas monitoring: development, current techniques, and clinical use of a commercial device." *British Journal of Anaesthesia* **2003**, *91*, 397-407.
- (6) Frost, M. C.; Meyerhoff, M. E. "Implantable chemical sensors for real-time clinical monitoring: progress and challenges." *Current Opinion in Chemical Biology* **2002**, *6*, 633-641.
- (7) Udd, E. "An overview of fiber-optic sensors." *Review of Scientific Instruments* **1995**, *66*, 4015-4030.
- (8) Wolfbeis, O. S. "Fiber-optic chemical sensors and biosensors." *Analytical Chemistry* **2004**, *76*, 3269-3283.
- (9) Oropello, J. M.; Manasia, A.; Hannon, E.; Leibowitz, A.; Benjamin, E. "Continuous fiberoptic arterial and venous blood gas monitoring in hemorrhagic shock." *Chest* **1996**, *109*, 1049-1055.
- (10) Ishikawa, S.; Makita, K.; Nakazawa, K.; Amaha, K. "Continuous intra-arterial blood gas monitoring during oesophagectomy." *Canadian Journal of Anaesthesia-Journal Canadien D Anesthesie* **1998**, *45*, 273-276.
- (11) Weiss, I. K.; Fink, S.; Harrison, R.; Feldman, J. D.; Brill, J. E. "Clinical use of continuous arterial blood gas monitoring in the pediatric intensive care unit." *Pediatrics* **1999**, *103*, 440-445.
- (12) Wisniewski, N.; Reichert, M. "Methods for reducing biosensor membrane biofouling." *Colloids and Surfaces B-Biointerfaces* **2000**, *18*, 197-219.

- (13) Radomski, M. W.; Rees, D. D.; Dutra, A.; Moncada, S. "S-nitroso-glutathione inhibits platelet activation in vitro and in vivo." *British Journal of Pharmacology* **1992**, *107*, 745-749.
- (14) Marxer, S. M.; Rothrock, A. R.; Nablo, B. J.; Robbins, M. E.; Schoenfisch, M. H. "Preparation of nitric oxide (NO)-releasing sol-gels for biomaterial applications." *Chemistry of Materials* **2003**, *15*, 4193-4199.
- (15) Zhou, Z. R.; Meyerhoff, M. E. "Preparation and characterization of polymeric coatings with combined nitric oxide release and immobilized active heparin." *Biomaterials* **2005**, *26*, 6506-6517.
- (16) Mowery, K. A.; Schoenfisch, M. H.; Saavedra, J. E.; Keefer, L. K.; Meyerhoff, M. E. "Preparation and characterization of hydrophobic polymeric films that are thromboresistant via nitric oxide release." *Biomaterials* **2000**, *21*, 9-21.
- (17) Kelm, M.; Yoshida, K. In *Methods in Nitric Oxide Research*, Feelisch, M.; Stamler, J. S., Eds. John Wiley and Sons Inc.: New York, 1996; pp 47-58.
- (18) Shin, J. H.; Schoenfisch, M. H. "Improving the biocompatibility of in vivo sensors via nitric oxide release." *Analyt* **2006**, *131*, 609-615.
- (19) Hrabie, J. A.; Klose, J. R.; Wink, D. A.; Keefer, L. K. "New nitric oxide-releasing zwitterions derived from polyamines." *Journal of Organic Chemistry* **1993**, *58*, 1472-1476.
- (20) Frost, M. C.; Rudich, S. M.; Zhang, H. P.; Maraschio, M. A.; Meyerhoff, M. E. "In vivo biocompatibility and analytical performance of intravascular amperometric oxygen sensors prepared with improved nitric oxide-releasing silicone rubber coating." *Analytical Chemistry* **2002**, *74*, 5942-5947.
- (21) Schoenfisch, M. H.; Mowery, K. A.; Rader, M. V.; Baliga, N.; Wahr, J. A.; Meyerhoff, M. E. "Improving the thromboresistivity of chemical sensors via nitric oxide release: Fabrication and in vivo evaluation of NO-releasing oxygen-sensing catheters." *Analytical Chemistry* **2000**, *72*, 1119-1126.
- (22) Gifford, R.; Batchelor, M. M.; Lee, Y.; Gokulrangan, G.; Meyerhoff, M. E.; Wilson, G. S. "Mediation of in vivo glucose sensor inflammatory response via nitric oxide release." *Journal of Biomedical Materials Research Part A* **2005**, *75A*, 755-766.
- (23) Frost, M. C.; Batchelor, M. M.; Lee, Y. M.; Zhang, H. P.; Kang, Y. J.; Oh, B. K.; Wilson, G. S.; Gifford, R.; Rudich, S. M.; Meyerhoff, M. E. "Preparation and characterization of implantable sensors with nitric oxide release coatings." *Microchemical Journal* **2003**, *74*, 277-288.

- (24) Schoenfish, M. H.; Zhang, H. P.; Frost, M. C.; Meyerhoff, M. E. "Nitric oxide-releasing fluorescence-based oxygen sensing polymeric films." *Analytical Chemistry* **2002**, *74*, 5937-5941.
- (25) Brinker, J.; Scherer, G. *Sol-Gel Science*. Academic Press: New York, 1990; Vol. 1989.
- (26) Nablo, B. J.; Schoenfish, M. H. "Antibacterial properties of nitric oxide-releasing sol-gels." *Journal of Biomedical Materials Research Part A* **2003**, *67A*, 1276-1283.
- (27) Nablo, B. J.; Chen, T. Y.; Schoenfish, M. H. "Sol-gel derived nitric-oxide releasing materials that reduce bacterial adhesion." *Journal of the American Chemical Society* **2001**, *123*, 9712-9713.
- (28) Marxer, S. M.; Robbins, M. E.; Schoenfish, M. H. "Sol-gel derived nitric oxide-releasing oxygen sensors." *Analyst* **2005**, *130*, 206-212.
- (29) Shin, J. H.; Marxer, S. M.; Schoenfish, M. H. "Nitric oxide-releasing sol-gel particle/polyurethane glucose biosensors." *Analytical Chemistry* **2004**, *76*, 4543-4549.
- (30) Oh, B. K.; Robbins, M. E.; Nablo, B. J.; Schoenfish, M. H. "Miniaturized glucose biosensor modified with a nitric oxide-releasing xerogel microarray." *Biosensors & Bioelectronics* **2005**, *21*, 749-757.
- (31) Grattan, K. T. V.; Badini, G. E.; Palmer, A. W.; Tseung, A. C. C. "Use of sol-gel techniques for fiber-optic sensor applications." *Sensors and Actuators A-Physical* **1991**, *26*, 483-487.
- (32) MacCraith, B. D.; McDonagh, C. "Enhanced fluorescence sensing using sol-gel materials." *Journal of Fluorescence* **2002**, *12*, 333-342.
- (33) MacCraith, B. D.; McDonagh, C. M.; Okeeffe, G.; McEvoy, A. K.; Butler, T.; Sheridan, F. R. "Sol-gel coatings for optical chemical sensors and biosensors." *Sensors and Actuators B-Chemical* **1995**, *29*, 51-57.
- (34) Grant, S. A.; Glass, R. S. "A sol-gel based fiber optic sensor for local blood pH measurements." *Sensors and Actuators B-Chemical* **1997**, *45*, 35-42.
- (35) Golden, J. P.; Anderson, G. P.; Rabbany, S. Y.; Ligler, F. S. "An evanescent wave biosensor 2: Fluorescent signal acquisition from tapered fiber optic probes." *IEEE Transactions on Biomedical Engineering* **1994**, *41*, 585-591.
- (36) Hoffmann, P.; Dutoit, B.; Salathe, R. P. "Comparison of mechanically drawn and protection layer chemically etched optical fiber tips." *Ultramicroscopy* **1995**, *61*, 165-170.

- (37) Cazenave, J.; Mulvihill, J. In *The role of platelets in blood-biomaterial interactions*, Missirlis, Y.; Wautier, J.-L., Eds. Kluwer: Dordrecht, 1993; pp 69-80.
- (38) Parker, J. W.; Laksin, O.; Yu, C.; Lau, M. L.; Klima, S.; Fisher, R.; Scott, I.; Atwater, B. W. "Fiber-optic sensors for pH and carbon dioxide using a self-referencing dye." *Analytical Chemistry* **1993**, *65*, 2329-2334.
- (39) Schubert, U.; Husing, N.; Lorenz, A. "Hybrid inorganic-organic materials by sol-gel processing of organofunctional metal alkoxides." *Chemistry of Materials* **1995**, *7*, 2010-2027.
- (40) McDonagh, C.; Sheridan, F.; Butler, T.; MacCraith, B. D. "Characterisation of sol-gel-derived silica films." *Journal of Non-Crystalline Solids* **1996**, *194*, 72-77.
- (41) Sanchez-Barragan, I.; Costa-Fernandez, J. M.; Sanz-Medel, A. "Tailoring the pH response range of fluorescent-based pH sensing phases by sol-gel surfactants co-immobilization." *Sensors and Actuators B-Chemical* **2005**, *107*, 69-76.
- (42) Nivens, D. A.; Schiza, M. V.; Angel, S. M. "Multilayer sol-gel membranes for optical sensing applications: single layer pH and dual layer CO₂ and NH₃ sensors." *Talanta* **2002**, *58*, 543-550.
- (43) Cajlakovic, M.; Lobnik, A.; Werner, T. "Stability of new optical pH sensing material based on cross-linked poly(vinyl alcohol) copolymer." *Analytica Chimica Acta* **2002**, *455*, 207-213.
- (44) Wallace, P. A.; Elliott, N.; Uttamlal, M.; Holmes-Smith, A. S.; Campbell, M. "Development of a quasi-distributed optical fibre pH sensor using a covalently bound indicator." *Measurement Science & Technology* **2001**, *12*, 882-886.
- (45) Makote, R.; Collinson, M. M. "Organically modified silicate films for stable pH sensors." *Analytica Chimica Acta* **1999**, *394*, 195-200.
- (46) Lobnik, A.; Oehme, I.; Murkovic, I.; Wolfbeis, O. S. "pH optical sensors based on sol-gels: Chemical doping versus covalent immobilization." *Analytica Chimica Acta* **1998**, *367*, 159-165.
- (47) Ismail, F.; Malins, C.; Goddard, N. J. "Alkali treatment of dye-doped sol-gel glass films for rapid optical pH sensing." *Analyst* **2002**, *127*, 253-257.
- (48) Ramamurthi, A.; Lewis, R. S. "Nitric oxide inhibition of platelet deposition on biomaterials." *Biomedical Sciences Instrumentation* **1999**, *35*, 333-338.
- (49) Robbins, M. E.; Hopper, E. D.; Schoenfisch, M. H. "Synthesis and characterization of nitric oxide-releasing sol-gel microarrays." *Langmuir* **2004**, *20*, 10296-10302.

- (50) Muller, C.; Hitzmann, B.; Schubert, F.; Scheper, T. "Optical chemo- and biosensors for use in clinical applications." *Sensors and Actuators B-Chemical* **1997**, *40*, 71-77.

Chapter 3:

Preparation and Characterization of *S*-Nitrosothiol (RSNO)-Modified Xerogels

3.1. Introduction

A number of problems continue to hinder the biocompatibility of indwelling medical devices. Biofouling of implanted materials, such as surface-induced aggregation of adhesion proteins and platelets and onto intravascular stents and sensors, lead to significant functional impairment of device operation and potentially disastrous health effects such as vessel occlusion.^{1, 2} Even in the absence of thrombus formation, the foreign body response results in the sequestration of tissue-implanted biomaterials within a dense avascular collagen capsule, thereby limiting interaction of the device with the surrounding environment.^{3, 4} All implanted materials also carry with them bacteria and the risk of implant-associated infection. Alarmingly, indwelling medical devices are responsible for >1,000,000 hospital-acquired infections per year in the U.S. alone.⁵

Clearly, methods to increase material biocompatibility and reduce the threat of implant-associated infection are drastically needed. The integral role of nitric oxide (NO) in the physiological processes governing platelet activation, angiogenesis, and the phagocytotic response to microbial infection make NO uniquely qualified as a potentially universal means to overcome problems associated with medical implants. Nitric oxide-releasing polymeric coatings have proven to be an effective strategy for reducing the body's response to foreign materials and improving the integration of biomedical devices into surrounding blood and

tissue.⁶⁻⁸ Polymeric materials are most often modified to release NO through physical entrapment or covalent attachment of NO-donor functionalities such as nitrosamines, metal complexes, *S*-nitrosothiols, or *N*-diazoniumdiolates.⁹ Nitrogen-bound diazeniumdiolates (NONOates) have been the most widely studied of these NO-donors.⁹ Several NO-releasing biomedical coatings and sensors with demonstrated antithrombotic and antibacterial effects have been fabricated through incorporation of NONOate donors in polymeric materials.^{6, 8, 9} Though a convenient and efficient means of generating NO, NONOates are not without drawbacks. Controlling the flux of NO from these materials can be difficult. NO generation is highly pH dependent, and strategies for overcoming localized elevated pH due to regeneration of parent amines upon NONOate decomposition are required to maintain high NO fluxes.¹⁰ The inclusion of high concentrations of amines in *N*-diazoniumdiolated materials may also have undesirable cytotoxic effects on nearby tissue. For example, Nablo et al. reported a high instance of cell death among L929 mouse fibroblasts directly contacting amine-modified xerogel materials.¹¹ Cytotoxicity was partially alleviated upon modification of the amines to NONOate donors, indicating the amines, not NO, were the root cause of the cytotoxicity.

Though not as widely studied as NONOate-based coatings, *S*-nitrosothiols (RSNOs) provide an appealing alternative for providing NO-release capability to a material. Created via the reaction of thiols with reactive nitrogen oxide species (e.g., N_2O_3 , HNO_2), RSNOs formed on free thiols (e.g., *S*-nitrosoglutathione; GSNO) and cysteine residues of blood proteins (e.g., serum albumin) are speculated to function as the body's reservoir and means of transporting the short-lived NO free radical throughout the bloodstream.^{12, 13} Small molecule RSNOs such as *S*-nitroso-*N*-acetyl-L-cysteine (SNAC) have been studied widely as

NO delivery agents, and the solution phase antimicrobial^{14, 15} and antithrombotic¹⁶⁻¹⁸ effects of RSNO NO donors have been well characterized. Nitric oxide release from RSNOs may be initiated through a number of trigger mechanisms, including thermal and light-initiated homolytic cleavage of the S-N bond,¹⁹ catalytic reaction with Cu⁺,²⁰ or reaction with other thiols through a nitroxyl (HNO) intermediate.²¹ As a mimic of physiological NO transport in the body, toxicity concerns due to side-product formation or regeneration of the parent thiol upon RSNO decomposition are minimal compared to NONOate donors, which are known to form potentially toxic nitrosamines upon recombination with NO-oxidation reaction intermediates.²²

Despite the potential benefits of RSNOs, relatively few reports of RSNO-modified polymeric coatings for NO generation exist. Bohl and West reported the formation of *S*-nitrosocysteine-modified polyethylene glycol (PEG) hydrogels.²³ The hydrogels were capable of generating NO for short periods (4-12 h) and reduced smooth muscle cell adhesion on sections of angioplasty-damaged arteries in rat models.²⁴ A number of NO-releasing polymers were reported by de Oliveira and co-workers wherein small molecule RSNOs such as SNAC and *S*-nitrosogluthathione (GSNO) were dispersed in PEG or solid poly(vinyl alcohol)/poly(vinyl pyrrolidone) films.²⁵⁻²⁸ However, NO delivery was accomplished in these cases by rapid physical leaching of the hydrophilic small-molecule RSNO out of the polymer matrix into the soak media, making the materials of limited use as implant coatings. Photoswitchable NO-generating materials have been described by Frost and co-workers through the incorporation of RSNO-modified fumed silica particles in the central region of tri-layer polymer films.²⁹ Such films generated detectable NO fluxes only under bright illumination and were capable of maintaining NO fluxes $\geq 1.7 \text{ pmol cm}^{-2} \text{ s}^{-1}$ for

nearly 12 h with 40 W illumination. Seabra et al. reported polynitrosated polyesters with covalently attached RSNO functionalities capable of high initial rates of NO release (475 $\mu\text{mol g}^{-1} \text{h}^{-1}$ for 2 h) at physiological temperature.³⁰ The polyester macromolecules did not form solid films, but remained water-insoluble liquids best suited for transdermal NO delivery.

In this chapter, a novel class of polymeric *S*-nitrosothiol films, RSNO-modified xerogels, is evaluated as a new type of NO-releasing material for use in the production of more biocompatible medical implant devices. Xerogels are sol-gel derived polymeric materials formed through the catalytic hydrolysis and condensation of alkoxy-terminated silane precursors.³¹ Previous studies have examined NONOate-modified xerogel films as a means of imparting NO-release capability to biomedical sensors and devices. Unfortunately, these materials have suffered from relatively short durations of NO production under physiological conditions and may exhibit undesirable cytotoxicity due to high concentrations of surface amines.¹¹ In the present work, the production of RSNO-modified films formed via nitrosation of mercaptoalkoxysilane-derived xerogels is described. The stability and NO-release properties of RSNO-modified xerogels are characterized, and the resistance of the films to platelet and bacterial adhesion are examined and compared to previously described NONOate-based NO-releasing materials.

3.2. Materials and Methods

Mercaptopropyltrimethoxysilane (MPTMS), ethyltrimethoxysilane (ETMOS), and isobutyltrimethoxysilane (BTMOS) were purchased from Gelest (Tullytown, PA). Methyltrimethoxysilane (MTMOS) and diethylenetriamine-pentaacetic acid (DTPA) were

purchased from Fluka. Glutaraldehyde (50% w:w in water), hexamethyldisilazane (HMDS), and L-glutathione (reduced) were purchased from Aldrich (Milwaukee, WI). *Pseudomonas aeruginosa* (ATCC #19143) was obtained from American Type Culture Collection (Manassas, VA). Nitric oxide calibration gas (27.6 ppm; balance N₂) was purchased from National Welders Supply Co. (Durham, NC). Whole blood was obtained from healthy pigs at the Francis Owen Blood Research Laboratory (Chapel Hill, NC). Other solvents and chemicals were analytical-reagent grade and used as received. Distilled water was purified to 18.2 MΩ·cm with a Millipore Milli-Q Gradient A-10 water purification system (Bedford, MA).

3.2.1. Xerogel Film Synthesis

Sols containing 20-80% (v:v total silane) MPTMS (balance MTMOS) were created by shaking ethanol (800 μL), MTMOS (160-640 μL), MPTMS (640-160μL; total silane volume = 800 μL), and 0.5 mM HCl (25 μl) for 1 h. Sols were allowed to age under ambient conditions for an additional 0-6 h, and 30 μl aliquots were cast onto 9 x 25 mm² glass substrates previously sonicated 20 min in ethanol, dried under N₂, and UV/O₃ cleaned for 20 min in a BioForce TipCleaner (Ames, IA). Films were allowed to dry at room temperature overnight, and transferred to a 70 °C oven for 1-2 d.

3.2.2. Nitrosothiol Formation

Pendant thiols of MPTMS/MTMOS xerogels were nitrosated by reaction with acidified nitrite.³² Films were protected from light and incubated for fixed intervals in 2 mL 0.5 M HCl containing a 10-fold molar excess of NaNO₂ (vs. moles thiol) and 100 μM DTPA. The xerogels were washed 3 times with 100 μM DTPA_(aq) and stored in the dark at -20 °C

until use. Spectral characterization of RSNO formation was performed by affixing the slides normal to the light path of a PerkinElmer Lambda 40 UV/Vis Spectrophotometer (Norwalk, CT) in cuvettes containing 2 mL phosphate buffered saline (PBS; 10mM phosphate, pH 7.4). Characteristic RSNO absorbance bands ($n_0 \rightarrow \pi^*$ and $n_N \rightarrow \pi^*$)^{33, 34} were monitored as a function of nitrosation reaction time and percentage mercaptosilane in the xerogel.

3.2.3. *Characterization of NO Release*

Real-time NO release from RSNO-modified xerogels was monitored using a Sievers NOA™ 280 Chemiluminescence Nitric Oxide Analyzer (Boulder, CO). Calibration of the instrument was performed daily using air passed through a Sievers NO zero filter and 27.6 ppm NO gas (balance N₂). Individual slides were immersed in 30 mL pH 7.4 PBS containing 100 μM DTPA and sparged with a 200 mL/min N₂ stream. Temperature control was achieved by immersing the sample flask in a water bath maintained between 0 and 37 °C. Chemiluminescence due to NO was monitored continuously in 1 s intervals. Thiol-initiated RSNO decomposition was monitored by the inclusion of 500 μM glutathione (GSH).

3.2.4. *Xerogel Film Stability*

Nitrosated xerogel films on glass slides (N = 5) were immersed in 10 mL pH 7.4 PBS and incubated at 37 °C. Films were removed and transferred to fresh solutions of PBS at fixed intervals. Leached Si concentrations in the PBS soak solutions were determined using a direct current plasma optical emission spectrometer (DCP-OES; ARL-Fisons Spectraspan 7; Beverly, MA) calibrated with 0–50 ppm Si standard solutions in PBS.

3.2.5. Bacterial Adhesion to RSNO Xerogels

P. aeruginosa was cultured at 37 °C in tryptic soy broth (TSB), pelleted by centrifugation, resuspended in 15% glycerol (v:v in PBS), and stored at -80 °C. Cultures for bacterial adhesion studies were grown from a -80 °C stock in 37 °C TSB overnight. A 1 mL aliquot of overnight culture was inoculated into 100 mL fresh TSB, incubated at 37 °C with rotation, and grown to a concentration of $\sim 10^8$ colony-forming units (cfu)/mL (verified by 10-fold serial dilutions in PBS, plating on tryptic soy agar nutrient plates, and subsequent cfu enumeration). The bacteria were pelleted by centrifugation, rinsed with ultrapure water, and resuspended in sterile PBS. Control and RSNO-modified xerogels were immersed in 4-mL aliquots of bacterial suspension and incubated at 37 °C. After 1 h, the xerogel substrates were removed from the bacterial suspension, gently immersed in ultrapure water to remove loosely-adhered cells, and gently dried under a stream of N₂. To quantify bacterial adhesion, substrates were imaged in phase-contrast mode with a Zeiss Axiovert 200 inverted optical microscope (Chester, VA) at 20x magnification. Digital micrographs were captured with a Zeiss AxioCam digital camera (Chester, VA). To determine the percent surface coverage of bacteria, each image was digitally processed by applying a threshold value to differentiate adhered cells from the background. The number of pixels corresponding to adhered bacterial cells was digitally enumerated and the extent of bacterial adhesion reported as the percent of the xerogel substrate surface covered with bacterial cells. For the time-based adhesion studies 60% MPTMS xerogels were incubated in PBS supplemented with 500 μM GSH for 24 h prior to the 1 h adhesion experiment described above.

3.2.6. Platelet Adhesion to RSNO Xerogels

Healthy porcine blood was drawn into acid citrate dextrose (ACD)-anticoagulated tubes (7:60 v:v, ACD:whole blood) and maintained in ambient conditions up to 30 min before use. Platelet enriched plasma (PRP) was obtained by centrifugation at 400g for 20 min at room temperature.³⁵ Normal platelet activity was reestablished by incubation with 2.0 mM $\text{CaCl}_2 \cdot 2\text{H}_2\text{O}$ at 37 °C for 5 min. Nitrosated xerogel films and controls were incubated in 2 mL PRP at 37 °C for 1 h. The PRP was carefully removed and the slides were washed thrice with 37 °C Tyrodes Buffer (137 mM NaCl, 2.7 mM KCl, 5.6 mM glucose, 3.3 mM KCl, pH 7.35). Adhered platelets were fixed by incubating with 1% glutaraldehyde solution (v:v, Tyrodes buffer) at 37 °C for 30 min. The films were rinsed with Tyrodes buffer and immersed twice in fresh Tyrodes buffer and once in Milli-Q water to minimize remaining non-adherent cells. To preserve cell morphology, the slides were chemically dried by exposure to 50, 75, and 95 and 100% ethanol (v:v, water) for 5 min. Phase-contrast images of adhered platelets were obtained at 20x magnification. Percent platelet surface coverages on nitrosated xerogels and controls were calculated via digital image processing and black/white thresholding as described above.

3.3. Results and Discussion

3.3.1. Xerogel Characterization

The relative ease of xerogel modification through variation of alkoxy silane precursors makes sol-gel chemistry a convenient scaffold for the production of NO-releasing materials and a versatile material for use in biomedical sensors and devices. In these experiments, sols were created using mercaptopropyltrimethoxysilane (MPTMS), a commercially available

thiol-terminated alkoxy silane, in conjunction with three alkylalkoxysilanes: methyltrimethoxysilane (MTMOS), ethyltrimethoxysilane (ETMOS), and isobutyltrimethoxysilane (BTMOS). The structures of these molecules are illustrated Figure 3.1. Incorporation of alkylalkoxysilanes as an inert polymer backbone material allows control over the NO fluxes generated by the material and has previously been used as a means of increasing the stability of NONOate-modified xerogel films.³⁶ While all sols appeared to form homogenous gels, curing of xerogel films formed with the bulky ETMOS and BTMOS alkylalkoxysilanes required prohibitively long periods, most likely due to the decreased rates of hydrolysis of sterically hindered alkoxy silanes.³¹ Even after overnight aging of the sol, films cast from these materials and stored in a 70 °C oven for >2 weeks remained viscous and tacky. Conversely, MPTMS/MTMOS sols aged 1-5 h rapidly solidified overnight under ambient conditions and formed clear, rigid films after 2 d drying at 70 °C. As such, MTMOS was selected as the backbone alkoxy silane in all further experiments.

To establish conditions for optimal RSNO formation in the xerogel, films were prepared containing 20, 40, 60, and 80% (v:v total silane) MPTMS. Nitrosation of the primary thiol of MPTMS was carried out by immersing the cured xerogel films in a solution of acidified nitrite containing 100 μ M DTPA to reduce catalytic RSNO decomposition by adventitious Cu^+ ions. Reaction of the pendant thiols of the xerogel network with nitrous acid resulted in *S*-nitrosothiol formation (Eq. 3.1), and was accompanied by a concomitant color shift of the transparent xerogel film to a deep pink hue.



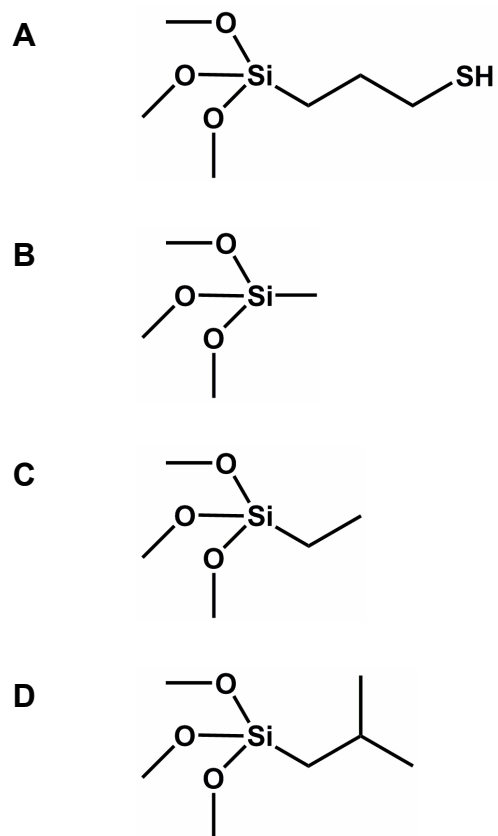


Figure 3.1. Chemical structures of (A) mercaptopropyltrimethoxysilane (MPTMS); (B) methyltrimethoxysilane (MTMOS); (C) ethyltrimethoxysilane (ETMOS); and (D) isobutyltrimethoxysilane (BTMOS).

The characteristic UV and visible absorbance maxima of the S-NO bond (at 336 and 545 nm, respectively) were monitored as a measure of the extent of thiol nitrosation. After 3 h immersion in acidified nitrite, no further absorbance increases in the films were observed, indicating maximal RSNO formation (data not shown). Extended soaking periods up to 24 h resulted in an overall decrease in measured absorbance. Such decrease was attributed to thermal decomposition of formed RSNOs. As shown in Figure 3.2, increasing the concentration of MPTMS in the xerogel films resulted in increased absorbance after nitrosation. A darker pink coloration of the more heavily thiol-functionalized films was readily apparent. The color shift associated with nitrosation may thus provide a useful indication of the concentration of RSNOs (and thus NO-release potential) in a xerogel film.

Nitric oxide production from the RSNO-modified xerogels was measured via chemiluminescence as a real-time flux from individual films immersed in 37 °C pH 7.4 PBS/DTPA containing physiological concentrations of glutathione. Glutathione is the most common free thiol present in blood (~500 μ M in healthy adults),³⁷ and is believed to be one of the main small-molecule thiol sources for endogenous RSNO formation.³⁸ Previous studies have indicated RSNO reaction with GSH as a potential pathway for NO production through an intermediate HNO species.²¹ Average NO fluxes from xerogel films prepared with 20-80% (v:v total silane) MPTMS are shown in Figure 3.3. As expected, NO generation was found to scale with the percentage of MPTMS incorporated in the film, mirroring the increased absorbances shown in Figure 3.2. In all cases, maximum NO flux was achieved within several minutes of xerogel immersion. Subsequent NO production decreased exponentially. In 37 °C PBS, significant NO fluxes were maintained from the RSNO-modified films for extended periods. Films incorporating 40 and 80% MPTMS were

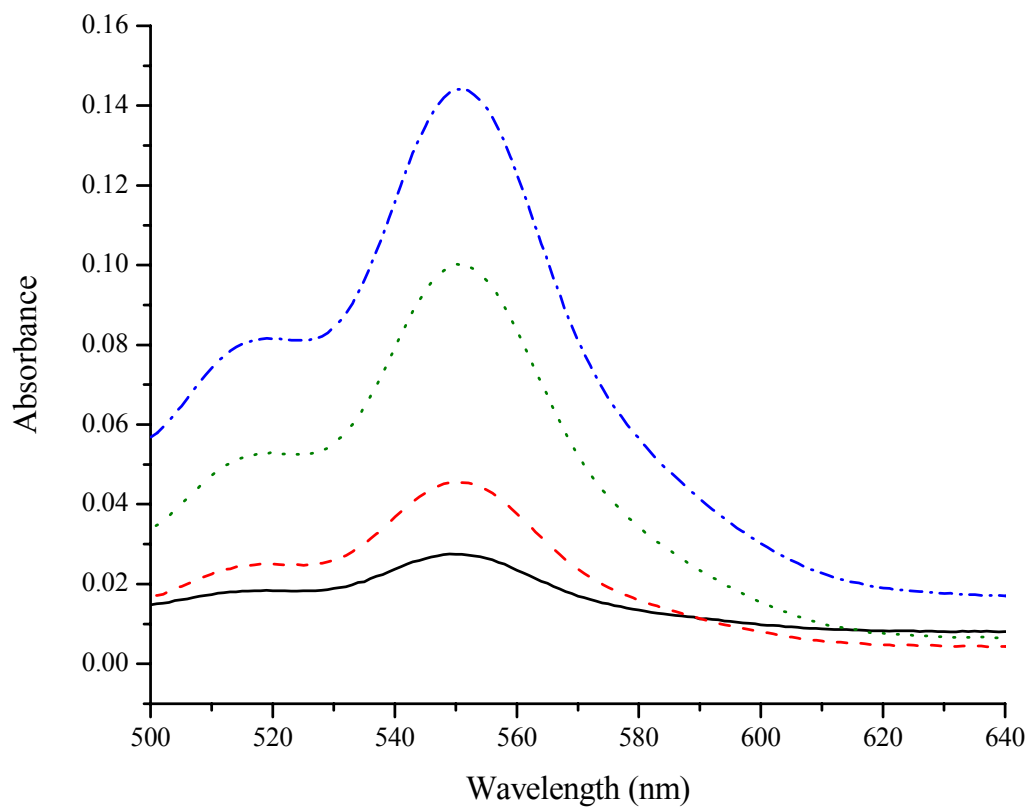


Figure 3.2. Absorbance spectrum of MTMOS films containing (—) 20% MPTMS; (---) 40% MPTMS; (···) 60% MPTMS; and (-·-) 80% MPTMS (v:v total silane).

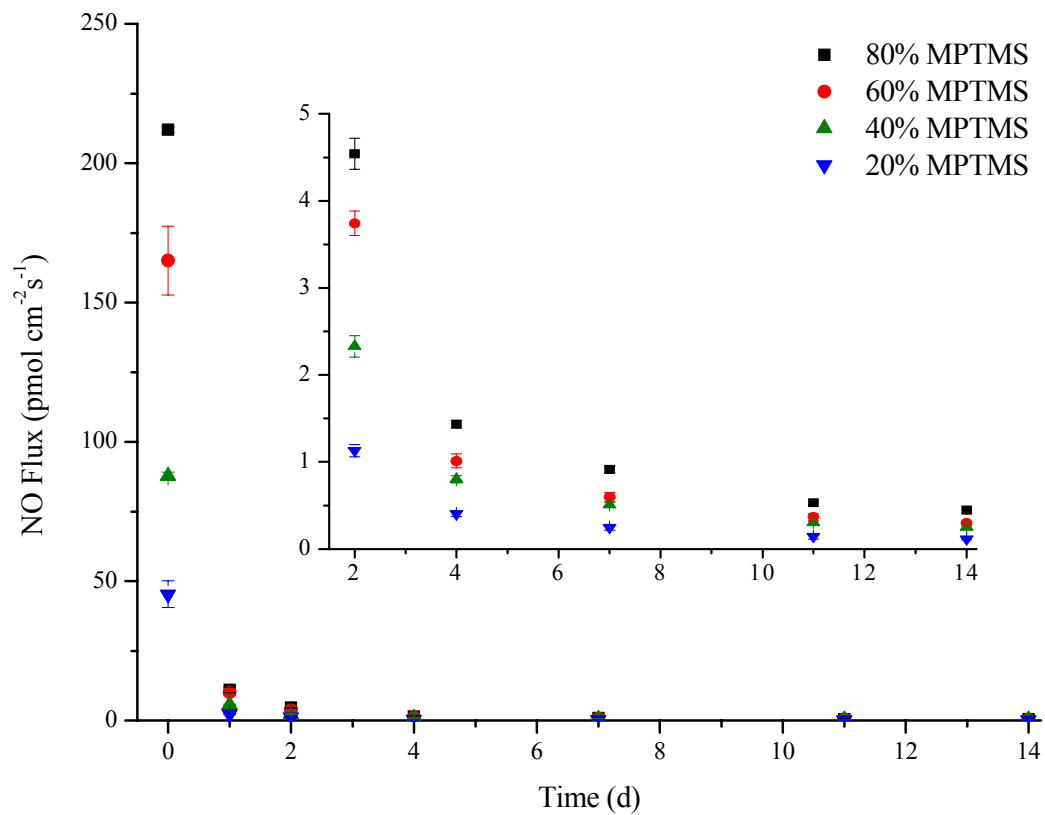


Figure 3.3. Average NO flux from RSNO-modified MPTMS/MTMOS films in 37 °C PBS/DTPA. Data points correspond to the average of 3 films incorporating (■) 80%; (●) 60%; (▲) 40% and (▼) 20% MPTMS (v:v total silane). [Inset: Magnified view of 2 – 14 d NO release.]

capable of maintaining fluxes $>0.5 \text{ pmol cm}^{-2} \text{ s}^{-1}$ for ~ 7 d and 14 d, respectively. Such a duration of NO-release is a significant improvement over previously reported NONOate-modified xerogels, wherein films of comparable thickness reached equivalent NO fluxes after only 24-72 h.^{7,39}

The presence of free thiol in solution was found to have negligible effect on NO-generation from RSNO-modified xerogel films as indicated by no observable change in NO production between films run in pure PBS or 500 μM GSH (data not shown). As free thiol concentration was previously reported to have direct effects on NO production from RSNOs,²¹ the data indicate that the xerogel network may be sufficiently cross-linked to prohibit penetration of GSH into the xerogel interior. Nitric oxide release was measured from films in the presence of DTPA copper chelator and protected from light, indicating the observed NO production proceeds via thermal-initiated homolytic cleavage of the RS-NO bond. Indeed, NO production from RSNO-modified xerogel films was found to be highly temperature dependent (Figure 3.4). Thermal decomposition is not surprising as primary *S*-nitrosothiols are known to be quite thermally labile in the absence of intramolecular hydrogen bonding.⁴⁰ The rapid initial burst of NO production observed may also be indicative of an autocatalytic reaction between freshly-formed $\text{RS}\cdot$ and neighboring RSNO groups:⁴⁰



Due to the covalent immobilization of RSNO in the xerogel network, however, this effect would be expected to occur only over short time scales before the population of directly adjacent RSNOs is depleted.

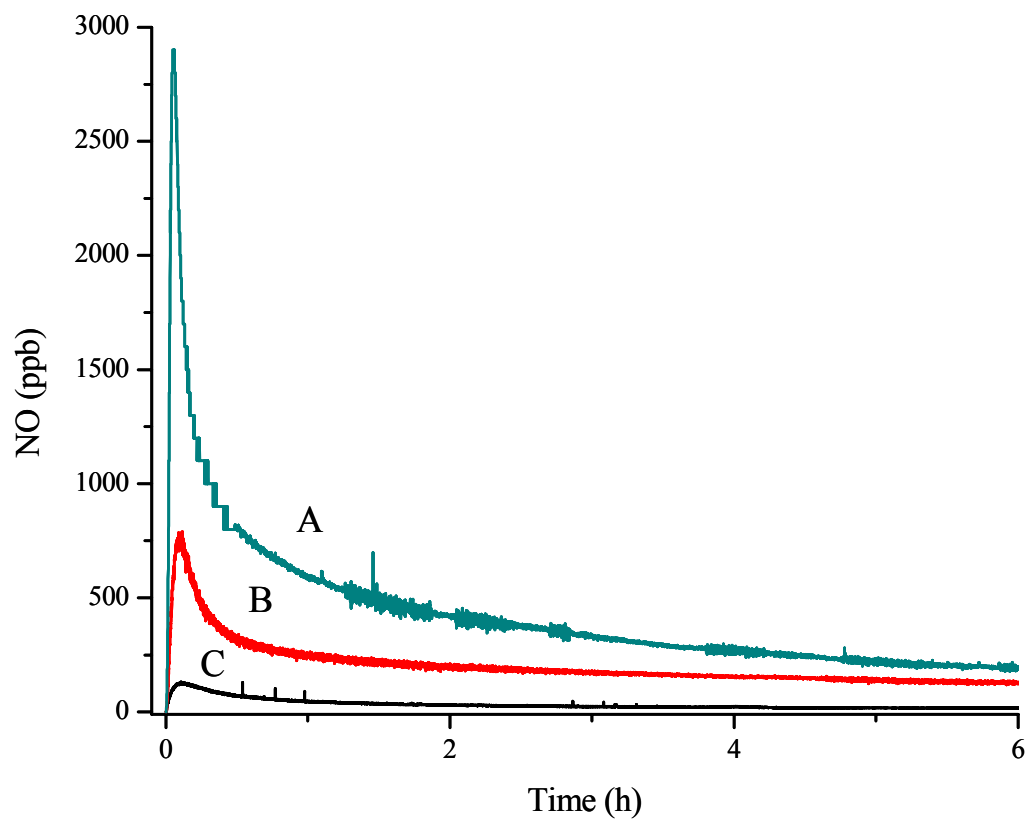


Figure 3.4. Nitric oxide flux from RSNO-modified 40% (v:v total silane) MPTMS/MTMOS films in pH 7.4 PBS / 100 μ M DTPA solutions held at (A) 37 $^{\circ}$ C; (B) 25 $^{\circ}$ C; or (C) 0 $^{\circ}$ C.

The long-term stability of RSNO-modified xerogels in 37 °C PBS solution was monitored by tracking siloxane network degradation through DCP-OES detection of leached Si. After two weeks immersion, solutions in which 20-80% MPTMS/MTMOS films had been soaked showed negligible levels of xerogel fragmentation (<0.5 ppm). In fact, detected Si in xerogel soak solutions was reduced compared to control samples containing only bare glass substrates, ostensibly due to masking of ~50% of the glass surface by the xerogel films. This level of stability is a marked improvement over previously described NONOate-modified xerogel films in which significant fragmentation (8.2 mol %) was observed after 14 d.³⁶

3.3.2. *Antibacterial Properties of RSNO-Xerogels*

Implant-associated infection remains a serious problem in the U.S., with indwelling devices responsible for nearly half of the cases of nosocomial infection reported annually.⁵ As these infections are a direct result of bacterial adhesion to implant materials, many active and passive strategies have been employed to decrease the amount of adherent bacteria on medical devices.^{8,41} Nitric oxide is one such strategy, and materials modified with NONOate donors have previously shown promising reductions in surface bacterial adhesion compared to non-NO-releasing controls.⁴²⁻⁴⁴ To evaluate the antibacterial properties of RSNO-modified xerogel films, the adhesion of *P. aeruginosa*, a common opportunistic pathogen, was evaluated on 60% MPTMS films exposed to highly concentrated ($\sim 10^8$ cfu) bacterial suspensions both during initial periods of peak NO production and after 24 h immersion in 37 °C PBS/GSH (to reduce overall NO fluxes from the films). Statistically significant reductions ($P < 0.05$) of average bacterial surface coverage on RSNO-modified films versus non-nitrosated controls were observed in both cases (Figure 3.5). Non-nitrosated control

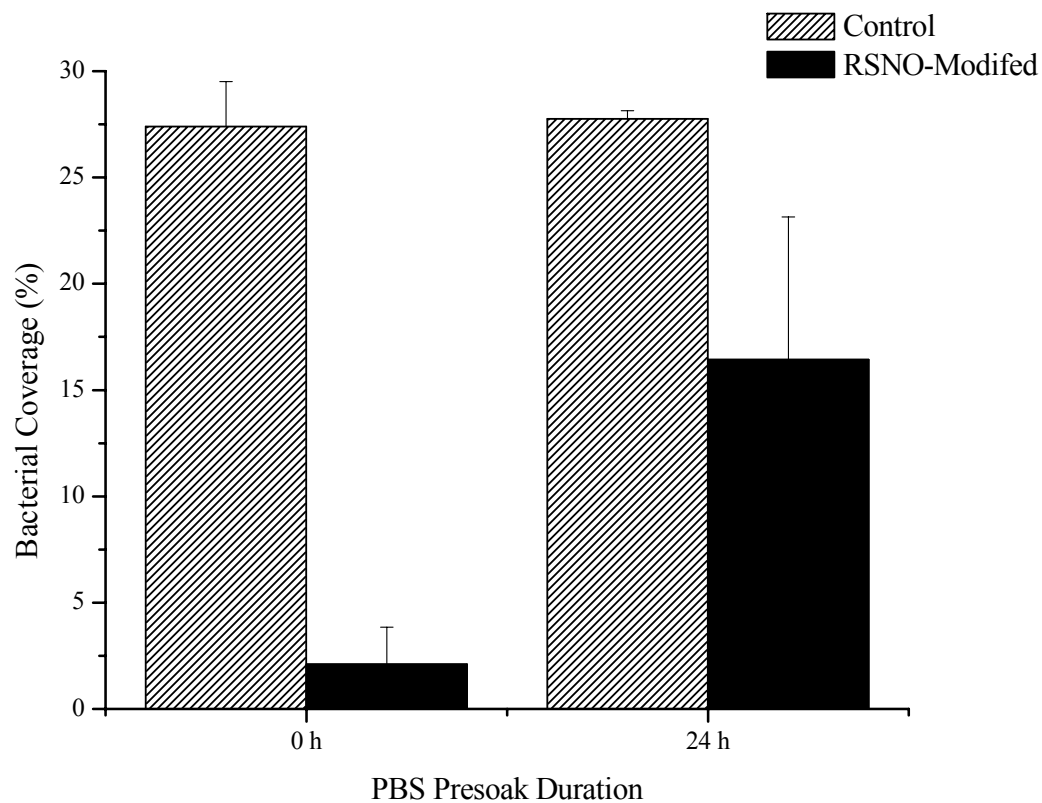


Figure 3.5. Average *P. aeruginosa* adhesion to 60% (v:v total silane) MPTMS/MTMOS films during 1 h immersion in $\sim 10^8$ cfu/mL bacterial suspensions. Average values were calculated from the mean of 5 images on control or RSNO-modified films (N = 3) soaked 0 or 24 h in 37 °C PBS/GSH.

films presoaked for 0 and 24 h were both characterized by average surface coverages of ~27%, indicating no significant change in the surface properties of the thiol-terminated films during extended exposure to PBS and GSH. During this period, an approximate 16 fold reduction in average NO-flux from the nitrosated films (from ~165 to ~10 pmol cm⁻²s⁻¹) resulted in an increase of observed bacterial surface coverage on the RSNO-modified films from 4 ± 2 to 16 ± 7%, respectively. This behavior is consistent with previous data showing reductions of bacterial adhesion to NO-releasing surfaces to be highly flux dependent.⁴² Although the exact mechanism of the antibacterial effects of NO-releasing films is unknown, NO's effect likely involves membrane damage due to lipid peroxidation⁴⁵ or protein inactivation through nitrosation of key tyrosine and cysteine residues by the reactive oxidation products of NO.⁴⁶ Direct transnitrosation reactions between RSNOs at the xerogel surface and bacterial thiols are possible,⁴⁷ and may account for some of the observed reduction in bacterial coverage at RSNO-xerogels. However, the majority of readily-accessible surface RSNOs are likely depleted after 24 immersion in PBS/GSH via thermal homolytic cleavage and transnitrosation reactions with solution GSH. We thus expect the observed antibacterial effects at longer periods are mediated by free NO radical. Of note, the antibacterial properties of RSNO-modified films are maintained when exposed to concentrated bacterial suspensions for extended periods. Previous studies using NONOate modified xerogels reported a general downward trend in bacterial adhesion to both control and NO-releasing surfaces when exposed to bacterial solutions for up to 4 h. This decrease in adhesion was attributed to both changes in the surface properties of the hydrated films and alterations in bacterial metabolism and protein expression during long-term suspension in nutrient poor PBS.⁴⁴ We observed a similar trend with RSNO-modified films. However,

whereas some NONOate-modified films showed insignificant antibacterial effects after as little as 1 h bacterial exposure,⁴⁴ the bacterial surface coverage of RSNO-modified xerogels remained approximately half that of non-nitrosated controls (1.3 ± 1.0 vs. $3.5 \pm 1.2\%$, respectively) during a full 24 h exposure to concentrated bacterial suspensions. This window of decreased bacterial adhesion is well in excess of the decisive “best treatment” period 6 h after device implantation during which introduced pathogens remain metabolically inactive.⁴⁸ Thus, RSNO-modified xerogel coatings may provide a useful means of reducing bacterial adhesion to implanted biomedical devices during the period most critical to reducing implant-associated infection.

3.3.3. *Antithrombotic Properties of RSNO Xerogels*

Another significant impediment to the practical application of indwelling vascular medical devices is the tendency for platelets to activate and adhere to the material surface.⁴⁹ Such buildup is problematic for vascular grafts and stents as it restricts blood flow and may ultimately result in vessel occlusion.⁵⁰ Likewise, platelet aggregation on intravascular sensors forms an effective barrier between sensor and analyte, leading to significantly impaired sensitivity to the surrounding environment.² Nitric oxide’s inhibitory role in the platelet activation cascade provides a promising solution to such issues. Multiple polymer coatings have displayed decreased thrombogenicity after modification to release NO via NONOate donor inclusion^{10, 51-53} or catalytically generate NO from blood components.⁵⁴ While small-molecule RSNO compounds have been widely studied as inhibitors of free platelet aggregation,⁵⁵⁻⁵⁷ limited studies have examined platelet aggregation to RSNO-modified surfaces. Bohl et al. demonstrated reductions in platelet adhesion to collagen-coated glass surfaces after incubation of whole blood samples with RSNO-doped hydrogel

materials, but platelet adhesion to the hydrogel material itself was not described.²³ Lewis and co-workers reported reductions in platelet adhesion to polyurethane and poly(ethylene terephthalate) polymers containing immobilized cysteines.^{58, 59} However, such materials were used to generate NO from a reservoir of solution RSNOs, and were not modified with RSNOs prior to the experiment.

The effect of RSNO inclusion on platelet adhesion to xerogel materials was examined by exposing 40% MPTMS/MTMOS (v:v total silane) xerogel films to platelet-rich porcine plasma for 1 h. Representative phase contrast images of platelet adhesion to RSNO-modified surfaces and non-nitrosated controls are shown in Figure 3.6. In general, overall platelet adhesion to MPTMS/MTMOS xerogels was quite low even at the elevated 2mM Ca²⁺ concentrations used to increase platelet activation in the experiment. Nevertheless, modification with RSNO resulted in an approximate 50% decrease in average platelet coverage on nitrosated films versus controls (2.48 ± 1.16 vs. $4.61 \pm 1.72\%$, respectively; $P < 0.05$), as determined from the mean platelet surface coverage of 6 images per film (N = 8). The 50% reduction of platelet adhesion to RSNO-modified films versus controls is slightly lower than that seen previously for NONOate-modified xerogel films despite overall increased NO flux during the period of PRP exposure.^{60, 61} This smaller reduction may be attributed to the decreased overall adhesion observed at thiol-terminated controls versus amine-terminated NONOate xerogels and is in agreement with previous observations that reductions in platelet adhesion are not achieved at NO-releasing surfaces beyond a certain NO flux threshold.⁶¹ As discussed previously, during initial exposure to RSNO-modified films direct transnitrosation between surface xerogel RSNOs and thiol residues on plasma and platelet proteins may occur. At longer time scales, however, the majority of RSNO-

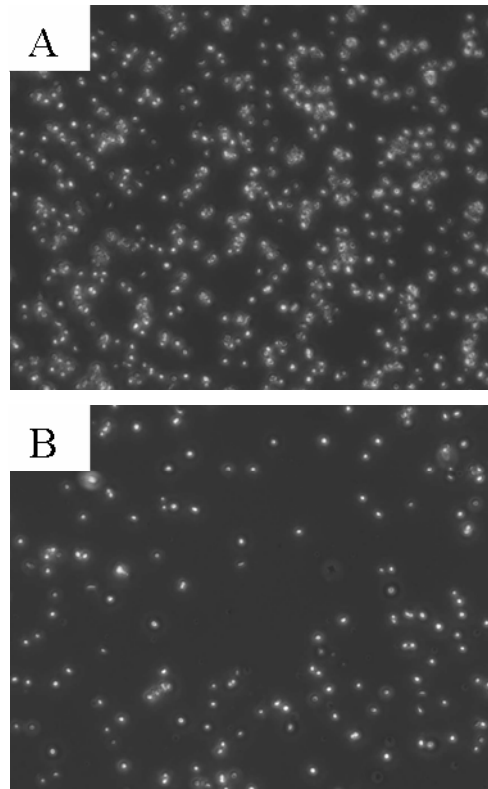


Figure 3.6. Representative phase-contrast images of platelet adhesion to (A) control and (B) RSNO-modified 40% (v:v total silane) MPTMS/MTMOS films after 1 h exposure to porcine PRP.

modified xerogel films antithrombotic activity would be expected to result from NO generated from the inaccessible interior of the xerogel. Previous work has found that NO fluxes as low as $0.4 \text{ pmol/cm}^2\text{s}$ are adequate for maintaining thromboresistive effects at a material surface.⁶¹ Nitric oxide release experiments indicate that RSNO-modified xerogels maintain fluxes over this threshold for up to 2 weeks. During in vivo application, minimum NO flux requirements are likely to increase due to rapid NO scavenging by other free radicals, thiols, and heme proteins in blood.⁶² Nevertheless, the low thrombogenicity and extended NO-release durations observed indicate the use of RSNO-modified xerogel coatings represents an effective strategy for reducing platelet adhesion to implanted biomaterial surfaces.

3.4. Conclusions

Nitric oxide-releasing polymer coatings have been shown to reduce biofouling and improve the performance of indwelling biomedical devices. We have developed RSNO-modified xerogel films as a novel and versatile class of NO-releasing materials. Formed via condensation and subsequent nitrosation of mercaptoalkoxysilane precursors, RSNO-modified xerogels showed tunable NO-release profiles with significantly improved durations of NO generation and solution stability compared to previously described NO-releasing xerogel films. The antibacterial and antithrombotic benefits expected of NO-releasing materials were confirmed. The power of sol-gel chemistry lies in its versatility. Future work will focus on further exploring the range of NO-release characteristics attainable through modification of the mercaptoalkoxysilane and alkylalkoxysilane precursors employed. Studies evaluating the potential benefits of RSNO-modified materials as a means of

enhancing tissue compatibility and controlling the foreign body response during in vivo application are currently underway.

3.5. References

- (1) Wisniewski, N.; Reichert, M. "Methods for reducing biosensor membrane biofouling." *Colloids and Surfaces B-Biointerfaces* **2000**, *18*, 197-219.
- (2) Frost, M. C.; Meyerhoff, M. E. "Implantable chemical sensors for real-time clinical monitoring: progress and challenges." *Current Opinion in Chemical Biology* **2002**, *6*, 633-641.
- (3) Ratner, B. D.; Bryant, S. J. "Biomaterials: Where we have been and where we are going." *Annual Review of Biomedical Engineering* **2004**, *6*, 41-75.
- (4) Ratner, B. D. "Reducing capsular thickness and enhancing angiogenesis around implant drug release systems." *Journal of Controlled Release* **2002**, *78*, 211-218.
- (5) Darouiche, R. O. "Current concepts - Treatment of infections associated with surgical implants." *New England Journal of Medicine* **2004**, *350*, 1422-1429.
- (6) Frost, M. C.; Reynolds, M. M.; Meyerhoff, M. E. "Polymers incorporating nitric oxide releasing/generating substances for improved biocompatibility of blood-contacting medical devices." *Biomaterials* **2005**, *26*, 1685-1693.
- (7) Hetrick, E. M.; Prichard, H. L.; Klitzman, B.; Schoenfisch, M. H. "Reduced foreign body response at nitric oxide-releasing subcutaneous implants." *Biomaterials* **2007**, *28*, 4571-4580.
- (8) Hetrick, E. M.; Schoenfisch, M. H. "Reducing implant-related infections: active release strategies." *Chemical Society Reviews* **2006**, *35*, 780-789.
- (9) Shin, J. H.; Schoenfisch, M. H. "Improving the biocompatibility of in vivo sensors via nitric oxide release." *Analyst* **2006**, *131*, 609-615.
- (10) Batchelor, M. M.; Reoma, S. L.; Fleser, P. S.; Nuthakki, V. K.; Callahan, R. E.; Shanley, C. J.; Politis, J. K.; Elmore, J.; Merz, S. I.; Meyerhoff, M. E. "More lipophilic dialkyldiamine-based diazeniumdiolates: Synthesis, characterization, and application in preparing thromboresistant nitric oxide release polymeric coatings." *Journal of Medicinal Chemistry* **2003**, *46*, 5153-5161.
- (11) Nablo, B. J.; Schoenfisch, M. H. "In vitro cytotoxicity of nitric oxide-releasing sol-gel derived materials." *Biomaterials* **2005**, *26*, 4405-4415.
- (12) Stamler, J. S. "S-nitrosothiols in the blood - Roles, amounts, and methods of analysis." *Circulation Research* **2004**, *94*, 414-417.

- (13) Tyurin, V. A.; Tyurina, Y. Y.; Liu, S. X.; Bayir, H.; Hubel, C. A.; Kagan, V. E. Quantitation of S-nitrosothiols in cells and biological fluids. In *Redox Cell Biology and Genetics, Part A*, 2002; Vol. 352, pp 347-360.
- (14) Fang, F. C. "Antimicrobial reactive oxygen and nitrogen species: Concepts and controversies." *Nature Reviews Microbiology* **2004**, *2*, 820-832.
- (15) de Souza, G. F. P.; Yokoyama-Yasunaka, J. K. U.; Seabra, A. B.; Miguel, D. C.; de Oliveira, M. G.; Uliana, S. R. B. "Leishmanicidal activity of primary S-nitrosothiols against *Leishmania major* and *Leishmania amazonensis*: Implications for the treatment of cutaneous leishmaniasis." *Nitric Oxide-Biology and Chemistry* **2006**, *15*, 209-216.
- (16) Langford, E. J.; Brown, A. S.; Wainwright, R. J.; Debelder, A. J.; Thomas, M. R.; Smith, R. E. A.; Radomski, M. W.; Martin, J. F.; Moncada, S. "Inhibition of Platelet Activity by S-Nitrosoglutathione During Coronary Angioplasty." *Lancet* **1994**, *344*, 1458-1460.
- (17) Salas, E.; Moro, M. A.; Askew, S.; Hodson, H. F.; Butler, A. R.; Radomski, M. W.; Moncada, S. "Comparative pharmacology of analogs of S-nitroso-N-acetyl-DL-penicillamine on human platelets." *British Journal of Pharmacology* **1994**, *112*, 1071-1076.
- (18) Radomski, M. W.; Rees, D. D.; Dutra, A.; Moncada, S. "S-Nitroso-glutathione inhibits platelet activation in vitro and in vivo." *British Journal of Pharmacology* **1992**, *107*, 745-749.
- (19) Wood, P. D.; Mutus, B.; Redmond, R. W. "The mechanism of photochemical release of nitric oxide from S-nitrosoglutathione." *Photochemistry and Photobiology* **1996**, *64*, 518-524.
- (20) Singh, R. J.; Hogg, N.; Joseph, J.; Kalyanaraman, B. "Mechanism of nitric oxide release from S-nitrosothiols." *Journal of Biological Chemistry* **1996**, *271*, 18596-18603.
- (21) Wong, P. S. Y.; Hyun, J.; Fukuto, J. M.; Shirota, F. N.; DeMaster, E. G.; Shoeman, D. W.; Nagasawa, H. T. "Reaction between S-nitrosothiols and thiols: Generation of nitroxyl (HNO) and subsequent chemistry." *Biochemistry* **1998**, *37*, 5362-5371.
- (22) Mowery, K. A.; Schoenfisch, M. H.; Saavedra, J. E.; Keefer, L. K.; Meyerhoff, M. E. "Preparation and characterization of hydrophobic polymeric films that are thromboresistant via nitric oxide release." *Biomaterials* **2000**, *21*, 9-21.
- (23) Bohl, K. S.; West, J. L. "Nitric oxide-generating polymers reduce platelet adhesion and smooth muscle cell proliferation." *Biomaterials* **2000**, *21*, 2273-2278.

- (24) Masters, K. S. B.; Lipke, E. A.; Rice, E. E. H.; Liel, M. S.; Myler, H. A.; Zygourakis, C.; Tulis, D. A.; West, J. L. "Nitric oxide-generating hydrogels inhibit neointima formation." *Journal of Biomaterials Science-Polymer Edition* **2005**, *16*, 659-672.
- (25) Shishido, S. M.; de Oliveira, M. G. "Polyethylene glycol matrix reduces the rates of photochemical and thermal release of nitric oxide from S-nitroso-N-acetylcysteine." *Photochemistry and Photobiology* **2000**, *71*, 273-280.
- (26) Shishido, S. M.; Seabra, A. B.; Loh, W.; de Oliveira, M. G. "Thermal and photochemical nitric oxide release from S-nitrosothiols incorporated in pluronic F127 gel: potential uses for local and controlled nitric oxide release." *Biomaterials* **2003**, *24*, 3543-3553.
- (27) Seabra, A. B.; Da Rocha, L. L.; Eberlin, M. N.; De Oliveira, M. G. "Solid films of blended poly(vinyl alcohol)/poly(vinyl pyrrolidone) for topical S-nitrosoglutathione and nitric oxide release." *Journal of Pharmaceutical Sciences* **2005**, *94*, 994-1003.
- (28) Seabra, A. B.; Pankotai, E.; Feher, M.; Somlai, A.; Kiss, L.; Biro, L.; Szabo, C.; Kollai, M.; de Oliveira, M. G.; Lacza, Z. "S-nitrosoglutathione-containing hydrogel increases dermal blood flow in streptozotocin-induced diabetic rats." *British Journal of Dermatology* **2007**, *156*, 814-818.
- (29) Frost, M. C.; Meyerhoff, M. E. "Synthesis, characterization, and controlled nitric oxide release from S-nitrosothiol-derivatized fumed silica polymer filler particles." *Journal of Biomedical Materials Research Part A* **2005**, *72A*, 409-419.
- (30) Seabra, A. B.; da Silva, R.; de Oliveira, M. G. "Polynitrosated polyesters: Preparation, characterization, and potential use for topical nitric oxide release." *Biomacromolecules* **2005**, *6*, 2512-2520.
- (31) Brinker, J.; Scherer, G. *Sol-Gel Science*. Academic Press, Inc.: New York, 1990.
- (32) Dasgupta, T. P.; Smith, J. N. Reactions of S-nitrosothiols with L-ascorbic acid in aqueous solution. In *Nitric Oxide, Pt D*, 2002; Vol. 359, pp 219-229.
- (33) Williams, D. L. H. "The chemistry of S-nitrosothiols." *Accounts of Chemical Research* **1999**, *32*, 869-876.
- (34) Barret, J.; Debenham, D. F.; Glauser, J. "The electronic spectrum and photolysis of S-nitrosotoluene- α -thiol." *Chemical Communications (London)* **1965**, *12*, 248-249.
- (35) Cazenave, J.; Mulvihill, J. In *The role of platelets in blood-biomaterial interactions*, Missirlis, Y.; Wautier, J.-L., Eds. Kluwer: Dordrecht, 1993; pp 69-80.

- (36) Marxer, S. M.; Rothrock, A. R.; Nablo, B. J.; Robbins, M. E.; Schoenfisch, M. H. "Preparation of nitric oxide (NO)-releasing sol-gels for biomaterial applications." *Chemistry of Materials* **2003**, *15*, 4193-4199.
- (37) Serru, V.; Baudin, B.; Ziegler, F.; David, J. P.; Cals, M. J.; Vaubourdoles, M.; Mario, N. "Quantification of reduced and oxidized glutathione in whole blood samples by capillary electrophoresis." *Clinical Chemistry* **2001**, *47*, 1321-1324.
- (38) Wink, D. A.; Nims, R. W.; Darbyshire, J. F.; Christodoulou, D.; Hanbauer, I.; Cox, G. W.; Laval, F.; Laval, J.; Cook, J. A.; Krishna, M. C.; Degraff, W. G.; Mitchell, J. B. "Reaction kinetics for nitrosation of cysteine and glutathione in aerobic nitric oxide solutions at neutral pH - Insights into the fate and physiological effects of intermediates generated in the NO/O₂ Reaction." *Chemical Research in Toxicology* **1994**, *7*, 519-525.
- (39) Dobmeier, K. P.; Charville, G. W.; Schoenfisch, M. H. "Nitric oxide-releasing xerogel-based fiber-optic pH sensors." *Analytical Chemistry* **2006**, *78*, 7461-7466.
- (40) de Oliveira, M. G.; Shishido, S. M.; Seabra, A. B.; Morgon, N. H. "Thermal stability of primary S-nitrosothiols: Roles of autocatalysis and structural effects on the rate of nitric oxide release." *Journal of Physical Chemistry A* **2002**, *106*, 8963-8970.
- (41) Gottenbos, B.; van der Mei, H. C.; Busscher, H. J. "Initial adhesion and surface growth of *Staphylococcus epidermidis* and *Pseudomonas aeruginosa* on biomedical polymers." *Journal of Biomedical Materials Research* **2000**, *50*, 208-214.
- (42) Hetrick, E. M.; Schoenfisch, M. H. "Antibacterial nitric oxide-releasing xerogels: Cell viability and parallel plate flow cell adhesion studies." *Biomaterials* **2007**, *28*, 1948-1956.
- (43) Nablo, B. J.; Rothrock, A. R.; Schoenfisch, M. H. "Nitric oxide-releasing sol-gels as antibacterial coatings for orthopedic implants." *Biomaterials* **2005**, *26*, 917-924.
- (44) Nablo, B. J.; Schoenfisch, M. H. "Antibacterial properties of nitric oxide-releasing sol-gels." *Journal of Biomedical Materials Research Part A* **2003**, *67A*, 1276-1283.
- (45) Rubbo, H.; Radi, R.; Trujillo, M.; Telleri, R.; Kalyanaraman, B.; Barnes, S.; Kirk, M.; Freeman, B. A. "Nitric oxide regulation of superoxide and peroxynitrite-dependent lipid peroxidation - Formation of novel nitrogen-containing oxidized lipid derivatives." *Journal of Biological Chemistry* **1994**, *269*, 26066-26075.
- (46) Miranda, K. M.; Espey, M. G.; Jourdeuil, D.; Grisham, M. B.; Fukuto, J.; Freilich, M.; Wink, D. A. In *Nitric Oxide: Biology and Pathobiology*, Ignarro, L. J., Ed. Academic Press: New York, 2000; pp 41-55.

- (47) Hogg, N. "The kinetics of S-transnitrosation - A reversible second-order reaction." *Analytical Biochemistry* **1999**, *272*, 257-262.
- (48) Emmerson, M. "A microbiologist's view of factors contributing to infection." *New Horizons-the Science and Practice of Acute Medicine* **1998**, *6*, S3-S10.
- (49) Sefton, M. V.; Gemmell, C. H.; Gorbet, M. B. "What really is blood compatibility?" *Journal of Biomaterials Science-Polymer Edition* **2000**, *11*, 1165-1182.
- (50) Roy-Chaudhury, P.; Kelly, B. S.; Zhang, J. H.; Narayana, A.; Desai, P.; Melhem, M.; Duncan, H.; Heffelfinger, S. C. "Hemodialysis vascular access dysfunction: From pathophysiology to novel therapies." *Blood Purification* **2003**, *21*, 99-110.
- (51) Fleser, P. S.; Nuthakki, V. K.; Malinzak, L. E.; Callahan, R. E.; Seymour, M. L.; Reynolds, M. M.; Merz, S. I.; Meyerhoff, M. E.; Bendick, P. J.; Zelenock, G. B.; Shanley, C. J. "Nitric oxide-releasing biopolymers inhibit thrombus formation in a sheep model of arteriovenous bridge grafts." *Journal of Vascular Surgery* **2004**, *40*, 803-811.
- (52) Frost, M. C.; Rudich, S. M.; Zhang, H. P.; Maraschio, M. A.; Meyerhoff, M. E. "In vivo biocompatibility and analytical performance of intravascular amperometric oxygen sensors prepared with improved nitric oxide-releasing silicone rubber coating." *Analytical Chemistry* **2002**, *74*, 5942-5947.
- (53) Smith, D. J.; Chakravarthy, D.; Pulfer, S.; Simmons, M. L.; Hrabie, J. A.; Citro, M. L.; Saavedra, J. E.; Davies, K. M.; Hutsell, T. C.; Mooradian, D. L.; Hanson, S. R.; Keefer, L. K. "Nitric oxide-releasing polymers containing the [N(O)NO](-) group." *Journal of Medicinal Chemistry* **1996**, *39*, 1148-1156.
- (54) Wu, Y. D.; Rojas, A. P.; Griffith, G. W.; Skrzypchak, A. M.; Lafayette, N.; Bartlett, R. H.; Meyerhoff, M. E. "Improving blood compatibility of intravascular oxygen sensors via catalytic decomposition of S-nitrosothiols to generate nitric oxide in situ." *Sensors and Actuators B-Chemical* **2007**, *121*, 36-46.
- (55) Mathews, W. R.; Kerr, S. W. "Biological activity of S-nitrosothiols - The role of nitric oxide." *Journal of Pharmacology and Experimental Therapeutics* **1993**, *267*, 1529-1537.
- (56) Mellion, B. T.; Ignarro, L. J.; Myers, C. B.; Ohlstein, E. H.; Ballot, B. A.; Hyman, A. L.; Kadowitz, P. J. "Inhibition of human platelet aggregation by S-nitrosothiols - Heme-dependent activation of soluble guanylate-cyclase and stimulation of cyclic-GMP accumulation." *Molecular Pharmacology* **1983**, *23*, 653-664.
- (57) Salas, E.; Langford, E. J.; Marrinan, M. T.; Martin, J. F.; Moncada, S.; de Belder, A. J. "S-nitrosoglutathione inhibits platelet activation and deposition in coronary artery saphenous vein grafts in vitro and in vivo." *Heart* **1998**, *80*, 146-150.

- (58) Gappa-Fahlenkamp, H.; Lewis, R. S. "Improved hemocompatibility of poly(ethylene terephthalate) modified with various thiol-containing groups." *Biomaterials* **2005**, *26*, 3479-3485.
- (59) Duan, X. B.; Lewis, R. S. "Improved haemocompatibility of cysteine-modified polymers via endogenous nitric oxide." *Biomaterials* **2002**, *23*, 1197-1203.
- (60) Marxer, S. M.; Robbins, M. E.; Schoenfisch, M. H. "Sol-gel derived nitric oxide-releasing oxygen sensors." *Analyst* **2005**, *130*, 206-212.
- (61) Robbins, M. E.; Hopper, E. D.; Schoenfisch, M. H. "Synthesis and characterization of nitric oxide-releasing sol-gel microarrays." *Langmuir* **2004**, *20*, 10296-10302.
- (62) Wink, D. A.; Mitchell, J. B. "Chemical biology of nitric oxide: Insights into regulatory, cytotoxic, and cytoprotective mechanisms of nitric oxide." *Free Radical Biology and Medicine* **1998**, *25*, 434-456.

Chapter 4:

Xerogel Optical Sensor Films for Quantitative Detection of Nitroxyl

4.1. Introduction

Nitrogen oxide compounds have become a topic of considerable interest in medicinal and biological chemistry.¹ Nitric oxide (NO) is the most widely studied and well-known of these molecules, and multiple reports have catalogued the role of NO in numerous physiological processes, including vasodilation, neurotransmission, wound-healing, and thrombosis.² As the effects of NO on physiology become better understood, more attention has focused on structurally similar nitrogen oxide compounds that may also have direct biochemical effects and/or function as intermediates in the NO-signaling cascade. Nitroxyl (HNO), the one electron reduced congener of NO, is one such molecule that has displayed a number of interesting physiological effects.³ Nitroxyl's high reactivity with thiols and metalloproteins has led to potential pharmaceutical application in protective preconditioning of ischemic injury,⁴ treatment for alcohol abuse through targeted inhibition of aldehyde dehydrogenase,⁵ ⁶ and as an efficient means of enhancing left ventricular contractility in victims of congestive heart failure.⁷ These discoveries have led to efforts focusing on the design and development of new HNO-donor molecules and prodrugs.⁸⁻¹¹ Research in this area has been hindered by an inability to easily monitor HNO. Indeed, no simple method currently exists for the quantitative determination of HNO in solution. In this chapter, this issue is addressed

through the development of optical sensors designed for the rapid quantitative screening of HNO released by nitroxyl-donor molecules.

Despite their similarities, HNO and NO have distinct chemical properties and reactivity. The relatively high standard reduction potentials for the formation of HNO from NO (< -0.4 V vs. NHE)¹² preclude the creation of HNO from NO under most physiological conditions. Conversely, while the oxidation of nitroxyl to NO would be expected to occur readily *in vivo*, this has not been observed. Oxidation to NO occurs most readily from nitroxyl's triplet-state anion form (NO^-) which is not present in significant concentration at physiological pH due to a $\text{pK}_a > 11$.¹³ The ground spin states of HNO and NO^- are singlet and triplet, respectively, making proton transfer between the two species spin-forbidden and kinetically slow.¹³ The recently described biological activities of HNO-donor compounds thus reflect reactivity of the HNO molecule itself and not a transformation to NO.

Knowledge of HNO chemistry lags behind that of other nitrogen oxides such as NO, which can in large part be explained by HNO's greater reactivity and difficulties in its handling and quantitation. Nitroxyl in solution undergoes dimerization to hyponitrous acid followed by rapid dehydration and the formation of nitrous oxide (N_2O):



The study and application of HNO must therefore be accomplished by *in situ* generation of nitroxyl by HNO-donor molecules such as Angeli's salt ($\text{Na}_2\text{N}_2\text{O}_3$) which decomposes upon protonation to form HNO and nitrite:



The situation is further complicated by the lack of a simple means to detect and quantify HNO. While specialized techniques such as infrared chemiluminescence may

directly assay HNO,¹⁴ such procedures are impractical in most laboratories. More commonly, indirect screening methods for HNO are employed. Gas chromatographic detection of the N₂O dimerization product is often viewed as a marker of HNO formation, but may be misleading as alternate NO reaction pathways not involving nitroxyl also result in the production of N₂O.^{15, 16} A more selective strategy reported by Donzelli et al. employed the rapid reaction of HNO with thiols as a marker of HNO generation in biological systems.¹⁷ Treatment of HNO producing systems with glutathione resulted in the formation of a sulfinamide reaction product that was subsequently detected via HPLC. Another commonly employed strategy involves reaction of HNO with ferric heme-containing proteins such as metmyoglobin.¹⁸ In the presence of HNO, ferric hemes undergo reductive nitrosylation, resulting in detectable shifts in the absorbance spectrum of the enzyme. This reaction provides a highly selective means of screening for HNO generation, but the resulting Fe^{II}(NO) complex is unstable in aerobic conditions and readily undergoes reoxidation and dissociation. Ferric porphyrin analogues have been reported that undergo similar absorbance shifts upon reaction with HNO.¹⁹ While easier to handle than the bulky metmyoglobin protein, ferric porphyrins suffered from the same oxygen instability and also react with NO, a common interferent in HNO-generating systems. Recently, Marti et al. reported on the kinetics of reductive nitrosylation of manganese porphyrins via HNO.²⁰ The reaction of manganese(III) *meso*-tetrakis(4-sulfonatophenyl) porphyrinate (Mn^{III}TPPS; Figure 4.1A) with nitroxyl:



resulted in strong shifts in the absorbance spectrum and displayed no cross-reactivity with NO or catalytic decomposition of the Angeli's salt HNO donor compound. This molecule

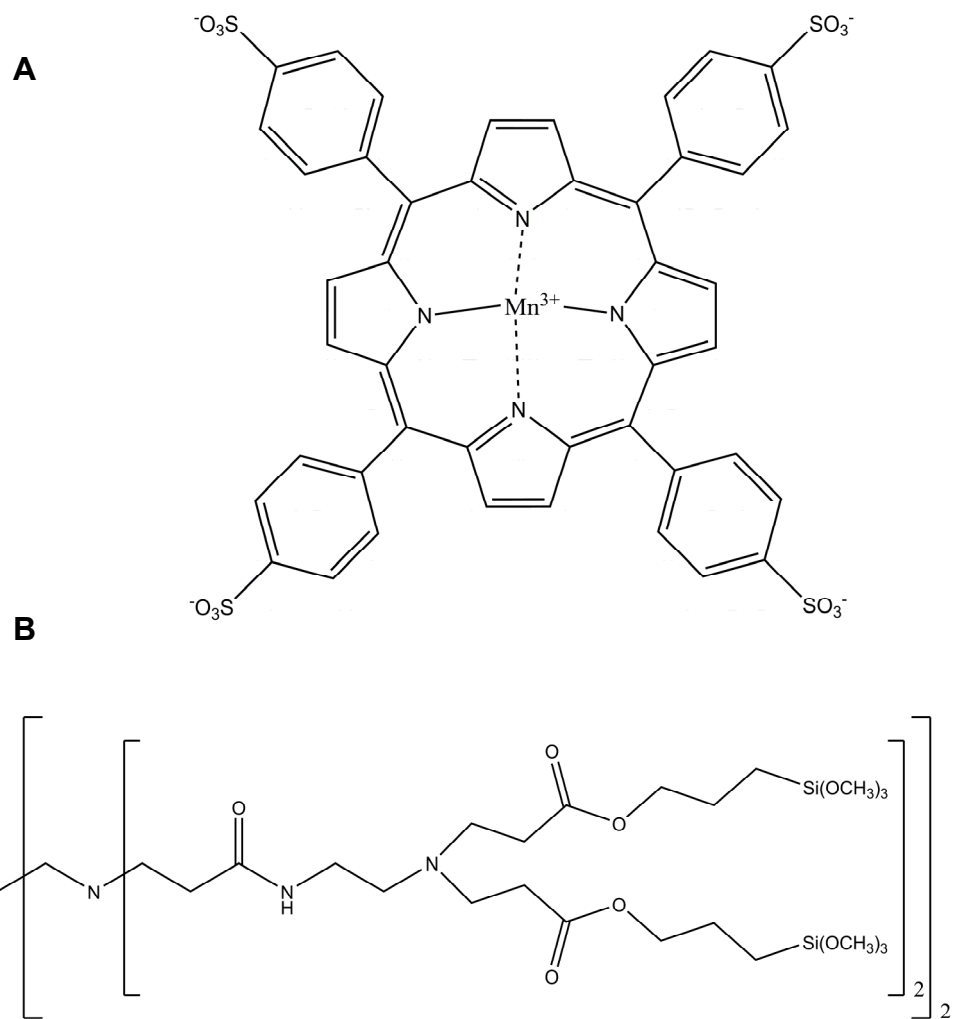


Figure 4.1. Chemical structures of (A) Mn^{III} TPPS and (B) generation-zero trimethoxysilyl-terminated PAMAMOS dendrimers.

may thus provide a simple and robust alternative to metmyoglobin for the selective detection of HNO. Unfortunately, the resultant $\text{Mn}^{\text{II}}(\text{NO})\text{TPPS}$ complex was found to be unstable in the presence of O_2 and rapidly dissociate back to $\text{Mn}^{\text{III}}\text{TPPS}$. The instability of the $\text{Mn}^{\text{II}}(\text{NO})$ complex in aerated solution makes it difficult to quantitatively determine HNO concentrations. Complex formation/dissociation is slower than the HNO dimerization rate ($8 \times 10^6 \text{ M}^{-1} \text{ s}^{-1}$),¹³ and thus a measured absorbance is not reflective of an instantaneous HNO concentration. As such, HNO complexation at metal centers has been limited to nonquantitative screening procedures and qualitative tests for the presence of HNO.

Herein, optical sensor coatings suitable for quantitative determination of HNO in solution were developed by increasing the stability of the $\text{Mn}^{\text{II}}(\text{NO})\text{TPPS}$ complex via encapsulation in an aminoalkoxysilane-based xerogel matrix. Xerogels are polymeric materials formed through the catalytic hydrolysis and condensation of alkoxy-terminated silane precursors.²¹ While NO diffusion through aminoalkoxysilane-derived xerogels has been shown to occur readily, oxygen permeability in these materials is quite low.²² Encapsulation of $\text{Mn}^{\text{III}}\text{TPPS}$ inside aminoalkoxysilane-xerogel films is thus expected to permit HNO diffusion while creating a localized anaerobic environment for the porphyrin, slowing dissociation of the $\text{Mn}^{\text{II}}(\text{NO})\text{TPPS}$ complex. Over short periods, HNO complexation by $\text{Mn}^{\text{III}}\text{TPPS}$ in these films may be considered largely irreversible, resulting in the creation of a cumulative HNO trap. By utilizing the detected rate of intra-film $\text{Mn}^{\text{II}}(\text{NO})\text{TPPS}$ formation, a kinetic strategy may be employed to estimate HNO concentrations. Aminoalkoxysilane-xerogel film properties were further optimized for this application through the inclusion of trimethoxysilyl-terminated poly(amidoamine-organosilicon) (PAMAMOS) dendrimers (Figure 4.1B). Such dendrimers create hydrophilic nanodomains

in the material and speed HNO diffusion through the membrane, increasing sensitivity and allowing application of the sensor films in a convenient 96-well plate format. The resulting HNO-sensing microtitre plates were used to quantify HNO and confirm the pH-dependent nature of nitroxyl generation from a recently described HNO/NO donor compound, sodium-1-(isopropylamino)diazene-1-ium-1,2-diolate (IPA/NO).²³⁻²⁵

4.2. Materials and Methods

Manganese(III) *meso*-tetrakis(4-sulfonatophenyl) porphine chloride (Mn^{III}TPPS) was purchased from Frontier Scientific (Logan, UT). (Aminoethylaminomethyl)phenethyltrimethoxysilane (AEMP3) was purchased from Gelest (Tullytown, PA). Methyltrimethoxysilane (MTMOS) and diethylenetriamine-pentaacetic acid (DTPA) were purchased from Fluka. Generation zero (G-0) trimethoxysilyl-terminated PAMAMOS dendrimer (10 wt% in isopropanol) was purchased from Aldrich (Milwaukee, WI). Angeli's Salt (disodium diazen-1-ium-1,2,2-triolate; Na₂N₂O₃) was purchased from Cayman Chemical (Ann Arbor, MI). Sodium-1-(isopropylamino)diazene-1-ium-1,2-diolate (IPA/NO) was provided as a generous gift from Dr. Katrina Miranda at the University of Arizona. Nitric oxide (99.5%) was purchased from National Welders Supply (Durham, NC). Untreated polystyrene round-bottom 96-well microtitre plates were purchased from Fisher Scientific. Other solvents and chemicals were analytical-reagent grade and used as received. Distilled water was purified to 18.2 MΩ·cm with a Millipore Milli-Q Gradient A-10 water purification system (Bedford, MA).

4.2.1. *Response of Mn^{III}TPPS to NO and HNO*

The selectivity of HNO binding over NO by Mn^{III}TPPS in aerobic conditions was examined in a PerkinElmer Lambda 40 UV/Vis spectrophotometer (Norwalk, CT). A ~0.01 M stock solution of the Angeli's salt HNO donor was prepared in 0.01 M NaOH and stored on ice until use. A deoxygenated, saturated NO stock solution (~1.9 mM) was created by sparging 30 mL pH 7.4 10 mM phosphate-buffered saline (PBS) with Ar for 40 min, and then bubbling with NO for 2 h. Aliquots (20-100 μL) of each solution were mixed with 2 mL 5.5 μM Mn^{III}TPPS in 10 mM PBS at room temperature, and the visible absorbance spectrum of the resulting solution was monitored for ~2 h.

4.2.2. *Xerogel Film Preparation*

Nitroxyl-sensing films were first evaluated as thin films on glass slides using a previously described 20/80% (v:v total silane) AEMP3/MTMOS aminoalkoxysilane-xerogel formulation.^{22, 26} Briefly, MTMOS (160 μL) and ethanol (200 μL) were combined with 0.25 - 2 mM (aq) Mn^{III}TPPS solution (11 μL). After 5 min sonication, AEMP3 (40 μL) was added and sonicated for an additional 5 min. The resulting sol was cast in 10 - 30 μL aliquots onto 9 x 25 mm² glass substrates that had been previously sonicated 20 min in ethanol, dried under N₂, and UV/O₃ cleaned for 20 min in a BioForce TipCleaner (Ames, IA). The resulting films were allowed to dry a minimum of 3 d in ambient conditions prior to subsequent characterization.

4.2.3. *Film Characterization*

Film depths and the corresponding volume of cured xerogel on glass slides were determined using a Tencor Alpha-Step 200 Profilometer (San Jose, CA). Spectral

characterization of Mn^{III}TPPS encapsulated in AEMP3/MTMOS films was performed by affixing the slides inside PBS-containing (2 mL) cuvettes normal to the light path of the spectrophotometer. The extinction coefficient of immobilized Mn^{III}TPPS was determined by plotting the measured 467 nm absorbance of xerogel films (depth ~29 μm) containing 0.32 – 2.55 x 10⁻⁷ moles/cm³ Mn^{III}TPPS versus porphyrin concentration. Aliquots of 10-100 μL Angeli's salt stock solution (~0.01 M in 10 mM NaOH) were added to pH 7.4 PBS to a final volume of 2.5 mL. Nitroxyl-sensing xerogel films that had been previously hydrated in PBS for a minimum of 20 min were placed in cuvettes with 2 mL of the Angeli's salt/PBS solution. The rates of Mn^{II}(NO)TPPS formation and dissociation in AEMP3/MTMOS films were determined by monitoring changes in the absorbance maxima of Mn^{III}TPPS and Mn^{II}(NO)TPPS at 467 and 432 nm, respectively, for ~2 h. The concentrations of Angeli's salt stock solutions were determined via Beer's law prior to each experiment by monitoring the absorbance at 250 nm ($\epsilon = 8000 \text{ M}^{-1} \text{ cm}^{-1}$).²⁷

4.2.4. Kinetic HNO Quantification

Stabilization of the Mn^{II}(NO)TPPS complex in AEMP3/MTMOS sensor films provides a means for kinetic quantification of HNO in solution. By eliminating the uncertain rate of competitive complex dissociation, steady-state reaction kinetics for HNO-donor systems are greatly simplified. Calibration with a well-characterized HNO-donor such as Angeli's salt under controlled reaction conditions allows determinations of an experimental kinetic coefficient (k_{on}) for Mn^{II}(NO)TPPS formation in xerogel films. The resulting rate constant may then be used to extrapolate solution HNO concentrations generated by alternate HNO-donors. In our system, three kinetic expressions (Eq. 4.4 – 4.6) were considered during

calibration, corresponding to Angeli's salt decomposition (Eq. 4.2), Mn^{II}(NO)TPPS formation (Eq. 4.3), and HNO scavenging through dimerization (Eq. 4.1):

$$\partial[HNO]/\partial t = -k_1[AS] \quad (4.4)$$

$$\partial[Mn^{II}(NO)TPPS]/\partial t = k_{on}[HNO][Mn^{III}TPPS] \quad (4.5)$$

$$\partial[HNO]/\partial t = -k_2[HNO]^2 \quad (4.6)$$

Application of steady-state kinetics to Eq. 4.4 – 4.6 yields:

$$\frac{\partial[Mn^{II}(NO)TPPS]}{\partial t} = \frac{-1 \pm \sqrt{1^2 + 4 \cdot k_2 / (k_{on}[Mn^{III}TPPS])^2 \cdot k_1[AS]}}{2 \cdot k_2 / (k_{on}[Mn^{III}TPPS])^2} \quad (4.7)$$

where $k_1[AS]$ is the rate of Angeli's salt decomposition, and k_2 is the kinetic coefficient of the HNO dimerization reaction ($8 \times 10^6 \text{ M}^{-1} \text{ s}^{-1}$).¹³ Angeli's salt decomposition rates were determined in PBS by monitoring the decrease in 250 nm absorbance over 60 min and fitting to an exponential decay model (absorbance = $Ae^{-kt} + c$).²⁸ For the experimental conditions employed herein (25 °C, pH 7.4, 10^{-4} DTPA, aerobic), k_1 was calculated at $8.1 \times 10^{-4} \text{ s}^{-1}$. After determination of k_{on} via Angeli's salt calibration, the observed rates of Mn^{II}(NO)TPPS formation were used to calculate HNO concentrations according to:

$$[HNO] = \frac{\partial[Mn^{II}(NO)TPPS]/\partial t}{k_{on}[Mn^{III}TPPS]} \quad (4.8)$$

where $[Mn^{II}(NO)TPPS]$ and $[Mn^{III}TPPS]$ concentrations in the film were monitored spectroscopically at 432 and 467 nm, respectively. Considering xerogel film thicknesses (~29 μm) as the optical path length, the extinction coefficient of Mn^{III}TPPS encapsulated in AEMP/MTMOS was calculated to be $90000 \text{ M}^{-1} \text{ cm}^{-1}$ at 467 nm via Beer's law. Although complete conversion of Mn^{III}TPPS to Mn^{II}(NO)TPPS was not attainable even with large

excesses of Angeli's salt, the differential rates of absorbance decrease at 467 nm and increase at 432 nm were used to estimate $\epsilon \sim 160000 \text{ M}^{-1} \text{ cm}^{-1}$ at 432 nm for $\text{Mn}^{\text{II}}(\text{NO})\text{TPPS}$.

4.2.5. Xerogel-Coating of 96-well Microtitre Plates

Nitroxyl-sensing xerogel films were optimized for deposition in 96-well plates. Sols were created using the general reaction scheme described above and varying the following: the volume and identity of solvent employed, including methanol, ethanol, isopropanol, and n-butanol; the concentration of aqueous $\text{Mn}^{\text{III}}\text{TPPS}$ solution included in the sol (2-8 mM); and the volume percentage of AEMP3 to MTMOS employed (10-50%). Aliquots (4-10 μL) of the resulting sols were pipetted into the bottom of round-bottom 96-well polystyrene microtitre plates and allowed to cure under ambient conditions. Xerogel films were evaluated for their transparency, smoothness, stability, and detectable absorbance at 467 nm. Film thickness was monitored via optical microscopy using a Zeiss Axiovert 200 inverted microscope.

4.2.6. Microtitre Plate Sensor Optimization

Sols containing 40/60% (v:v) AEMP/MTMOS and ~0-2% PAMAMOS dendrimer (v:v total silane) were created by shaking MTMOS (120 μL), 10% (w:w) PAMAMOS dendrimer in isopropanol (0 – 40 μL), methanol (420-380 μL ; total methanol and PAMAMOS volume = 420 μL), and 4mM (aq) $\text{Mn}^{\text{III}}\text{TPPS}$ (11 μl) for 10 min, followed by the addition of AEMP3 (80 μL) and a subsequent 5 min additional shaking. Aliquots (4-10 μL) of the resulting sol were pipetted into wells and allowed to cure for a minimum of 3 d under ambient conditions. Initial screening procedures monitoring the rate of $\text{Mn}^{\text{II}}(\text{NO})\text{TPPS}$ complex formation in the gel were performed using a Labsystems Multiskan RC plate reader

outfitted with 430 and 467 nm narrow bandpass interference filters (10 nm full-width at half max) purchased from Edmund Optics (Barrington, NJ). All wells were soaked with 50-100 μL PBS for a minimum of 3 h prior to use to achieve a steady 430 nm baseline absorbance. To initiate HNO generation, 40 μL of the initial Angeli's salt stock solution was mixed and shaken with 1960 μL pH 7.4 PBS containing 100 μM DTPA for 30 s. The pre-soaked wells were emptied and 10-100 μL of the Angeli's salt-PBS solution and a balance PBS/DTPA was added to wells for a total volume of 100 μL . To ensure accurate kinetics, care was taken so that timing remained consistent. The HNO-sensing wells were loaded and the recording of kinetic absorbance data began at exactly 40 and 60 s, respectively, after initial mixing of Angeli's salt and PBS. The absorbance at 430 nm, corresponding to formation of $\text{Mn}^{\text{II}}(\text{NO})\text{TPPS}$ in the films, was monitored every 10 s for 15 min. Initial rates were obtained from the slope of linear fits of the first 5 min of collected data. Only fits with $R^2 \geq 0.99$ were retained for subsequent calculations. After optimization, characterization of the most favorable sensor formulation's dynamic range and sensitivity was performed following the same procedures with a monochromator-equipped Molecular Devices Spectramax 340PC plate reader (Sunnyvale, CA) capable of monitoring both 432 and 467 nm absorbance maxima simultaneously. Baseline absorbance from control xerogel films containing no $\text{Mn}^{\text{III}}\text{TPPS}$ was subtracted from all measurements.

4.2.7. *Oxygen Permeability Testing*

The permeability of oxygen (O_2) through PAMAMOS-modified HNO-sensing xerogels was examined by measuring O_2 reduction at xerogel-coated electrodes. Sols containing 40/60% (v:v total silane) AEMP3/MTMOS with $\sim 0, 0.25, 0.5, 1.0,$ and 2.0% (v:v total silane) trimethoxysilyl-terminated PAMAMOS dendrimer were prepared using the

formula described above. Control MTMOS sols containing no AEMP3 were synthesized by shaking MTMOS (750 μL) with 0.1 M HCl (140 μL) for 10 min. Platinum electrodes (2 mm dia.) were mechanically polished with a 0.05 μM alumina slurry, rinsed, sonicated in water for 15 min, coated with 2 μL of the corresponding sol and allowed to dry for three days. The diffusion of O_2 through the xerogel films as a function of PAMAMOS amount was examined with a CH Instruments 660A potentiostat (Austin, TX). A three-electrode system consisting of the xerogel-modified Pt electrode, Pt wire auxiliary electrode (0.5 mm), and a Ag/AgCl (3.0 M KCl) reference electrode was used to monitor O_2 reduction. Electrodes placed in 40 mL of PBS (100 μM DTPA, pH 7.4) with constant stirring were exposed to atmospheric levels of O_2 . Current was recorded at an applied potential of -0.65 V vs. Ag/AgCl with a sampling frequency of 1 Hz. Xerogel permeability to oxygen was determined by taking the ratio of the peak current for O_2 for the xerogel-coated electrode to that of the corresponding uncoated electrode. Coated electrodes were soaked in PBS (100 μM DTPA, pH 7.4) for 3 h prior to the electrochemical experiments to mimic hydration conditions of the HNO sensing films at time of use.

4.2.8. *HNO-Generation from IPA/NO*

Generation of HNO from an IPA/NO nitroxyl donor compound was quantified using the developed 96-well microtitre plate sensing scheme. Sols containing 40/60% (v:v total silane) AEMP3/MTMOS and ~0.25% PAMAMOS dendrimer (v:v total silane) were prepared and pre-hydrated as described above. An IPA/NO stock solution was prepared by dissolving 29.3 mg IPA/NO in 1 mL 0.01 M NaOH. The solution was stored at -20 $^\circ\text{C}$ until use. Immediately prior to measurement, 80 μL of the IPA/NO stock was added to 1.92 mL 10 mM PBS/100 μM DTPA, and shaken for 30 s. Using the strategy described above, 25-100

μL of the IPA/NO-PBS solution was added to wells containing a balance of PBS/DTPA buffer for a total volume of 100 μL . The formation of $\text{Mn}^{\text{II}}(\text{NO})\text{TPPS}$ from $\text{Mn}^{\text{III}}\text{TPPS}$ was monitored by measuring the absorbance at 432 and 467 nm, respectively. The effect of pH on HNO production was examined by adjusting the starting pH of the PBS solution employed prior to mixing (pH 3-10). To compensate for the poor buffering capacity of PBS outside the neutral pH region, final solution pH was determined after IPA/NO stock addition. The concentrations of IPA/NO stock solutions were determined prior to each experiment by monitoring absorbance at 250 nm ($\epsilon = 10000 \text{ M}^{-1} \text{ cm}^{-1}$).²⁵

4.3. Results and Discussion

4.3.1. $\text{Mn}^{\text{III}}\text{TPPS}$ HNO Selectivity

The selectivity of $\text{Mn}^{\text{III}}\text{TPPS}$ for complexation of HNO over NO in oxygenated media was examined directly using a UV/Vis spectrophotometer. As expected, mixing $\text{Mn}^{\text{III}}\text{TPPS}$ with HNO generated via Angeli's salt resulted in a rapid increase in the absorbance of the solution at 423 nm and a concurrent decrease in absorbance at 467 nm, corresponding to the formation of $\text{Mn}^{\text{II}}(\text{NO})\text{TPPS}$ from $\text{Mn}^{\text{III}}\text{TPPS}$ (Figure 4.2). Maximum 423 nm absorbance occurred within 5 min of HNO addition and then slowly decreased to baseline absorbances within 90 min. Negligible absorbance change was observed upon addition of saturated NO solution, indicating that $\text{Mn}^{\text{III}}\text{TPPS}$ retains its selectivity for HNO in aerobic solution conditions.

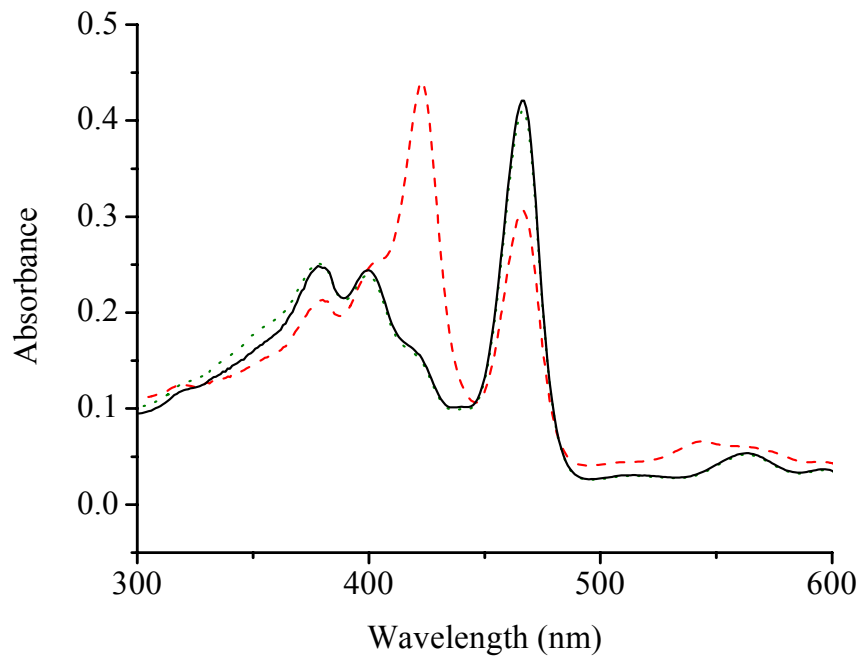


Figure 4.2. The UV/Vis spectral response of (—) Mn^{III}TPPS in pH 7.4 PBS upon exposure to 100 μ M (---) Angeli's salt and (···) NO. Spectra were recorded 8 min after the addition of Angeli's salt or NO.

4.3.2. $Mn^{II}(NO)TPPS$ Formation in Xerogel Films

Amine-terminated xerogels have previously been used in the production of multiple optical (e.g., pH),²⁹ amperometric (e.g., CO₂, NO)^{30, 31} and enzyme-based (e.g. glucose)^{32, 33} sensors and biosensors. While the diffusion of NO through these materials was rapid, the intrinsic permeability of O₂, a highly nonpolar molecule, was quite low.³⁴ Robbins and co-workers measured oxygen permeability at xerogel-coated electrodes, and reported that the oxygen permeability at a Pt electrode coated with 20/80% (v:v total silane) AEMP3/MTMOS was diminished by ~97% compared to a bare electrode.²² By encapsulating Mn^{III}TPPS in this material we thus sought to provide an anaerobic localized environment for the porphyrin, slowing dissociation of the Mn^{II}(NO)TPPS complex formed upon reaction with HNO. Spectroscopic observation of Mn^{III}TPPS encapsulated in an AEMP3/MTMOS xerogel revealed the presence of both the expected absorbance maxima at 467 nm and a second unidentified peak centered at 445 nm. Upon immersion of the film in PBS, the 445 nm peak disappeared rapidly concomitant with a rise in 467 nm absorbance. This behavior may be attributed to temporary association of the Mn center with surface silanols or amines present in the dry xerogel film. All films were hydrated a minimum of 20 min prior to HNO exposure to overcome this effect. Upon introducing HNO, a rise and fall of absorbance maxima at 432 and 467 nm, respectively, were observed. While red-shifted compared to the 423 nm absorbance maximum observed in solution, the correlation between the 432 and 467 nm maxima is a strong indication that 432 nm absorbance may be assigned to Mn^{II}(NO)TPPS formation via reductive nitrosylation of Mn^{III}TPPS. As shown in Figure 4.3, encapsulation of the porphyrin in AEMP3/MTMOS xerogel resulted in a dramatic decrease in Mn^{II}(NO)TPPS dissociation. While Mn^{II}(NO)TPPS formation was slowed relative to in

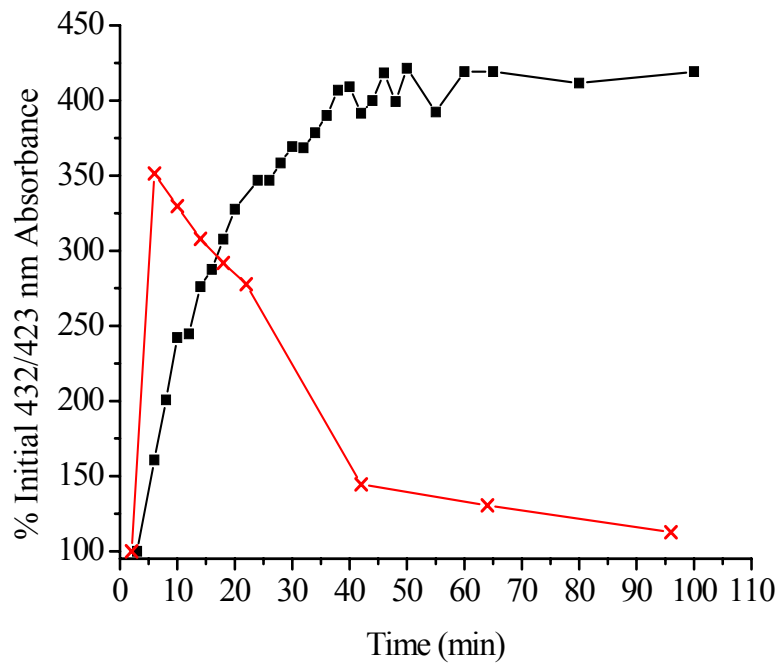


Figure 4.3. $\text{Mn}^{\text{II}}(\text{NO})\text{TPPS}$ formation in (■) AEMP3/MTMOS or (x) free in aerobic PBS as measured by absorbance at 432 or 423 nm, respectively, after the addition of $100 \mu\text{M}$ Angeli's salt.

solution, the resulting complex remained stable over the time course of the experiment (2 h), indicating that Mn^{III}TPPS in AEMP3/MTMOS functions largely as a cumulative HNO trap over short periods.

4.3.3. *Microtitre Plate Sensor Optimization via PAMAMOS*

Long-term exposure (>24 h) of HNO-sensing films to media containing ambient O₂ concentrations was found to regenerate Mn^{III}TPPS and restore initial absorbance maxima. However, the largely irreversible short-term nature of HNO complexation in AEMP3/MTMOS films makes HNO quantitation with a single film impractical for analytical measurements. To maximize the utility of HNO-sensing films, xerogel coatings were optimized for use in a 96-well microtitre plate format. Such a configuration allows a large number of HNO assays to be run in parallel while permitting calibration to be performed at the time of analysis to account for variations in individual films and changes that may occur in the xerogel with time. Curing of sols deposited in flat-bottom polystyrene microtitre plates resulted in clustering of xerogel around the edges of the well and the formation of concave films. More uniform coatings were achieved using round-bottom plates. In general, the reduced sensitivity of the microtitre plate reader format versus the UV/Vis spectrophotometer required thicker xerogel layers and larger Mn^{III}TPPS concentrations to bring measured absorbance values above baseline noise. Several solvents and reaction conditions were evaluated to form reproducibly thicker, crack-free xerogel films in the round-bottom wells. Ultimately, a mixture of 40/60% (v:v total silane) AEMP3/MTMOS, 4 mM Mn^{III}TPPS (aq) and methanol (co-solvent) provided the proper balance between sol-gel condensation rates and solvent evaporation, resulting in smooth, uniform films of adequate thickness (~90-140 μm, for 6-10 μL sol cast).

Unfortunately, nitroxyl diffusion through pure AEMP3/MTMOS films proved inadequate for the sensitivity constraints imposed by the 96-well plate format. To increase the formation rate of $\text{Mn}^{\text{II}}(\text{NO})\text{TPPS}$, trimethoxysilyl-terminated PAMAMOS dendrimers were evaluated as a means of selectively enhancing HNO permeability through the xerogel. Dvornic and co-workers previously reported on the utility of such macromolecules to form honeycomb-like hydrophilic-nanodominated networks upon sol-gel hydrolysis and condensation.^{35, 36} The generation-zero PAMAMOS dendrimers employed are characterized by a branched hydrophilic polyamidoamine interior surrounded by 8 terminal trimethoxysilyl groups enabling their incorporation into the surrounding xerogel structure via condensation reactions. By incorporating PAMAMOS dendrimers as bridging molecules in the surrounding AEMP3/MTMOS network, hydrophilic pockets were created in the final xerogel, providing preferential enhancement of HNO diffusion over the more lipophilic O_2 molecule. The percentage change in 430 nm absorbance observed from xerogel films containing ~0.25-2.0% (v:v total silane) PAMAMOS dendrimer upon introduction of Angeli's salt is shown in Figure 4.4. In films containing ~0.25% (v:v total silane) PAMAMOS, the initial rates of $\text{Mn}^{\text{II}}(\text{NO})\text{TPPS}$ formation increased by nearly an order of magnitude versus rates measured in pure AEMP3/MTMOS films. Surprisingly, increasing the percentages of PAMAMOS >0.25% resulted in an overall decrease in the rate of $\text{Mn}^{\text{II}}(\text{NO})\text{TPPS}$ formation measured in the films. This effect may be attributed to increased competition with oxygen as larger amounts of the PAMAMOS bridge would lead to less dense crosslinking of the alkoxy silane precursors and thus a more open xerogel network. Indeed, macroscopic holes were observed in multiple wells at percentages of PAMAMOS

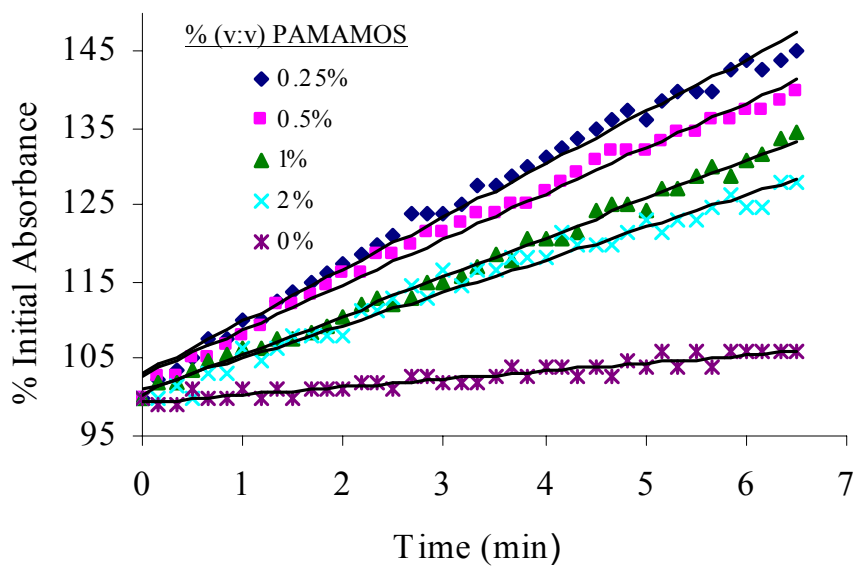


Figure 4.4. Initial rates of $\text{Mn}^{\text{II}}(\text{NO})\text{TPPS}$ formation detected as 430 nm absorbance in AEMP3/MTMOS films modified with 0-2% (v:v total silane) trimethoxysilyl-terminated PAMAMOS dendrimers upon the addition of 320 μM Angeli's salt/PBS.

inclusion above 2% likely due to termination of growing silane networks by the inclusion of multiple dendrimers.

4.3.4. Oxygen Permeability in PAMAMOS-Modified Films

To evaluate the effect of PAMAMOS dendrimer incorporation on O₂ diffusion in the HNO-sensing xerogel films, the amperometric response of xerogel-coated O₂-reducing electrodes was examined. Films comprised of 40/60% (v:v total silane) AEMP3/MTMOS with ~0, 0.25, 0.5, 1.0 and 2.0% (v:v total silane) trimethoxysilyl-terminated PAMAMOS dendrimers were tested and compared to control films consisting of 100% MTMOS. Initially, the amperometric response of bare Pt electrodes to ambient concentrations of dissolved O₂ was evaluated. The electrodes were then coated with MTMOS, AEMP3/MTMOS, and PAMAMOS-modified xerogels. The change in oxygen peak current was determined and correlated to percent O₂ permeability relative to the bare electrode (Table 4.1). Whereas MTMOS-only control films retained nearly 70% of the oxygen signal of a bare electrode, the oxygen permeability of pure AEMP3/MTMOS films was reduced to ~8% of the value observed for bare electrodes. Of note, ANOVA statistical tests showed no significant oxygen permeability difference ($P > 0.05$) in films modified with 0.25% PAMAMOS compared to AEMP3/MTMOS alone. While O₂ permeability in all PAMAMOS-modified AEMP3/MTMOS films remained well below the permeability of MTMOS controls, all films with >0.25% PAMAMOS incorporation were found to yield small, but statistically significant increases in oxygen permeability compared to both 0 and 0.25% PAMAMOS-modified xerogels. Thus, enhanced oxygen permeation may account for the downward trend in the Mn^{II}(NO)TPPS formation rates observed with increasing %PAMAMOS inclusion. Nevertheless, the inclusion of small percentages of PAMAMOS

Table 4.1. Oxygen permeability of 0-2% (v:v) PAMAMOS-modified AEMP3/MTMOS xerogels and controls.

% PAMAMOS (v:v total silane)	O ₂ Permeability (%) ^a	ANOVA <i>P</i> value (vs. 0.0 % PAMAMOS)	ANOVA <i>P</i> value (vs. MTMOS Control)
0.0	8.19 ± 1.90	1	3.23E-03
0.25	9.61 ± 0.23	2.56E-01	5.44E-04
0.5	16.92 ± 1.08	1.64E-03	1.90E-04
1.0	14.69 ± 0.72	4.57E-02	4.84E-03
2.0	15.98 ± 0.58	5.68E-03	9.24E-04
MTMOS Control	68.90 ± 12.79	3.23E-03	1

^a relative to uncoated electrode

dendrimer in the AEMP3/MTMOS network provided a clear enhancement in the sensitivity of HNO-sensing films with minimal detrimental effects on oxygen permeability.

4.3.5. Nitroxyl Sensing

Nitroxyl sensor films comprised of the optimized xerogel formulation were fabricated by depositing 8 μl of 40/60% (v:v total silane) AEMP3/MTMOS with 0.25% (v:v total silane) PAMAMOS dendrimer in each well of a 96-well microtitre plate and cured up to 7 d before use. Sol-gel condensation reactions continue to occur after xerogel solidification, and thus long term storage may have detrimental effects on sensor sensitivity as the siloxane network of the gel becomes more densely crosslinked.³⁷ As such, sensor calibration at the time of nitroxyl detection is important. Calibration of the sensor plate was performed by monitoring the initial rates of $\text{Mn}^{\text{II}}(\text{NO})\text{TPPS}$ formation in the films upon exposure to Angeli's salt and fitting the response to Eq. 4.7. A representative response curve is shown in Figure 4.5. Obtaining a strong coefficient of determination ($R^2 \geq 0.99$) at rates $< 8 \times 10^{-9} \text{ M}^{-1} \text{ s}^{-1}$ (corresponding to $\sim 13 \mu\text{M}$ Angeli's salt) became difficult due to intrinsic noise. Rates $> \sim 1 \times 10^{-7} \text{ M}^{-1} \text{ s}^{-1}$ ($\sim 1 \text{ mM}$ Angeli's salt) began to deviate from the theoretical model of Eq. 4.7. Fitting the initial rates over this concentration range using Eq. 4.7 resulted in an experimental $k_{\text{on}} \sim 1 \times 10^3 \text{ M}^{-1} \text{ s}^{-1}$ for $\text{Mn}^{\text{II}}(\text{NO})\text{TPPS}$ formation in the xerogel films. As expected, this value was significantly lower than that established by Marti for $\text{Mn}^{\text{III}}\text{TPPS}$ in anaerobic solution ($4 \times 10^4 \text{ M}^{-1} \text{ s}^{-1}$)²⁰ due to diffusion constraints imposed by encapsulation of the porphyrin in the film. Substitution of these values into Eq. 4.8 resulted in an estimated dynamic range of 24-290 nM HNO, a relatively small range reflective of the rapid scavenging of HNO via dimerization at higher nitroxyl concentrations limiting free HNO in solution. Example real-time HNO release data from $\sim 700 \mu\text{M}$ and $50 \mu\text{M}$ Angeli's salt

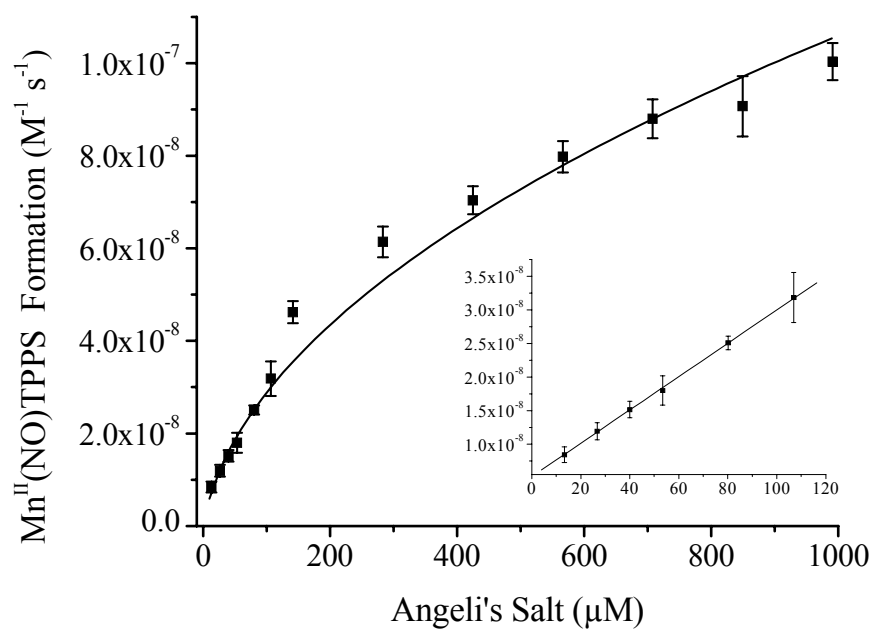


Figure 4.5. Initial rates of Mn^{II}(NO)TPPS formation in 40/60% (v:v total silane) AEMP3/MTMOS films modified with 0.25% (v:v total silane) trimethoxysilyl-terminated PAMAMOS dendrimers. Data corresponds to the average of 7 individual films. [Inset: Magnified view of linear region.]

solutions derived via Eq. 4.8 by spectroscopically monitoring intra-film $\text{Mn}^{\text{III}}\text{TPPS}$ concentrations and $\text{Mn}^{\text{II}}(\text{NO})\text{TPPS}$ formation rates over 60 s time intervals are shown in Figure 4.6. At the larger HNO-donor concentration, a steady decrease in solution HNO was observed due to the prevalence of the second order HNO dimerization reaction and N_2O formation. Dimerization was slowed considerably at the lower HNO concentration. Further improvement of the working dynamic range of HNO-sensing films would therefore best be achieved by increasing k_{on} , expanding the range of measurable initial rates and improving sensitivity at lower donor concentrations. The rates of $\text{Mn}^{\text{II}}(\text{NO})\text{TPPS}$ formation scale with the square root of the nitroxyl donor employed (Eq. 4.7). However, sensor response can be approximated as linear at low donor concentrations (Figure 4.5 inset). In this region, a sensitivity of $\sim 2.5 \times 10^{-10} \text{ M}^{-1} \text{ s}^{-1}$ (change in initial rates) per μmol Angeli's salt was obtained, correlating to an estimated minimum resolvable shift of approximately 10 nM HNO as derived from twice the average standard deviation of the measured initial rates. Although sensors regenerated by long-term (>24 h) exposure to PBS containing ambient O_2 concentrations showed consistent response to HNO, the lengthy soaking periods required often had detrimental effects on xerogel stability, leading to cracking and peeling of the xerogel films. Because of this issue and the relative ease of film fabrication, films were typically utilized only once.

To illustrate the usefulness of the developed HNO-sensing films for the screening of HNO-donor compounds, nitroxyl production from the *N*-bound diazeniumdiolate (NONOate) compound IPA/NO was measured using the microtitre plate format. Formed upon exposure of amines to high pressures of NO, NONOate compounds have been widely employed as NO-storage and delivery agents. Recent studies indicate that primary amine NONOates such

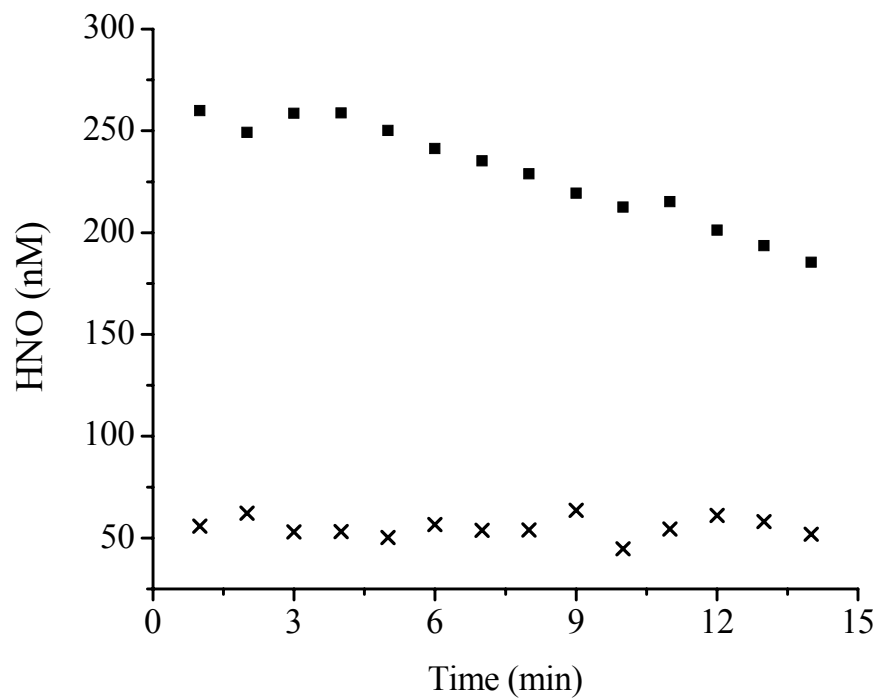


Figure 4.6. Time-resolved HNO concentrations obtained from (■) 700 μM and (x) 50 μM Angeli's salt in pH 7.4 PBS. Rates were acquired over 60 s intervals.

as IPA/NO have the capacity to produce both NO and HNO under certain conditions.^{25, 38} While overall decomposition of *N*-bound NONOates is proton initiated, HNO production is predicted to be thermodynamically favored over NO at high pH values.²⁶ The transition of IPA/NO from a HNO to NO-donor is proposed to occur gradually, with NO production increasing at pH <7 at the expense of HNO generation. This behavior was experimentally confirmed by examining the rates of Mn^{II}(NO)TPPS formation using the HNO-sensing plates. After Angeli's salt calibration, nitroxyl concentrations generated from 6.1 mM IPA/NO in pH 4-10.5 PBS were determined at 15 min time intervals (Figure 4.7). The nitroxyl concentrations at elevated pH trended upwards with decreasing pH to near neutral conditions, after which HNO concentrations began to decline. Gas evolution did not follow this trend, but rather was observed to consistently increase at decreasing pH values. Enhanced gas evolution is consistent with increased proton-initiated decomposition rates of the NONOate donor, and a strong indication that the reduced HNO concentrations detected were the result of an increase in IPA/NO decomposition to NO. Optical noise due to bubble formation in the sensor light path likely contributed to the high variability in recovered HNO concentrations observed at low pH in Figure 4.7. To compare the HNO production efficiencies of IPA/NO versus Angeli's salt, HNO concentrations were calculated from 1-6 mM IPA/NO in pH 7.4 PBS over 15 min intervals and compared to equivalent HNO concentrations derived from Angeli's salt (Figure 4.8). Despite similar rates of donor decomposition,²⁷ generation of equivalent HNO concentrations required significantly larger concentrations of IPA/NO. Such a trend is consistent with previous reports of decreased metmyoglobin reductive nitrosylation efficiency by equimolar amounts of IPA/NO and

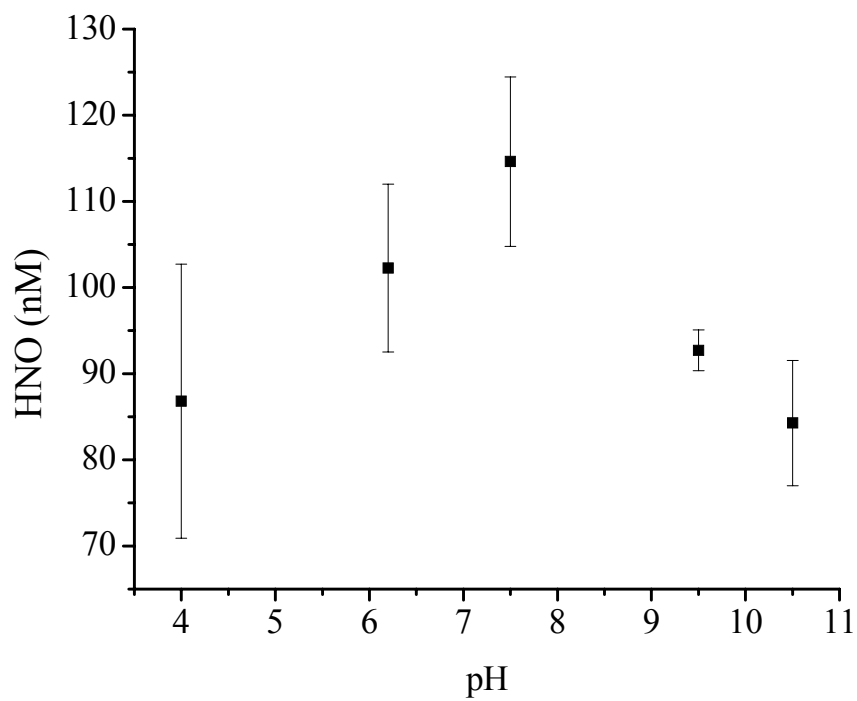


Figure 4.7. Effect of pH on HNO production from 6.1 mM IPA/NO in PBS. Data corresponds to the average of 7 individual films.

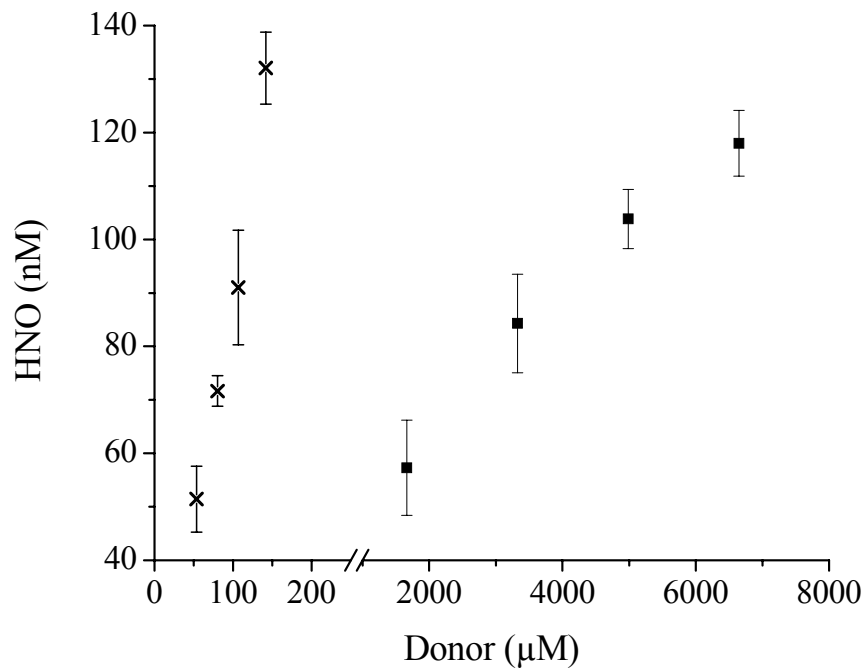


Figure 4.8. Concentrations of HNO versus required donor concentrations of (■) IPA/NO or (x) Angeli's salt in ph 7.4 PBS. Data corresponds to the average of 7 individual films. Note the scale break along the x-axis.

Angeli's salt,²⁵ and may be attributed to the concurrent formation of NO that is both formed competitively with HNO and scavenges existing HNO from solution.¹³

4.4. Conclusions

Despite a growing number of potential pharmaceutical applications, difficulties associated with nitroxyl detection and quantification have complicated the study of HNO and the characterization of new HNO-donor compounds. Through encapsulation of HNO-selective Mn^{III}TPPS within the anaerobic local environment of an aminoalkoxysilane xerogel membrane the first reported optical sensor films suitable for the quantitative determination of HNO were developed in a convenient 96-well microtitre plate format. At present, the rapid dimerization of HNO at high concentrations and relatively slow rate of HNO complexation in the xerogel film limit optimal sensor performance to environments with restricted HNO scavenging conditions and a narrow dynamic range. Future work should focus on increasing both the sensor range and sensitivity by increasing the rate of HNO diffusion into the films and the corresponding experimental kinetic coefficient (k_{on}) for intra-film complex formation. Nevertheless, the described HNO-sensing plates provide a simple, rapid means for determining HNO concentrations in aerobic solution and may thus prove useful as tools for characterizing novel HNO-releasing compounds.

4.5. References

- (1) Keefer, L. K. "Nitric oxide (NO)- and nitroxyl (HNO)-generating diazeniumdiolates (NONOates): Emerging commercial opportunities." *Current Topics in Medicinal Chemistry* **2005**, *5*, 625-634.
- (2) Moncada, S.; Higgs, A. "The L-arginine nitric oxide pathway." *New England Journal of Medicine* **1993**, *329*, 2002-2012.
- (3) Paolocci, N.; Jackson, M. I.; Lopez, B. E.; Miranda, K.; Tocchetti, C. G.; Wink, D. A.; Hobbs, A. J.; Fukuto, J. M. "The pharmacology of nitroxyl (HNO) and its therapeutic potential: Not just the janus face of NO." *Pharmacology & Therapeutics* **2007**, *113*, 442-458.
- (4) Pagliaro, P.; Mancardi, D.; Rastaldo, R.; Penna, C.; Gattullo, D.; Miranda, K. M.; Feelisch, M.; Wink, D. A.; Kass, D. A.; Paolocci, N. "Nitroxyl affords thiol-sensitive myocardial protective effects akin to early preconditioning." *Free Radical Biology and Medicine* **2003**, *34*, 33-43.
- (5) Nagasawa, H. T.; Kawle, S. P.; Elberling, J. A.; Demaster, E. G.; Fukuto, J. M. "Prodrugs of nitroxyl as potential aldehyde dehydrogenase inhibitors vis-a-vis vascular smooth muscle relaxants." *Journal of Medicinal Chemistry* **1995**, *38*, 1865-1871.
- (6) Lee, M. J. C.; Nagasawa, H. T.; Elberling, J. A.; Demaster, E. G. "Prodrugs of nitroxyl as inhibitors of aldehyde dehydrogenase." *Journal of Medicinal Chemistry* **1992**, *35*, 3648-3652.
- (7) Paolocci, N.; Saavedra, F. W.; Miranda, K. M.; Espey, M. G.; Isoda, T.; Wink, D. A.; Kass, D. A. "Novel and potent inotropic and selective venodilatory action of nitroxyl anion in intact dogs." *Circulation* **2000**, *102*, 161-161.
- (8) Miranda, K. M.; Nagasawa, H. T.; Toscano, J. P. "Donors of HNO." *Current Topics in Medicinal Chemistry* **2005**, *5*, 647-664.
- (9) Sha, X.; Isbell, T. S.; Patel, R. P.; Day, C. S.; King, S. B. "Hydrolysis of acyloxy nitroso compounds yields nitroxyl (HNO)." *Journal of the American Chemical Society* **2006**, *128*, 9687-9692.
- (10) King, S. B. "N-hydroxyurea and acyl nitroso compounds as nitroxyl (HNO) and nitric oxide (NO) donors." *Current Topics in Medicinal Chemistry* **2005**, *5*, 665-673.
- (11) Pennington, R. L.; Sha, X.; King, S. B. "N-hydroxy sulfonimidamides as new nitroxyl (HNO) donors." *Bioorganic & Medicinal Chemistry Letters* **2005**, *15*, 2331-2334.

- (12) Bartberger, M. D.; Liu, W.; Ford, E.; Miranda, K. M.; Switzer, C.; Fukuto, J. M.; Farmer, P. J.; Wink, D. A.; Houk, K. N. "The reduction potential of nitric oxide (NO) and its importance to NO biochemistry." *Proceedings of the National Academy of Sciences of the United States of America* **2002**, *99*, 10958-10963.
- (13) Shafirovich, V.; Lyman, S. V. "Nitroxyl and its anion in aqueous solutions: Spin states, protic equilibria, and reactivities toward oxygen and nitric oxide." *Proceedings of the National Academy of Sciences of the United States of America* **2002**, *99*, 7340-7345.
- (14) Butkovskaya, N. I.; Muravyov, A. A.; Setser, D. W. "Infrared chemiluminescence from the NO+HCO reaction: Observation of the 2 $\nu(1)$ - $\nu(1)$ hot band of HNO." *Chemical Physics Letters* **1997**, *266*, 223-226.
- (15) Cho, J. Y.; Dutton, A.; Miller, T.; Houk, K. N.; Fukuto, J. M. "Oxidation of N-hydroxyguanidines by copper(II): model systems for elucidating the physiological biosynthetic intermediate chemistry of the nitric oxide N-hydroxyl-L-arginine." *Archives of Biochemistry and Biophysics* **2003**, *417*, 65-76.
- (16) Yoo, J.; Fukuto, J. M. "Oxidation of N-hydroxyguanidine by nitric oxide the possible generation of vasoactive species." *Biochemical Pharmacology* **1995**, *50*, 1995-2000.
- (17) Donzelli, S.; Espey, M. G.; Thomas, D. D.; Mancardi, D.; Tocchetti, C. G.; Ridnour, L. A.; Paolucci, N.; King, S. B.; Miranda, K. M.; Lazzarino, G.; Fukuto, J. M.; Wink, D. A. "Discriminating formation of HNO from other reactive nitrogen oxide species." *Free Radical Biology and Medicine* **2006**, *40*, 1056-1066.
- (18) Bazylnski, D. A.; Hollocher, T. C. "Metmyoglobin and methemoglobin as efficient traps for nitrosyl hydride (nitroxyl) in neutral aqueous solution." *Journal of the American Chemical Society* **1985**, *107*, 7982-7986.
- (19) Bari, S. E.; Marti, M. A.; Amorebieta, V. T.; Estrin, D. A.; Doctorovich, F. "Fast nitroxyl trapping by ferric porphyrins." *Journal of the American Chemical Society* **2003**, *125*, 15272-15273.
- (20) Marti, M. A.; Bari, S. E.; Estrin, D. A.; Doctorovich, F. "Discrimination of nitroxyl and nitric oxide by water-soluble Mn(III) porphyrins." *Journal of the American Chemical Society* **2005**, *127*, 4680-4684.
- (21) Brinker, J.; Scherer, G. *Sol-Gel Science*. Academic Press, Inc.: New York, 1990.
- (22) Robbins, M. E.; Hopper, E. D.; Schoenfish, M. H. "Synthesis and characterization of nitric oxide-releasing sol-gel microarrays." *Langmuir* **2004**, *20*, 10296-10302.
- (23) Katori, T.; Tocchetti, C. G.; Miranda, K. M.; Champion, H. C.; Fukuto, J. M.; Wink, D. A.; Kass, D. A.; Paolucci, N. "The novel organic nitroxyl donor,

- isopropylamine/nitric oxide exerts beta-independent positive inotropy/lusitropy in failing hearts." *Journal of the American College of Cardiology* **2004**, *43*, 218A-218A.
- (24) Mancardi, D.; Ridnour, L.; Donzelli, S.; Miranda, K. M.; Thomas, D.; Katori, T.; Espey, M.; Paolocci, N.; Wink, D. "The nitroxyl donors Angeli's salt and IPA/NO afford equal cardiac early preconditioning-like effect that is independent of mitochondrial katp channel activation." *Free Radical Biology and Medicine* **2004**, *37*, S86-S87.
- (25) Miranda, K. M.; Katori, T.; de Holding, C. L. T.; Thomas, L.; Ridnour, L. A.; McLendon, W. J.; Cologna, S. M.; Dutton, A. S.; Champion, H. C.; Mancardi, D.; Tocchetti, C. G.; Saavedra, J. E.; Keefer, L. K.; Houk, K. N.; Fukuto, J. M.; Kass, D. A.; Paolocci, N.; Wink, D. A. "Comparison of the NO and HNO donating properties of diazeniumdiolates: Primary amine adducts release HNO in vivo." *Journal of Medicinal Chemistry* **2005**, *48*, 8220-8228.
- (26) Dobmeier, K. P.; Schoenfisch, M. H. "Antibacterial properties of nitric oxide-releasing sol-gel microarrays." *Biomacromolecules* **2004**, *5*, 2493-2495.
- (27) Maragos, C. M.; Morley, D.; Wink, D. A.; Dunams, T. M.; Saavedra, J. E.; Hoffman, A.; Bove, A. A.; Isaac, L.; Hrabie, J. A.; Keefer, L. K. "Complexes of NO with nucleophiles as agents for the controlled biological release of nitric oxide - Vasorelaxant effects." *Journal of Medicinal Chemistry* **1991**, *34*, 3242-3247.
- (28) Miranda, K. M.; Dutton, A. S.; Ridnour, L. A.; Foreman, C. A.; Ford, E.; Paolocci, N.; Katori, T.; Tocchetti, C. G.; Mancardi, D.; Thomas, D. D.; Espey, M. G.; Houk, K. N.; Fukuto, J. M.; Wink, D. A. "Mechanism of aerobic decomposition of Angeli's salt (sodium trioxodinitrate) at physiological pH." *Journal of the American Chemical Society* **2005**, *127*, 722-731.
- (29) Dobmeier, K. P.; Charville, G. W.; Schoenfisch, M. H. "Nitric oxide-releasing xerogel-based fiber-optic pH sensors." *Analytical Chemistry* **2006**, *78*, 7461-7466.
- (30) Marxer, S. M.; Schoenfisch, M. H. "Sol-gel derived potentiometric pH sensors." *Analytical Chemistry* **2005**, *77*, 848-853.
- (31) Shin, J. H.; Weinman, S. W.; Schoenfisch, M. H. "Sol-gel derived amperometric nitric oxide microsensor." *Analytical Chemistry* **2005**, *77*, 3494-3501.
- (32) Schoenfisch, M. H.; Rothrock, A. R.; Shin, J. H.; Polizzi, M. A.; Brinkley, M. F.; Dobmeier, K. P. "Poly(vinylpyrrolidone)-doped nitric oxide-releasing xerogels as glucose biosensor membranes." *Biosensors & Bioelectronics* **2006**, *22*, 306-312.
- (33) Shin, J. H.; Marxer, S. M.; Schoenfisch, M. H. "Nitric oxide-releasing sol-gel particle/polyurethane glucose biosensors." *Analytical Chemistry* **2004**, *76*, 4543-4549.

- (34) Marxer, S. M.; Robbins, M. E.; Schoenfisch, M. H. "Sol-gel derived nitric oxide-releasing oxygen sensors." *Analyst* **2005**, *130*, 206-212.
- (35) Dvornic, P. R. "PAMAMOS: The first commercial silicon-containing dendrimers and their applications." *Journal of Polymer Science Part A-Polymer Chemistry* **2006**, *44*, 2755-2773.
- (36) Dvornic, P. R.; Li, J. M.; de Leuze-Jallouli, A. M.; Reeves, S. D.; Owen, M. J. "Nanostructured dendrimer-based networks with hydrophilic polyamidoamine and hydrophobic organosilicon domains." *Macromolecules* **2002**, *35*, 9323-9333.
- (37) Tang, Y.; Tehan, E. C.; Tao, Z. Y.; Bright, F. V. "Sol-gel-derived sensor materials that yield linear calibration plots, high sensitivity, and long-term stability." *Analytical Chemistry* **2003**, *75*, 2407-2413.
- (38) Dutton, A. S.; Suhrada, C. P.; Miranda, K. M.; Wink, D. A.; Fukuto, J. M.; Houk, K. N. "Mechanism of pH-dependent decomposition of monoalkylamine diazeniumdiolates to form HNO and NO, deduced from the model compound methylamine diazeniumdiolate, density functional theory, and CBS-QB3 calculations." *Inorganic Chemistry* **2006**, *45*, 2448-2456.

Chapter 5:

Summary and Future Directions

5.1. Summary

The versatility of sol-gel chemistry makes xerogels an extremely adaptable and useful medium for creating sensor membranes and devices. Through manipulation of sol-gel processing conditions and selective incorporation of functional organoalkoxysilane precursors into the siloxane backbone of the material, the physical and chemical properties of the xerogel can be tuned for a desired application. Sensor membranes can be optimized for enhanced analyte selectivity and increased material compatibility with an intended sensing environment. Developing strategies to best utilize the unique properties of xerogel membranes for the enhancement of chemical sensor function has been the major focus of my doctoral work.

Chapter 2 detailed the design and development of a xerogel-based nitric oxide (NO)-releasing optical pH sensor. Real-time pH detection was achieved by monitoring the ratio of fluorescent emission from the acid and base isomers of the pH-sensitive fluorophore seminaphthorhodamine-1 carboxylate (SNARF-1) physically doped into xerogel films on tapered fiber optic probes. Direct immobilization of SNARF-1 in *N*-diazoniumdiolate (NONOate)-modified NO-releasing xerogels resulted in significantly reduced sensitivity to bulk pH due to the low solution permeability of NONOate-modified xerogels and localized pH buffering by covalently-bound aminoalkoxysilanes. However, a two-layer sensor

configuration wherein the NONOate-modified film was deposited directly onto the fiber-optic surface and the SNARF-1 pH indicator was immobilized in an overlying tetramethyl orthosilicate (TMOS) xerogel dramatically improved sensor performance. Two-layer sensor response to pH throughout the physiological range (pH 7.0-7.8) was fast ($\leq 14 \pm 2$ s) and linear. An estimated minimum resolvable pH shift of ~ 0.04 pH units was determined. Real-time chemiluminescence measurements confirmed the presence of the overlying indicator-doped TMOS layer had no inhibitory effect on NONOate formation or NO release. The NO-releasing coatings were capable of maintaining NO fluxes > 0.4 pmol cm⁻² s⁻¹ up to 16 h, and enhanced biocompatibility of the sensor films was confirmed by exposure to porcine platelet-rich plasma.

In Chapter 3, a novel class of NO-releasing xerogel coatings to improve sensor biocompatibility was described. *S*-nitrosothiol (RSNO)-modified xerogels were formed through the co-condensation of mercaptopropyltrimethoxysilane (MPTMS) and methyltrimethoxysilane (MTMOS) precursors. Nitrosation of the covalently-bound pendant thiols of MPTMS resulted in deep pink xerogel films capable of releasing NO for significantly longer periods than previously described NONOate-modified xerogels. Coloration of the film and NO release were found to scale with the percent of nitrosated-MPTMS incorporated in the sol. Thermal-initiated NO release from highly RSNO-modified films maintained NO fluxes > 0.5 pmol cm⁻² s⁻¹ for up to 14 d in 37 °C phosphate-buffered saline (PBS). The RSNO-modified xerogels demonstrated excellent solution stability as negligible siloxane network fragmentation was observed during 2 week immersion in 37 °C PBS. Significant reductions in adhesion of both *Pseudomonas aeruginosa* and activated porcine platelets were observed on nitrosated films versus non-nitrosated controls, indicating

that RSNO-modified films are capable of providing similar biocompatibility benefits as other NO-releasing xerogels.

In Chapter 4, the unique properties of aminoalkoxysilane-derived xerogels were employed to create the first reported optical sensor coatings for quantitative determination of nitroxyl (HNO), the one-electron reduced congener of NO. Sensors were created by encapsulating manganese(III) *meso*-tetrakis(4-sulfonatophenyl) porphyrinate ($\text{Mn}^{\text{III}}\text{TPPS}$) in (aminoethylaminomethyl)phenethyltrimethoxysilane (AEMP3)/MTMOS xerogel films. Upon reaction with HNO, the reductive nitrosylation of $\text{Mn}^{\text{III}}\text{TPPS}$ to $\text{Mn}^{\text{II}}(\text{NO})\text{TPPS}$ resulted in a concurrent shift in the absorbance spectrum of the complex. While the nitrosylated compound was unstable in air, encapsulation of $\text{Mn}^{\text{II}}(\text{NO})\text{TPPS}$ in the anaerobic interior of the AEMP3/MTMOS xerogel significantly slowed reoxidation of the complex. Thus, xerogel-encapsulated $\text{Mn}^{\text{III}}\text{TPPS}$ operated as a cumulative HNO trap over short time scales. Sensor calibration was achieved by spectroscopically monitoring the initial rates of $\text{Mn}^{\text{II}}(\text{NO})\text{TPPS}$ formation in the films during exposure to the HNO-donor compound Angeli's salt. Steady-state kinetics were employed to compensate for HNO scavenging reactions and determine the kinetic coefficient (k_{on}) of $\text{Mn}^{\text{II}}(\text{NO})\text{TPPS}$ formation in the xerogel environment. The determined k_{on} and spectroscopically observed rates of $\text{Mn}^{\text{II}}(\text{NO})\text{TPPS}$ formation were subsequently used to calculate HNO concentrations in sample solutions.

Nitroxyl-sensing xerogel films were further optimized for use in a 96-well microtitre plate format through the incorporation of trimethoxysilyl-terminated poly(amidoamine-organosilicon) (PAMAMOS) dendrimers. The co-condensed PAMAMOS dendrimers selectively enhanced HNO diffusion through the material via the creation of hydrophilic

nanodomains in the siloxane network, resulting in greater k_{on} values and increased overall HNO sensitivity of the films. Amperometric oxygen permeability studies confirmed that PAMAMOS inclusion had no detrimental effect on the ability of the xerogel to exclude O₂. Nitroxyl-sensing films containing 0.25% (v:v total silane) PAMAMOS were capable of resolving a minimum shift of approximately 10 nM HNO over a working dynamic range of 24-290 nM HNO. The developed 96-well microtitre sensor plates were subsequently used to characterize HNO-release from a recently described HNO/NO donor, sodium-1-(isopropylamino)diazene-1-ium-1,2-diolate (IPA/NO), illustrating their potential as a useful tool in the evaluation of novel HNO donor compounds.

5.2. Future Research Directions

The optical sensing configuration employed in the development of the NO-releasing pH sensor described in Chapter 2 may be easily adapted for the fabrication of other NO-releasing optical sensors. Muller and co-workers have reported fiber-optic biosensors for penicillin, urea, creatinin and glucose created through immobilization of the appropriate enzyme (e.g., glucose dehydrogenase) at the surface of pH-sensitive optodes.¹ As described previously, inert, porous xerogels provide a near ideal host matrix for enzyme encapsulation. Nitric oxide-releasing analogs of the four biosensors mentioned above could be created by coencapsulating a desired enzyme in the upper TMOS xerogel layer and monitoring pH changes associated with enzyme function through fluorescent emission of the SNARF-1 indicator. Replacing SNARF-1 with an alternate luminescent indicator for a desired analyte (e.g., phosphorescent erythrosin B for quenchometric oxygen detection^{2, 3}) can also easily extend the capabilities of the two-layer xerogel optical sensor. By bundling multiple NO-

releasing xerogel-modified optical sensors together (i.e., O₂, CO₂, pH), biocompatible intravascular sensor arrays may be developed for real-time blood gas sensing during critical care situations.

A host of other intravascular sensor applications become possible if NO-release can be extended beyond the 16 h window achieved by the NONOate-modified xerogel films described in Chapter 2. For example, a rapid drop in brain parenchyma pH has been reported by McKinley et al. during the onset of stroke.⁴ Detecting this pH shift in unconscious or comatose patients at high risk of stroke could be an important early warning sign used to reduce brain damage caused by ischemic insult. Nitric oxide-releasing xerogels may provide a biocompatibility enhancement extending the functional lifetime of intravascular pH sensors used for long-term brain pH monitoring; prolonged durations of NO-release would be beneficial in such a task to reduce the necessary frequency of sensor replacement. The RSNO-modified xerogel films presented in Chapter 3 may be of potential use in this type of long-term sensing application.

At present time, no RSNO-modified polymeric coatings have been utilized for indwelling sensor applications. While the pink coloration of RSNOs may pose problems for optical sensor platforms, the stability and extended duration of NO-release attainable by RSNO-modified xerogels makes them potentially well-suited as a membrane material for intravascular and subcutaneous electrochemical sensors. Future work should evaluate the fabrication of RSNO-modified xerogel sensors and biosensors. However, as the materials are still in the beginning stages of development, further characterization of RSNO-modified xerogel properties is required before practical application.

Membrane porosity and permeability is particularly important in electrochemical sensor applications. As RSNO-modified xerogels are not exposed to the high pressures of NO required for NONOate formation, the extremely low porosity observed in NONOate-modified xerogels attributed to free-radical catalyzed cross-linking should not be an issue.⁵ Nevertheless, the permeability of RSNO-modified xerogels to common analytes (e.g., oxygen, glucose) should be assessed. The choice of organoalkoxysilane precursors employed may have important effects on material permeability. By utilizing silane precursors with highly branched terminal side chains or precursors subject to lower degrees of siloxane bonding (e.g., mercaptopropylmethyldimethoxysilane), more open and accessible xerogel networks may be created.

Optimization of NO-release from RSNO-modified xerogels remains largely to be explored. For example, porous networks may be more accessible to acidified nitrite, resulting in increased thiol nitrosation and enhanced NO flux from the material. The kinetics of thermal RSNO decomposition are influenced by factors such as the degree of substitution of the thiol-bonded carbon and/or presence of intramolecular hydrogen bonds.⁶ These structural considerations as well as other RSNO decomposition methods (e.g., light, Cu⁺)⁷ should all be examined as a means of regulating NO flux and duration from RSNO-modified xerogels.

Future work regarding the development of the HNO-sensing xerogel films described in Chapter 4 should focus on improving the working dynamic range and sensitivity of the optical sensors. As the rapid dimerization reaction limits HNO concentrations in solution, expanding the usable range of the sensor must necessarily focus on decreasing current limits of HNO detection. The most straightforward method of achieving this would be to improve

HNO complexation rates (i.e., k_{on}) in the film. While using alternate indicator molecules such as metmyoglobin⁸ or ferric porphyrins⁹ with higher reported rates of HNO reaction than the Mn^{III}TPPS indicator employed may increase HNO complexation rates, the determined values of k_{on} for Mn^{II}(NO)TPPS formation in the xerogel films remain ~30-40 times lower than those reported by Marti et al. for Mn^{III}TPPS in free solution.¹⁰ Thus the speed of HNO diffusion through the xerogel material likely plays a large role in determining the reaction rates observed. The inclusion of small amounts of hydrophilic trimethoxysilyl-terminated PAMAMOS dendrimer effectively increased HNO permeation, but larger percentages of inclusion resulted in higher oxygen permeability and decreased sensor response. The introduction of alternate sol-gel precursors for preferential enhancement of HNO over O₂ permeability in the xerogel may be required. Accelerating HNO diffusion through the optical sensor films to increase k_{on} and bring about concomitant improvements in HNO sensitivity while maintaining the anaerobic environments necessary for complex stability within the material remains a difficult and rewarding challenge.

5.3. References

- (1) Muller, C.; Hitzmann, B.; Schubert, F.; Scheper, T. "Optical chemo- and biosensors for use in clinical applications." *Sensors and Actuators B-Chemical* **1997**, *40*, 71-77.
- (2) Gillanders, R. N.; Tedford, M. C.; Crilly, P. J.; Bailey, R. T. "A composite sol-gel/fluoropolymer matrix for dissolved oxygen optical sensing." *Journal of Photochemistry and Photobiology A-Chemistry* **2004**, *163*, 193-199.
- (3) Gillanders, R. N.; Tedford, M. C.; Crilly, P. J.; Bailey, R. T. "Erythrosin B encapsulated in a fluoropolymer matrix for dissolved oxygen optical sensing in aggressive aqueous environments." *Journal of Photochemistry and Photobiology A-Chemistry* **2004**, *162*, 531-535.
- (4) McKinley, B. A.; Morris, W. P.; Parmley, C. L.; Butler, B. D. "Brain parenchyma PO₂, PCO₂, and pH during and after hypoxic, ischemic brain insult in dogs." *Critical Care Medicine* **1996**, *24*, 1858-1868.
- (5) Shin, J. H.; Marxer, S. M.; Schoenfisch, M. H. "Nitric oxide-releasing sol-gel particle/polyurethane glucose biosensors." *Analytical Chemistry* **2004**, *76*, 4543-4549.
- (6) de Oliveira, M. G.; Shishido, S. M.; Seabra, A. B.; Morgon, N. H. "Thermal stability of primary S-nitrosothiols: Roles of autocatalysis and structural effects on the rate of nitric oxide release." *Journal of Physical Chemistry A* **2002**, *106*, 8963-8970.
- (7) Singh, R. J.; Hogg, N.; Joseph, J.; Kalyanaraman, B. "Mechanism of nitric oxide release from S-nitrosothiols." *Journal of Biological Chemistry* **1996**, *271*, 18596-18603.
- (8) Bazylinski, D. A.; Hollocher, T. C. "Metmyoglobin and methemoglobin as efficient traps for nitrosyl hydride (nitroxyl) in neutral aqueous solution." *Journal of the American Chemical Society* **1985**, *107*, 7982-7986.
- (9) Bari, S. E.; Marti, M. A.; Amorebieta, V. T.; Estrin, D. A.; Doctorovich, F. "Fast nitroxyl trapping by ferric porphyrins." *Journal of the American Chemical Society* **2003**, *125*, 15272-15273.
- (10) Marti, M. A.; Bari, S. E.; Estrin, D. A.; Doctorovich, F. "Discrimination of nitroxyl and nitric oxide by water-soluble Mn(III) porphyrins." *Journal of the American Chemical Society* **2005**, *127*, 4680-4684.

Appendix 1:

Antibacterial Properties of NO-Releasing Xerogel Microarrays

A1.1. Introduction

Nitric oxide-releasing polymers have been shown to enhance the biocompatibility of intravascular and subcutaneous materials.^{1,2} As a key element in vasodilation and the regulation of platelet activity and aggregation, NO has been used to substantially increase the thromboresistivity of blood-contacting biomaterials.³⁻⁵ Nitric oxide has also been linked to phagocytosis and the body's response to microbial invaders.⁶ Polymeric coatings capable of NO-release have been shown to inhibit bacterial adhesion, suggesting that the use of such coatings for implant materials may aid in decreasing the incidence of implant-associated infection.^{7,8}

A simple method of imparting NO-release capability to a polymer is through the inclusion of NO-donor moieties termed *N*-diazoniumdiolates. *N*-diazoniumdiolates are readily formed through exposure of diamine functional groups to high pressures of NO, resulting in the coordination of two NO molecules.⁹ This configuration remains stable until exposed to a proton donor such as water, which results in the decomposition of the *N*-diazoniumdiolate and NO release. Previously, xerogels have been demonstrated as useful matrices capable of controlled NO release.⁸ Through condensation of diaminoalkoxysilanes into the siloxane backbone of a xerogel network, xerogel coatings capable of tunable picomolar NO fluxes have been synthesized.¹⁰

For certain applications such as intravascular and subcutaneous electrochemical sensors, a uniform xerogel coating may not be ideal. In such cases, the thromboresistive

benefits of NO-releasing polymers may be neutralized by the dense coating itself serving as an analyte diffusion barrier, resulting in decreased analytical sensitivity. Indeed, a recent study reported a greater than 10^4 -fold decrease in hydrogen peroxide permeation to a NO-releasing xerogel-based glucose sensor.¹¹ This problem may be alleviated by using micropatterning techniques to create NO-releasing xerogel arrays of micrometer dimensions separated by regions of unmodified sensor surface. As such, NO diffusing from the xerogel microstructures may permit enhanced biocompatibility at the sensor's surface while concurrently decreasing the analyte barrier effect caused by a uniform xerogel coating. Previous *in vitro* studies by Robbins *et al.* have shown that NO-releasing microarrays are capable of reducing platelet adhesion and activation.¹² Recent work has confirmed these microarrays as a viable means of increasing the sensitivity and response of xerogel-modified electrochemical oxygen sensors.¹³ Herein, the antibacterial effects of micropatterned NO-releasing xerogel arrays are evaluated. Fewer adherent bacteria would correspond to a decrease in biofilm nucleation sites, implying that NO-releasing xerogel arrays may be useful in reducing biofouling and associated infection at an implant site. *Pseudomonas aeruginosa*, an opportunistic pathogen, was selected as a model bacterium because of its medical relevance and capacity for biofilm formation.¹⁴ Reductions in bacterial adhesion to NO-releasing xerogel microarrays were quantified relative to controls, and the effect of microarray geometry was examined.

A1.2. Materials and Methods

Methyltrimethoxysilane (MTMOS), (aminoethylaminomethyl)-phenethyltrimethoxysilane (AEMP3), and dimethylsiloxane-(60% propylene oxide, 40% ethylene oxide) block polymer were purchased from Gelest (Morrisville, PA). *P. aeruginosa*

(ATCC #19143) was obtained from American Type Culture Collection (Manassas, VA). A BacLight LIVE/DEAD Cell Viability Fluorescence kit was purchased from Molecular Probes (Eugene, OR). Nitric oxide (99.5%) was acquired from National Welders Supply Co. (Durham, NC) and purified over KOH prior to use. Distilled water was purified with a Millipore Milli-Q Gradient A-10 system (Bedford, MA) to 18.2 M Ω . Sylgard 184 Silicone Elastomer (Dow Corning) polydimethylsiloxane (PDMS) and all other reagents were purchased from Fisher Scientific (Pittsburgh, PA) and used as received.

A1.2.1. Xerogel Micropatterning

A 20% AEMP3 / 80% MTMOS sol was prepared by mixing 160 μ L MTMOS with 200 μ L ethanol (EtOH), 11 μ L H₂O and 40 μ L of AEMP3. The resulting mixture was immersed in an ultrasonic bath for 5 min. Xerogel microarrays were formed on glass substrates through the micromolding in capillaries (MIMIC) soft lithographic technique described by Whitesides and coworkers.¹⁵ Master molds with the desired array dimensions were photolithographically produced in a silicon (Si) wafer by MCNC (Research Triangle Park, NC). Elastomeric negative-relief templates were formed by fluorinating the Si master with (heptadecafluoro-1,1,2,2-tetra-hydrodecyl)-trichlorosilane vapor for approximately 45 min to reduce PDMS adhesion,¹⁶ and then coating the master with Sylgard 184 elastomer and curing at 70 °C for 1 h. To enhance PDMS wettability toward the sol, the hydrophilicity of the PDMS channel walls was increased by immersing the PDMS templates in 5% PDMS-polyethylene glycol (PEG) block polymer in EtOH (v/v) for 30 min.¹⁷ The PDMS templates were then rinsed with EtOH, dried, and brought into contact with a glass substrate, forming an array of microchannels with the dimensions of the original Si master features. A 10 μ L drop of the sol placed adjacent to this template was drawn into the microchannels by

capillary action and allowed to cure under ambient conditions for 24 h, after which the PDMS template was removed. In this manner, arrays of lines 1.5 μm high with widths of 10 or 50 μm and separation distances ranging from 10 to 200 μm were produced.

A1.2.2. NO-Release

N-diazoniumdiolate formation was achieved by exposure of the xerogel arrays to 5 atm NO for 3 d in an in-house reactor, as described previously.¹⁰ Nitric oxide flux from the xerogel patterns was measured in deoxygenated phosphate buffered saline (PBS, 7.4 pH) at 37 °C via chemiluminescence using a Nitric Oxide Analyzer 280 (Sievers Inc., Boulder, CO).

A1.2.3. Array Stability

The extended solution stability of the NO-releasing xerogel arrays was evaluated using a PicoPlus (Molecular Imaging, Tempe, AZ) atomic force microscope (AFM). Microarrays were incubated in PBS at 37 °C. After discrete immersion intervals, arrays were dried and contact-mode images were acquired using SiN₃ AFM tips (nominal spring constant ~ 0.12 N/m).

A1.2.4. Evaluation of Bacterial Retention

P. aeruginosa stocks were cultured in tryptic soy broth (TSB) at 37 °C, pelleted, washed, suspended in 15% glycerol, and stored at -80 °C until use. Stocks were inoculated in TSB and grown for 12 h at 37 °C. A 1 mL aliquot of this culture was then grown in 200 μL TSB at 37 °C until the suspensions reached an optical density ($\text{OD}_{\lambda=600}$) of approximately 0.2, corresponding to $\sim 10^8$ colony forming units (cfu) per mL. The bacteria were pelleted, washed, and resuspended in a BacLight Syto 9 / PBS solution for 30 min to

fluorescently stain the cells. Following subsequent centrifugation and washing, the cells were resuspended in PBS. Control and NO-releasing arrays were immersed in 37 °C PBS for 30 min to initiate NO release. The samples were transferred to 5 mL bacterial suspensions at 37 °C for an additional 30 min and agitated mildly (~ 1 rev/s). The arrays were then rinsed lightly with deionized water to remove loosely adhered cells, and dried under a stream of nitrogen. A Zeiss Axiovert 200 inverted microscope fitted with a Syto 9 optical filter and Zeiss AxioCam (Chester, VA) was utilized to image fluorescently-tagged bacteria retained on the arrays. Bacterial surface coverage was determined through digital processing as percent white for each imaged 340 μm x 430 μm region. For each array geometry, the average of 5 randomly positioned images was determined for each of 9 sample arrays. Overall surface coverage was determined as the mean of the 9 individual sample averages (n = 9).

A1.3. Results and Discussion

The 20% AEMP3 / 80% MTMOS sol-gel formulation was employed because of the low sol viscosity afforded through use of the simple MTMOS precursor; which is necessary for MIMIC patterning procedures prior to curing.¹² Chemiluminescence analysis verified that the *N*-diazoniumdiolate-containing arrays were capable of releasing NO. After normalization to surface area, xerogel arrays were found to release NO at a flux of approximately $1.0 \pm 0.1 \text{ pmol cm}^{-2} \text{ s}^{-1}$ over the 30 min time window of the bacterial adhesion studies. This flux is similar to the NO released endogenously by activated human endothelial cells ($\sim 6 \text{ pmol cm}^{-2} \text{ s}^{-1}$),¹⁸ and that reported previously to reduce bacterial adhesion via NO-releasing xerogel films.^{7,8} AFM images at distinct intervals after immersion in PBS solution (pH 7.4) at 37 °C indicated that the xerogel patterns were stable in aqueous solution for up to 7 d (data not shown.)

As shown in Figure A1.1, a marked decrease in adhesion to substrates was observed for NO-releasing xerogel arrays compared to non-releasing controls. The veracity of this reduction was confirmed through ANOVA statistics. The average percent-surface covered by bacteria on controls, NO-releasing arrays, and the appropriate ANOVA P values for each group comparison are listed in Table A1.1. The reduction in *P. aeruginosa* adhesion displayed for all arrays comprised of 50 μm lines was determined to be significant ($P < 0.05$). For these arrays, a reduction in adhesion of approximately 50% was noted for all arrays, regardless of line separation. In 10 μm line arrays, a similar $\sim 50\%$ significant reduction was found for all line separations up to 50 μm . At larger line separations, however, the apparent reduction begins to decrease and P begins to rise above the significance threshold ($P > 0.05$). This is evident at 100 and 200 μm line separations.

These results may indicate a limit to the surface area of a substrate that may be left unmodified by xerogel under current experimental conditions. It may be expected that for a given NO flux (herein $1.0 \pm 0.1 \text{ pmol cm}^{-2} \text{ s}^{-1}$) there would exist a threshold ratio of unmodified/modified surface beyond which NO surface concentrations would be insufficient to achieve full inhibitory effects. The apparent breakdown in significant reduction of bacterial adhesion on 10 μm line arrays separated by 100 and 200 μm may indicate that this limit is approached at a 10:1 unmodified/modified surface ratio in this experiment. The inherently high variability of bacterial adhesion onto a surface makes an absolute limit difficult to determine conclusively, however, as evidenced by the larger adherence reduction displayed at 150 μm separations. In any case, such a threshold would depend heavily on experimental conditions (ie. substrate identity, NO flux, array geometry, etc.). Maximization of line separation is desirable as bacteria tend to become trapped near the raised edge of a

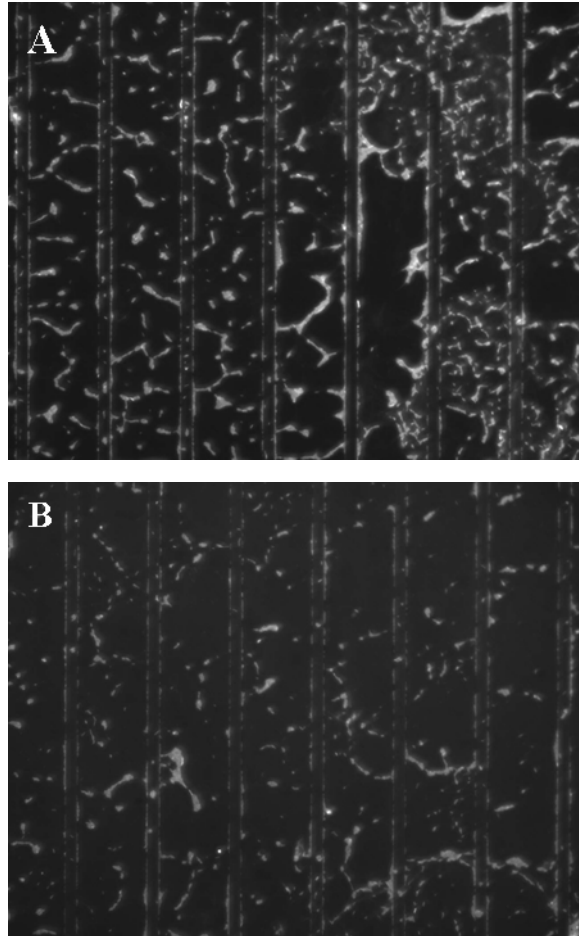


Figure A1.1. *P. aeruginosa* adhesion on (A) control and (B) NO-releasing 10 μm xerogel lines separated by 50 μm spacings. Cells are white.

Table A1.1. Average bacterial surface coverage on 20% AEMP3 / 80% MTMOS xerogel arrays

Line width x separation (μm) ^a	<u>Bacterial Coverage (%)</u>		ANOVA <i>P</i> value	Line width x separation (μm) ^a	<u>Bacterial Coverage (%)</u>		ANOVA <i>P</i> value
	Control	NO-array ^b			Control	NO-array ^b	
10x10	9.3 ± 2.6	4.7 ± 1.4	2.3x10 ⁻⁴	50x10	8.8 ± 2.8	3.8 ± 1.8	4.4x10 ⁻⁴
10x25	11.0 ± 2.4	5.2 ± 1.2	5.9x10 ⁻⁶	50x25	8.7 ± 3.2	3.3 ± 1.7	4.0x10 ⁻⁴
10x50	9.2 ± 2.1	4.2 ± 0.9	6.7x10 ⁻⁶	50x50	7.5 ± 4.4	4.0 ± 2.3	4.1x10 ⁻²
10x100	8.4 ± 3.5	6.0 ± 2.1	9.4x10 ⁻²	50x100	10.3 ± 3.2	5.6 ± 3.0	5.6x10 ⁻³
10x150	10.2 ± 4.0	4.8 ± 2.0	2.5x10 ⁻³	50x150	9.6 ± 2.9	4.7 ± 1.6	4.5x10 ⁻⁴
10x200	9.0 ± 4.7	6.1 ± 2.7	1.2x10 ⁻¹	50x200	10.7 ± 1.4	5.2 ± 2.1	7.4x10 ⁻⁶

^aLine height = 1.5 μm . ^bNO flux $\sim 1.0 \pm 0.1$ pmol/cm²•s

xerogel line. Thus, a reduction in the number of raised surfaces reduces the number of edges that may serve as potential biofilm nucleation sites.

These results indicate that NO release from micropatterned arrays of xerogels effectively reduces the adhesion of *P. aeruginosa* to adjacent unmodified substrate regions. As such, the application of these arrays onto the surface of an implant may reduce biofouling while minimizing substrate modification. However, two factors must be considered further before extrapolation of these results to in vivo conditions. As these experiments were performed in an aqueous cell suspension, NO degradation is limited to cellular interactions and direct oxidation to nitrite by dissolved O₂. In a biological environment, the presence of other NO scavengers (e.g., proteins, thiols, transition metals, etc.) is expected to significantly decrease the half-life of free NO.¹⁹ In such a situation, NO diffusion path lengths would be decreased, resulting in a reduction in the line separation distances that may be utilized while effectively maintaining NO concentrations adequate to impede bacterial adhesion. It should also be noted that extremely large *P. aeruginosa* cell concentrations (10⁸ cfu/mL) were used in this study to ensure regular substrate/cell interactions during the time of the experiment. The number of bacteria present would naturally be far lower in clinical situations.

A1.4. Conclusions

Arrays of xerogel lines capable of controlled release of NO via *N*-diazoniumdiolate modification have been produced through soft lithographic procedures. These NO-releasing arrays proved capable of reducing *P. aeruginosa* adhesion to regions of unmodified glass substrates by approximately 50% at a NO flux of $1.0 \pm 0.1 \text{ pmol cm}^{-2} \text{ s}^{-1}$ versus non-releasing controls in arrays comprised of unmodified/modified surface ratios up to 10:1. As such, micropatterning NO-releasing xerogels may provide a valuable means for reducing the

biofouling of certain materials while concurrently maintaining portions of unmodified surface that required for implant function.

A1.5. References

- (1) Frost, M. C.; Batchelor, M. M.; Lee, Y. M.; Zhang, H. P.; Kang, Y. J.; Oh, B. K.; Wilson, G. S.; Gifford, R.; Rudich, S. M.; Meyerhoff, M. E. "Preparation and characterization of implantable sensors with nitric oxide release coatings." *Microchemical Journal* **2003**, *74*, 277-288.
- (2) Zhang, H. P.; Annich, G. M.; Miskulin, J.; Osterholzer, K.; Merz, S. I.; Bartlett, R. H.; Meyerhoff, M. E. "Nitric oxide releasing silicone rubbers with improved blood compatibility: preparation, characterization, and in vivo evaluation." *Biomaterials* **2002**, *23*, 1485-1494.
- (3) Mowery, K. A.; Schoenfisch, M. H.; Saavedra, J. E.; Keefer, L. K.; Meyerhoff, M. E. "Preparation and characterization of hydrophobic polymeric films that are thromboresistant via nitric oxide release." *Biomaterials* **2000**, *21*, 9-21.
- (4) Schoenfisch, M. H.; Mowery, K. A.; Rader, M. V.; Baliga, N.; Wahr, J. A.; Meyerhoff, M. E. "Improving the thromboresistivity of chemical sensors via nitric oxide release: Fabrication and in vivo evaluation of NO-releasing oxygen-sensing catheters." *Analytical Chemistry* **2000**, *72*, 1119-1126.
- (5) Frost, M. C.; Rudich, S. M.; Zhang, H. P.; Maraschio, M. A.; Meyerhoff, M. E. "In vivo biocompatibility and analytical performance of intravascular amperometric oxygen sensors prepared with improved nitric oxide-releasing silicone rubber coating." *Analytical Chemistry* **2002**, *74*, 5942-5947.
- (6) Fang, F. C. "Mechanisms of nitric oxide-related antimicrobial activity." *Journal of Clinical Investigation* **1997**, *99*, 2818-2825.
- (7) Nablo, B. J.; Schoenfisch, M. H. "Antibacterial properties of nitric oxide-releasing sol-gels." *Journal of Biomedical Materials Research Part A* **2003**, *67A*, 1276-1283.
- (8) Nablo, B. J.; Chen, T. Y.; Schoenfisch, M. H. "Sol-gel derived nitric-oxide releasing materials that reduce bacterial adhesion." *Journal of the American Chemical Society* **2001**, *123*, 9712-9713.
- (9) Hrabie, J. A.; Klose, J. R.; Wink, D. A.; Keefer, L. K. "New nitric oxide-releasing zwitterions derived from polyamines." *Journal of Organic Chemistry* **1993**, *58*, 1472-1476.
- (10) Marxer, S. M.; Rothrock, A. R.; Nablo, B. J.; Robbins, M. E.; Schoenfisch, M. H. "Preparation of nitric oxide (NO)-releasing sol-gels for biomaterial applications." *Chemistry of Materials* **2003**, *15*, 4193-4199.

- (11) Shin, J. H.; Marxer, S.; Schoenfisch, M. H. "Nitric oxide-releasing Sol-Gel Particle/Polyurethane Glucose Biosensors." *Analytical Chemistry* **2004**, *76*, 4543-4549.
- (12) Robbins, M. E.; Schoenfisch, M. H. "Surface-localized release of nitric oxide via sol-gel chemistry." *Journal of the American Chemical Society* **2003**, *125*, 6068-6069.
- (13) Robbins, M. E.; Hopper, E. D.; Schoenfisch, M. H. "Nitric oxide-releasing sol-gel microarrays for biosensor applications." *Langmuir* **2004**, *accepted for publication*.
- (14) O'Toole, G.; Kaplan, H. B.; Kolter, R. "Biofilm formation as microbial development." *Annual Review of Microbiology* **2000**, *54*, 49-79.
- (15) Kim, E.; Xia, Y. N.; Whitesides, G. M. "Polymer microstructures formed by molding in capillaries." *Nature* **1995**, *376*, 581-584.
- (16) James, C. D.; Davis, R. C.; Kam, L.; Craighead, H. G.; Isaacson, M.; Turner, J. N.; Shain, W. "Patterned protein layers on solid substrates by thin stamp microcontact printing." *Langmuir* **1998**, *14*, 741-744.
- (17) Kim, Y. D.; Park, C. B.; Clark, D. S. "Stable sol-gel microstructured and microfluidic networks for protein patterning." *Biotechnology and Bioengineering* **2001**, *73*, 331-337.
- (18) Vaughn, M. W.; Kuo, L.; Liao, J. C. "Estimation of nitric oxide production and reaction rates in tissue by use of a mathematical model." *American Journal of Physiology-Heart and Circulatory Physiology* **1998**, *43*, H2163-H2176.
- (19) Kelm, M. "Nitric oxide metabolism and breakdown." *Biochimica Et Biophysica Acta-Bioenergetics* **1999**, *1411*, 273-289.